## Bauhaus-Universität Weimar

# Assessment of coupled models of bridges considering time-dependent vehicular loading

Bewertung gekoppelter Modelle im Brückenbau unter
Berücksichtigung zeitabhängiger Fahrzeugeinwirkungen

## DISSERTATION

zur Erlangung des akademischen Grades

Doktor-Ingenieur

an der Fakultät Bauingenieurwesen
der
Bauhaus-Universität Weimar

vorgelegt von

## Ghada Karaki

geb. am 2.Dezember 1982 in Bethlehem

Gutachter :  Prof. Dr.-Ing. Ursula Freundt
Prof. Dr. Geert Lombaert
Prof. Dr.-Ing Guido Morgenthal

Tag der Disputation: 13. Februar 2011

*To my parents, Dayna and Jamil*

# Acknowledgements

The present work was written during my work as a research associate within the "Graduierten-kolleg 1462: Bewertung gekoppelter numerischer Partialmodelle in Konstruktiven Ingenieur-bau" at the Bauhaus-Universität Weimar supported by the German Research Institute (DFG) which is gratefully acknowledged.

I am most thankful to my advisor and supervisor Professor Ursula Freundt, whose encouragement, guidance and support from the initial to final stages enabled me to complete my research work. I appreciate her contributions of time, ideas and openness in discussions. I would also like to thank Dr. Ralf Vogt for his assistance during my work. It is also a pleasure to be able to thank those who made this thesis possible: Dr. Thomas Most for his support and the discussions related to the assessment problem, Dr. Tom Lahmer and Holger Keitel for taking the time and having the patience to answer my many questions.

I had the pleasure of spending some time at the Katholieke Universiteit Leuven as a visiting scholar under the supervision of Professor Geert Lombaert. I am indebted to Professor Lombaert for his constructive feedback, and insightful discussions. I am also grateful to Dr. Kai Liu and Mohammad Amin Lak of the Department of Structural Mechanics at the Katholieke Universiteit Leuven, for their help and assistance. I would like also to extend my thanks to Professor Chul W. Kim, who I had the pleasure of meeting during my stay in Leuven; I sincerely appreciate his support and the time he took to answer my questions and concerns.

I am also thankful for Prof. Morgenthal and Prof. Lombaert for agreeing to serve as examiners for my dissertation and taking the time to review my work.

Many people have told me that the experience and the journey is what I will take with me from my doctorate studies. Therefore, I have to thank my companions on this journey, my colleagues and friends, Holger, Idna, Mathias, Markus, Peter, Susanne, Tina, Toni, Thomas, and Tom. Our informal meetings at the coffee machine and afterwork events and activities helped me to manage the long working days.

My time in Weimar was made enjoyable in large part because of the friends that I shared an apartment with, took a language course with or met in the many cool places in Weimar.

Therefore, I would like to extend my deepest thanks to all of my friends for the memorable moments we shared in and outside of Weimar.

A huge thank you goes to my family, my brothers, Ashraf and Samer, my sister Flair and their families Faten, Iman, Aseel, Rand, Jamil and Dayna, for always calling and checking on me. I felt involved in their lives, which made me see the bigger picture and got me through some difficult days. Finally, I want to express my sincere appreciation and absolute gratitude to my parents. They have been always there for me, which gives me the strength to go on. I simply cannot thank them enough for their support, encouragement and love.

<div style="text-align: right;">

Ghada Karaki

Weimar 2011

</div>

# Abstract

Bridge vibration due to traffic loading has been a subject of extensive research in the last decades. The focus of such research has been to develop solution algorithms and investigate responses or behaviors of interest. However, proving the quality and reliability of the model output in structural engineering has become a topic of increasing importance. Therefore, this study is an attempt to extend concepts of uncertainty and sensitivity analyses to assess the dynamic response of a coupled model in bridge engineering considering time-dependent vehicular loading. A setting for the sensitivity analysis is proposed, which enables performing the sensitivity analysis considering random stochastic processes. The classical and proposed sensitivity settings are used to identify the relevant input parameters and models that have the most influence on the variance of the dynamic response. The sensitivity analysis exercises the model itself and extracts results without the need for measurements or reference solutions; however, it does not offer a means of ranking the coupled models studied. Therefore, concepts of total uncertainty are employed to rank the coupled models studied according to their fitness in describing the dynamic problem. The proposed procedures are applied in two examples to assess the output of coupled subsystems and coupled partial models in bridge engineering considering the passage of a heavy vehicle at various speeds.

# Zusammenfassung

Brückenschwingungen infolge von Verkehrslasten sind seit mehreren Jahrzehnten Gegenstand intensiver Forschung. Im Fokus stand hierbei im Besonderen die Entwicklung von Lösungsalgorithmen zur Ermittlung des dynamischen Bauwerkverhaltens. Begleitet ist diese Entwicklung von der Frage nach der Qualität und Zuverlässigkeit dieser Modelle für den Gebrauch im konstruktiven Ingenieurbau. In diesem Zusammenhang werden in der vorliegenden Arbeit Konzepte der Unsicherheits- und Sensitivitätsanalyse erweitert, um das dynamische Bauwerkverhalten unter Berücksichtigung transienter Fahrzeuglasten bei gekoppelten Modellen des Brückenbaus zu bewerten. Bestehende Sensitivitätsanalysen werden ergänzt, um diese auch unter Berücksichtigung von stochastischen Prozessen durchführen zu können. Die klassische und die erweiterte Methode werden angewandt, um relevante Eingangsparameter sowie Partialmodelle mit wesentlichem Einfluss auf die Varianz der dynamischen Strukturantwort zu identifizieren. Die mit Hilfe der Sensitivitätsanalyse ermittelbaren Kennzahlen können ohne Bezug zu einer Referenzlösung in die Modellbewertung einfließen, allerdings ist es nicht möglich, die Modelle hinsichtlich der realitätsnahen Abbildung des dynamischen Problems zu bewerten. Um dies zu ermöglichen, wurden Konzepte der Gesamtunsicherheit verwendet. Die vorgestellten Methoden wurden auf zwei Beispiele angewandt, um die Ergebnisse von gekoppelten Subsystemen und gekoppelten Partialmodellen des Brückenbaus zu evaluieren. Hierbei handelt es sich um die Überfahrt von schweren Fahrzeugen mit verschiedenen Geschwindigkeiten.

# Contents

# List of Figures

# List of Tables

# Symbols

Symbols which are only used locally are not included.

## *Abbreviations*

| | |
|---|---|
| $BVI$ | bridge-vehicle interaction |
| $DIF$ | dynamic incremental factor |
| $DOF$ | degrees of freedom |
| $MC$ | model choice |
| $MCS$ | Monte Carlo simulation |
| $MQ$ | model quality |
| $MLS$ | moving least squares |
| $PM$ | partial model |
| $POLY$ | polynomial regression surfaces |
| $SA$ | sensitivity analysis |

## *Bridge and Vehicle Dynamics*

| | |
|---|---|
| $c$ | damping of a beam element |
| $c_s$ | damping of the suspension system for 2DOF vehicle model |
| $c_t$ | damping of the tire for 2DOF vehicle model |
| $c_1$ | damping of the tractor front axle suspension system for 8DOF vehicle model |
| $c_2$ | damping of the tractor rear axle suspension system for 8DOF vehicle model |

| | |
|---|---|
| $c_{31}$, $c_{32}$, $c_{33}$ | damping of the semi-trailer tridem axle suspension systems for 8DOF vehicle model |
| $f_{max}$ | a chosen upper frequency of a bridge system |
| $k_s$ | stiffness of the suspension system for 2DOF vehicle model |
| $k_t$ | stiffness of the tire for 2DOF vehicle model |
| $k_{t1}$ | stiffness of the tractor front axle tire for 8DOF vehicle model |
| $k_{t2}$ | stiffness of the tractor rear axle tire for 8DOF vehicle model |
| $k_1$ | stiffness of the tractor front axle suspension system for 8DOF vehicle model |
| $k_2$ | stiffness of the tractor rear axle suspension system for 8DOF vehicle model |
| $k_{31}$, $k_{32}$, $k_{33}$ | stiffness of the semi-trailer tridem axle suspension systems for 8DOF vehicle model |
| $m$ | mass per unit length of a bridge |
| $m_S$ | semi-trailer sprung mass for 8DOF vehicle model |
| $m_T$ | tractor sprung mass for 8DOF vehicle model |
| $m_1$ | tractor front axle mass for 8DOF vehicle model |
| $m_2$ | tractor rear axle mass for 8DOF vehicle model |
| $m_{31}$, $m_{32}$, $m_{33}$ | semi-trailer tridem masses for 8DOF vehicle model |
| $r_i(t)$ | road unevenness underneath the $i^{th}$ axle at instant $t$ |
| $t_d$ | time needed for a load to cross a bridge |
| $v$ | speed of a vehicle |
| $y_b(x_i, t)$ | displacement of the bridge underneath the $i^{th}$ axle at instant $t$ |
| $y_s$ | sprung mass vertical displacement |
| $y_u$ | unsprung mass vertical displacement |
| $y_w(x_i, t)$ | displacement of the vehicle's tire at the $i^{the}$ contact point at instant $t$ |
| $y_S$ | semi-trailer force-aft displacement for 8DOF vehicle model |
| $y_T$ | tractor vertical displacement for 8DOF vehicle model |
| $y_1$ | tractor front unsprung mass vertical displacement for 8DOF vehicle model |
| $y_2$ | tractor rear unsprung mass vertical displacement for 8DOF vehicle model |
| $y_{31}$, $y_{32}$, $y_{33}$ | semi-trailer unsprung masses vertical displacements for 8DOF vehicle model |
| $EI$ | bending stiffness of a bridge cross-section |
| $F^{int}$ | interaction forces between the vehicle and bridge |

| | |
|---|---|
| $F^g$ | forces acting on the bridge independent from the interaction |
| $I_S$ | semi-trailer pitch moment of inertia for 8DOF vehicle model |
| $I_T$ | tractor pitch moment of inertia for 8DOF vehicle model |
| $C_b$ | damping matrix of the bridge |
| $C_b^n$ | generalized damping of the bridge |
| $C_v$ | damping matrix of the vehicle |
| $K_b$ | stiffness matrix of the bridge |
| $K_b^n$ | generalized stiffness of the bridge |
| $K_R^{br}$ | rotational stiffness of elastomeric bearings |
| $K_V^{br}$ | vertical stiffness of elastomeric bearings |
| $K_v$ | stiffness matrix of the vehicle |
| $M_b$ | mass matrix of the bridge |
| $M_b^n$ | generalized mass of the bridge |
| $M_v$ | stiffness matrix of the vehicle |
| $N_{mode}$ | number of mode shapes |
| $N_d$ | number of discretized frequencies used in the realization of a stochastic process |
| $P_b$ | force vector acting on the bridge |
| $P_b^n$ | generalized load |
| $P_v$ | dynamic force vector acting on the vehicle |
| $S_{FF}(\kappa)$ | spacial power spectral density function of road unevenness |
| $S_{FF}(\omega)$ | temporal power spectral density function of road unevenness |
| $\zeta_n$ | damping ratio of $n^{th}$ mode |
| $\theta_S$ | tractor pitch angle for 8DOF vehicle model |
| $\theta_T$ | tractor pitch angle for 8DOF vehicle model |
| $\kappa$ | wavenumber of road unevenness |
| $\kappa_r^{max}$ | largest wavenumber of the road unevenness |
| $\phi_n(x)$ | deflected shape of $n^{th}$ mode |
| $z_n(t)$ | modal contribution of $n^{th}$ mode at instant $t$ |
| $\omega$ | temporal frequency |
| $\omega_l$ | lower cut-off frequency |
| $\omega_n$ | natural frequency of $n^{th}$ mode |

$\omega_u$            upper cut-off frequency

### Assessment

| | |
|---|---|
| $n_s$ | number of supporting points |
| $n_t$ | number of base function in approximation model |
| $n_v$ | number of input parameters |
| $\hat{y}^{poly}$ | polynomial response surface approximation |
| $\hat{y}^{MLS}$ | moving least squares approximation |
| $\hat{y}^{Hybd}$ | hybrid algorithm approximation |
| $E\left(\dots\right)$ | expected value |
| $M_i$ | class of partial models |
| $R^2$ | coefficient of determination |
| $R^2_{cross}$ | predictive coefficient of determination |
| $S_i$ | first order sensitivity index |
| $S_{Ti}$ | total effect sensitivity index |
| $V\left(\dots\right)$ | variance |
| $V(Y)$ | unconditional variance |
| $V(Y\|X)$ | conditional variance |
| $V(E(Y\|X))$ | variance of conditional expectation |
| $X_i^M$ | discrete parameter to activate/deactivate model class $M_i$ |
| $X_i^{MC}$ | discrete parameter to select a model from model class $M_i$ |
| $Y^{ref}$ | assumed reference model |
| $\epsilon^{ref}$ | additive error term |

# Chapter 1

# Introduction

## 1.1 Motivation

Numerical models in structural engineering demands increasingly procedures for model assessment as the models vary in their complexity and the uncertainty accompanying their output. A question concerned with the significance and appropriateness of a model within a set of possible models for the engineering problem arises and attracts further examination and testing. The engineering problem of interest here is the bridge-vehicle interaction. There has been an increasing attention to develop procedures to solve bridge-vehicle interaction problems, which is encouraged by the advent computational power of digital computers and the increasing number and weights of vehicles traveling on bridges. Hence, researchers and modelers had been concerned with deriving solutions of the dynamic problem of bridge-vehicle interaction, for which different models for the vehicle, bridge and solution algorithms have been derived and employed. In examining some of the studies concerned with bridge-vehicle interaction, one can detect attempts, which may be seen as steps of model assessment, such as studies that used measurement data to validate the derived solutions, which is a trivial model validation step. Probabilistic studies had also been employed to assess the effects of random input parameters and road unevenness on the dynamic response using direct comparisons between the obtained output without commenting on its uncertainty, which can indicate model quality. Therefore, it can be said from the above that the limits

of these studies can be pushed further to perform a more detailed analysis in order to assess the model output and its quality.

As mentioned before, there have been initial steps to evaluate the model output, however, they are not clearly established or defined, which justifies the extension, adaptation and derivation of procedures to specifically assess the output quality. Especially, in cases where measurement or reference data are not available, thus, the output quality of the models is examined using the models themselves.

## 1.2 State of the Art

The study is concerned with the assessment of coupled models of bridges considering vehicular loading. The assessment methods need an objective response, therefore the attention is given to the assessment of engineering model as well as the analysis of its output. Hence, the following sections present a brief review on the modeling and the solution procedures of bridge-vehicle interaction, a classification of coupled models in bridges, and a review on general assessment concepts in numerical modeling.

### 1.2.1 Bridge-Vehicle Interaction

The analysis of bridge-vehicle interaction is a special branch of structural dynamics. The interaction forces of a vehicle traveling over a bridge can lead to additional dynamic effects on it. These dynamic effects are governed by the way the bridge and the vehicle interact with each other, which is determined by the inherent frequencies of both subsystems and the driving frequency. The types of bridges studied when observing the traffic are highway or railway bridges. In reviewing the existing research on bridge-vehicle interaction, it is difficult to distinguish between the interaction solutions derived for highway and railway bridges since the general solution algorithms are similar. However, the nature of the excitation of vehicles on highway and railway bridges is different. The characteristics of vehicle movements on highway bridges are of a random nature, whereas a moving train is regarded as a sequence of identical vehicles moving according to a repetitive pattern. These differences would be

included when building the equations of motion for the systems, however, they would not affect the solution algorithm.

Research on the dynamic response of bridges dates back to the mid-nineteenth century. *Willis*(1849) and *Stockes* (1849) investigated the failure of Chaster Rail Bridge in England in 1847. Their investigation was based on modeling a mass moving at a constant speed over the bridge [1]. This investigation was the beginning of a special discipline in bridge and dynamic analysis. Since then, many studies have followed in which variant levels of modeling and different solution algorithms for the dynamic analysis have been used. In addition, there has been a considerable increase in studies on bridge-vehicle interaction solutions in the last two decades. This can be attributed not only to the enhanced computational capacity of digital computers, but also because of the flourishing and demanding transport service in Europe and East Asia. It is difficult to review all the work related to this area of research because the interests behind those studies have been different over the years. The dynamic response of bridges was of the highest priority in the early stages of this area of study, e.g. *Frýba* [2], *Kim and Nowak* [3], as well as others. Then attention was given to safety, ride comfort, and the optimum design of suspension systems, e.g. *Xu and Guo* [4], *Green et al.* [5]. This was followed by studies on the vibrational effects of bridge-vehicle interaction on the surrounding environment and the service components of a bridge, e.g. *Kim et al.* [6]. The following focuses on the different descriptions of the vehicle models and the main solution algorithms of the bridge-vehicle interaction problem.

The vehicle can be modeled in different ways: as a moving load (weight), in which the bridge-vehicle interaction and inertia effects are ignored; as a moving mass, in which the inertia effects are considered; or as a suspended mass, in which the inertia and dynamic characteristics of the vehicle are included in the interaction. A significant amount of research has been done on the vibration of bridges in relation to different models of vehicles. It is only appropriate to cite a few of the more recent studies in this field. The moving weight model is the simplest model that has been used by many researchers in studying the vibration of bridges caused by moving vehicles, e.g., *Weaver et al.* [7], *Wang* [8], *Zheng et al.* [9], and *Rao* [10]. Using the moving weight model, the essential dynamic characteristics of the bridge caused by a moving vehicle is obtained in reasonable modeling and computational efforts, which is advantageous in formulating the relations describing the dynamic effects of

a moving vehicle on a bridge as done by *Pesterev et al.* [11]. When the mass of the vehicle is comparable to the mass of the bridge, its inertial effects are important and included using the mass model of the vehicle, e.g. *Stanišič* [12]. Moreover, *Akin and Mofid* [13] have used the moving mass model to calculate the dynamic response of beams with various boundary conditions. The mass model can then be enhanced by considering the suspension system and the tires of the vehicle. Multiple axle or tractor-trailer trucks can be represented by a number of discrete masses supported by a set of springs and dashpot, e.g. *Humar and Kashif* [14], *Green and Cebon* [15], *Fafard et al.* [16] and in some cases frictional devices can be included in the vehicle model, e.g. *Chatterjee et al.* [17] and *Tan et al.* [18].

Several algorithms have been derived to solve the interaction problem, which can be applied to any of the vehicle models described in the previous studies. *F. Yang et al.* [19] and *Yang et al.* [1] reviewed the different methods with their corresponding mathematical and computational descriptions. The solution of the dynamic response of the bridge and/or the vehicle starts by writing the equations of motion for both subsystems. These equations are either written in an integrated (coupled) form or left separate prior to the solution. The integrated (coupled) equations for the bridge-vehicle interaction are built by substituting for the dynamic interaction forces, e.g. *Cheung et al.* [20]. The coupled set of equations are often solved using direct time integration methods. For the latter, the two sets of differential equations of the vehicle and the bridge are left uncoupled contingent on satisfying the compatibility constraints at the contact points. The solution of the differential equations can be also determined by using direct integration methods in an iterative or non-iterative procedure, e.g. *F. Yang et al.* [19] and *Liu et al.* [21], respectively. However, there are other methods for solving the dynamic problem. For example, the bridge-vehicle interaction can be solved by using the dynamic condensation method to eliminate all degrees of freedom associated with the vehicle to the element level of the beam. This solution is quite efficient if the bridge response is of interest, *Garg and Dukkipati* [22], *Yang and Lin* [23], *Wu and Yang* [24]. Another method is to solve the equations of motion in the frequency domain, e.g. *Green and Cebon* [15], *Zhu et al.* [25].

Another concern related to the bridge-vehicle interaction is the inclusion of road unevenness in the dynamic analysis since it can significantly affect the bridge response. Road unevenness is often obtained by measuring the existing roadways, which is a laborious procedure.

Therefore, *Dodds and Robson* [26] suggested simplified means to describe the unevenness of road surfaces. They came up with a treatment of road unevenness as a realization of a stationary Gaussian homogeneous random process described by its power spectral density function (PSD) in the space domain. The work of *Dodds and Robson* [26] has served as the basis for the ISO 8608 standards [27], which classifies the roadway profiles into classes according to their degree of roughness. The realization of road profiles is often obtained as a series of cosine terms with random phase angles. Methods similar to those mentioned above have been widely adopted by researchers in studying the bridge-vehicle interaction in relation to road unevenness, e.g. *Inbanathan and Wieland* [28], *Coussy et al.* [29], *Hwang and Nowak* [30], and *Henchi et al.* [31]. Moreover, road unevenness can be treated as one component in describing the initial road conditions. Potholes and bumps can be included in the road profile as local irregularities to examine their influence on the dynamic response. Moreover, with regard to reinforced concrete beam bridges in particular, long-term deflections, which could have an influence on bridge response due to vehicles traveling on it, can be considered in the dynamic analysis.

The superstructure of highway beam or girder bridges are often supported by elastomeric bearings, which affect the dynamic responses when considering bridge-vehicle interaction. Most researchers study the elastomeric bearing as an element of its own, the investigation of which can be based on either theoretical or experimental concepts, e.g. *Chang* [32] and *Warn et al.* [33], respectively. Few researchers study the behavior of elastomeric bearings when integrated in the bridge structure and investigate the dynamic behavior of elastically supported beams subjected to moving vehicles. Kawatani et al. [34] performed a three-dimensional analysis, which examines the dynamic response of bridges due to moving vehicles when steel bearings are replaced with elastomeric bearings. The authors noticed that the use and modeling of elastomeric bearings for the bridge system studied did not significantly change the system's resonant frequencies. Moreover, the inclusion of bearings in the dynamic analysis resulted in larger displacements, especially the horizontal displacements in the direction of the bridge's main axis. *Kim et al.* [6] performed a vibrational analysis of a two-girder steel bridge supported by elastomeric bearings. The authors concluded that the traffic-induced accelerations and dynamic reaction forces of the bridge when considering the elastomeric bearings were greater than those of the bridge with pin bearings.

Further, *Yau et al.* [34] showed that the insertion of elastic bearings at the supports of the single-span beam to isolate earthquake forces may adversely amplify the dynamic response of the beam to moving loads; it was determined that this observation depends on the speed of the vehicle. In the aforementioned studies, the elastomeric bearings were modeled as independent linear springs in vertical, horizontal, and lateral directions depending on the dimensionality of the bridge model. Hence the interaction between the deformations and forces in the different directions of the elastomeric bearing were not considered. *Vogt and Freundt* [35] proposed an element to model the bearing, which is able to map the interaction between the vertical, horizontal, and rotational forces. The authors concluded that using a combination of independent springs to represent the elastomeric bearings is sufficient when the global response of the bridge is of interest.

Most of the investigations carried out in this discipline were based on deterministic values of the system's input parameters, even though they intrinsically contain randomness, such as the parameters of the vehicle; suspension stiffness and damping, may vary with respect to the nominal value due to production tolerances and/or wear, aging, etc., as mentioned by *Gao et al.* [36]. In addition, the random vibration of a vehicle due to road unevenness was often examined for passenger comfort checks, road deterioration studies, or for designing an optimum suspension system for the vehicle, which was studied numerous times by *Cebon* [37]. Extending the analysis to investigate the dynamic response of a bridge structure while a vehicle is passing, in which not only the randomness of road unevenness is considered, but the randomness of a vehicle's input parameters as well, is a current area of research. A number of researchers have studied this problem. *Hwang and Nowak* [30] presented a procedure to calculate statistical parameters for the dynamic loading of bridges. These parameters were based on surveys and tests and included vehicle mass, suspension system, tires and road roughness, which were simulated by stochastic processes. *Kirkegaard and Nielsen* [38, 39] studied the randomness of vehicle input parameters and the randomness of road unevenness in two separate studies. One conducted for vehicle input parameters and the other for the effects of random road profiles on the dynamic response of highway bridges. Further, *González et al.* [40] investigated the critical speed for trucks moving on bridges with a smooth road surface. The authors investigated a dashpot truck on a relatively smooth surface and performed a full probabilistic study considering random input variables

of the vehicle and random road profiles to validate the results obtained from the moving weights model. Moreover, solutions for the statistical characteristics of a bridge's response to the passage of a vehicle over a random rough surface have been of interest in a number of research works, such as *Lin et al.* [41], *Lombaert and Conte* [42], and *Wu and Law* [43]. More recently, *N. Liu et. al.* [44] considered both the randomness of the vehicle input parameters and road unevenness, and calculated the statistical characteristics of the bridge response by using the random variable functional moment method.

In general, one of the main methods used in the dynamic analysis of structures with random parameters is the Monte Carlo simulation (MCS). *Shinozuka and Deodatis* [45] advocated the use of MCS to solve both the random vibration and system stochasticity problems. They maintain that the MCS gives accurate results for any problem, linear or nonlinear, stationary or non-stationary, as long as its analytical or numerical solution is known.

The dynamic response of the bridge is usually studied and quantified by a magnification factor for engineering design purposes. This factor is applied to the static loading to take into account the additional effects due to the transient nature of the loading. *Paultre et. al.* [46] give an extended review on the theoretical and experimental studies on this factor, which is also known as a dynamic amplification factor, dynamic impact factor, or dynamic incremental factor, depending on the definition used. The authors discuss the wide spectrum of variation in the values of this factor with respect to different bridge systems, vehicle models and response measures used in the dynamic analysis.

### 1.2.2   Couplings in Bridge Engineering

The coupling in this study is classified according to a coupling of subsystems and a coupling of partial models. This is done merely for convenience in presenting the output of the assessment procedures. A bridge superstructure, a bridge substructure, and a vehicle are considered subsystems; the bridge-vehicle interaction solution algorithm is considered a coupling between the superstructure and the vehicle, whereas a bearing is a coupling element between the superstructure and the substructure. Thus, the modeling of bridge-vehicle interaction and elastomeric bearings is categorized as a coupling of subsystems. On the other

hand, the creep model of concrete or the dynamic loading of a heavy vehicle, among others, can be denoted as a partial model. Therefore, the consideration of long-term deflections as an excitation for a vehicle traveling over a bridge can be categorized as a coupling of partial models, which are the dynamic loading model and the material model of creep. As mentioned above, this classification is for convenience only and not meant to imply that these definitions are fundamentally fixed.

### 1.2.3   Concepts of Assessment

*"While the world and the model are each internally entailed, nothing entails the world with the model."*

Robert Rosen

The statement above simply states that the portion of the world captured by the model is an arbitrary "enclosure" of an otherwise open and interconnected system, *Saltelli et al.* [47]. Therefore, engineers "Modelers" accept the fact that several models may be compatible with a specific set of data. Moreover, these models indicate different levels of complexity in their structure and the parameters included in their description. The complexity of the models can be tested against Occam's razor principle. This principle generally recommends the simplest explanation when facing two theories with the same predictions. These notions have raised the level of awareness with regard to the study of model assessment, which has been an attractive area of research in recent years. Model quality and assessment studies have become popular as the practice of building numerical models for engineering problems has had to deal with the challenge of having to prove the quality of a model with or without measurement data.

One kind of trivial quality assessment is to compare the model output with analytical or benchmark solutions, which controls the model's output to the limits of the reference solution. Therefore, another reference solution is required outside of these limits. Such a procedure is not practical because engineering applications tend to be diverse, complicated and have varying temporal and spatial domains of application, *Babuska and Oden* [48]. Another concept uses model error estimators to quantify the error resulting from simplification

of a model, *Oden and Prudhomme* [49]. The size of this error term may justify the use of complex models over simpler ones and vice versa. Therefore, these error terms can be viewed as a model assessment. However, such estimators do not assess the model as an abstraction of a system or a phenomenon, therefore, further investigations would be needed.

It is worth mentioning that the models assessed are data dependent. The data in this context includes information on the physical environment of the event to be depicted by the model, e.g., geometric information and physical parameters. The form in which the data occurs may be deterministic or statistical. The model and the data are thus always related. In other words, the use of the model will take the nature of the data into account. Further, when different models are used to represent the same system or phenomenon, the model should cover the underlying systems or phenomenon and additional over-parameterizations must be avoided. To address the issue of over-parametrization, uncertainty and sensitivity analyses can be employed.

Uncertainty is the acknowledgment of the existence of more possibilities, therefore, it is inevitably involved in assessing the plausible models created for a system or phenomenon. In order to investigate uncertainties, one requires a clear understanding of their different types. *Zio and Apostolakis* [50] reviewed the different taxonomies of uncertainty. They state that it is useful to classify uncertainties as being aleatory or epistemic. This does not imply that other terminologies are fundamentally different types of uncertainties. An aleatory uncertainty is a type of uncertainty, which is a result of a random or stochastic variability of a phenomenon and is contained in the formulation of the model, it can be known also as stochastic uncertainty. Epistemic uncertainty represents our knowledge regarding the numerical values of the parameters and the validity of the model's assumptions, and is also known as state-of-knowledge uncertainty. Furthermore, parameter uncertainties are represented by epistemic probability distribution functions. A separation between the model and parameter uncertainties is viable in assessment practice.

Sensitivity analysis is the study of how uncertainties in the output of a model are apportioned to different sources of input parameter uncertainties. The reasons for running a sensitivity analysis can be to prioritize the research by identifying and ranking the input parameters and their underlying systems or phenomena, to simplify a model by fixing input parameters

that do not influence the output uncertainty, or to identify the interactions between inputs and how they affect the output uncertainty. Therefore, different settings guided by the rationale for the sensitivity analysis can be proposed and used in obtaining the adequate results. There are various methods for performing a sensitivity analysis, such as scatter plots, derivatives, regression coefficients, or variance-based measures. *Helton et al.* [51] and *Saltelli et al.* [47] give an overview for the different methods.

One cannot discuss model assessment and quality without mentioning model ranking and selection, which has drawn attention to adjustment factor formulation and Bayesian model class selection. The adjustment factor formulation needs a reference model to be identified and its prediction to be modified through an adjustment factor that accounts for the uncertainty in the models, e.g. *Zio and Apostolakis* [50], while the Bayesian model class selection amounts to constructing a suitable set of plausible models and evaluating their parsimony. *Akaike* [52] proposes an estimate called the minimum information theoretic criterion (AIC), which is defined as the mean log-likelihood. It provided a mathematical formulation of the principle of parsimony in the field of model construction. Furthermore, *Schwarz* [53] proposes the selection of one model from a set of models with different dimensions by finding the Bayes solution for them. The Bayesian approach to model selection has been further developed in the last two decades, which has led to deriving more quantitative expressions of the principle of model parsimony, e.g. *Gull* [54], *Mackay* [55], *Sivia* [56], and *Beck and Yuen* [57].

## 1.3 Objective of Study

The current area of research for bridge-vehicle interaction is often not concerned with the aforementioned concepts of model assessment. Since state-of-the-art of the bridge-vehicle interaction is focused on developing and validating solutions for the dynamic problem to be used for design or prediction purposes later on, hence a detailed explanation of the dynamic responses and patterns obtained requires further examination. Moreover, a viable question concerns how the model itself can be exploited to assess its quality before moving on to validation using benchmarks or measurement data is raised.

The main objective of this study is to find expressions and measures that can help to study and assess the output of models, which considers bridge-vehicle interaction and support the choice to derive such models knowing their inherent output uncertainty. The dynamic responses of highway beam bridges (pinned or elastically supported) subjected to the passage of a heavy vehicle and considering the conditions of roadways are the scenarios under study. The variances of the dynamic responses are used as an indicator for their quality.

## 1.4   Contribution of the Thesis

It is also worth mentioning that the tested models ensure convergence and robustness, therefore these will not be tested in this study.

This study contributes to the current research area of the dynamic problem as follows:

- Concepts of sensitivity analysis are used to detect the influential inputs on the dynamic output. This detection is quantified by using measures of sensitivity indices. A setting for the sensitivity analysis is proposed to enable the examination of random stochastic processes of road profiles. The classical and proposed settings are used to quantify the subsystem's contribution to the variance of the output of the coupled subsystems

- Meta-models are developed to map the input-output relationship since the computational cost influences the numerical analysis. The hybrid meta-model of polynomial regression and moving least squares is developed to capture efficiently the input-output relationship, which has different patterns and localities depending on the inputs

- Concepts of total uncertainty are used to rank the models studied according to their fitness in describing the engineering problem. Total uncertainty represents the sum of the input uncertainty and the model uncertainty. A mathematical expression for the model uncertainty is derived by using the adjustment factor approach formulations. The model uncertainty can be estimated as the difference between the average of a single model and the average of an adjusted response

- A further extension of the sensitivity analysis is used to identify the influence that the partial models have on the dynamic response by introducing an input parameter representing the choice of a model within a global one.

- For the engineering problem investigated, the dynamic estimates of the displacements, strains, and normalized accelerations of the bridge system are thoroughly examined in order to explain some of the patterns observed for the responses, which serves as means of a better understanding of the dynamic problem and the output of a probabilistic study

## 1.5 Outline

The text of the dissertation has six main parts, which are presented in Chapters 2-7. The assessment procedures based on the sensitivity and uncertainty analyses are found in Chapter Two; their algorithms and detailed aspects of their implementation are described and explained. Chapter Three addresses the dynamic problem and its modeling possibilities. Since experimental data are not used in this study, a validation example using numerical and analytical solutions for the dynamic problem has been used and presented in Chapter Three. The modeling and assessment procedures presented are used in the application examples in Chapters Four, Five and Six. The first example in Chapters Four and Five focuses on the coupling of subsystems in bridges, i.e., bridge-vehicle interaction. In Chapter Four a general dynamic analysis is performed and a thorough examination of the dynamic responses is presented. In Chapter Five, sensitivity and uncertainty analyses are used to identify the influential input parameters on the dynamic response, and the different descriptions of the models of coupled subsystems are ranked using their total uncertainty. Chapter Six tackles the assessment of the dynamic response for coupled partial models, i.e. the dynamic loading model of a vehicle and the material model of creep. Finally, Chapter Seven deals with the conclusions derived from the results obtained from the examples of the dynamic problem. Further recommendations and the possible extension of the study are also discussed in the same chapter.

# Chapter 2

# Assessment Methods

## 2.1 Introduction

Computer-based models can be used to approximate real life processes. These models are usually based on mathematical equations, which are dependent on several variables. Therefore, the predictive capability of models is limited by the assumptions used to build the mathematical equations and the uncertainty in the value of the input variables, among others.

There is a demand for procedures that can serve as guidelines for drawing conclusions and assessing the quality of prognosis of engineering models. Assessments based on methods of uncertainty and sensitivity analyses are significant since they are generic in application. Such procedures are employed to rank input parameters and modules in order to identify the main contributors to the uncertainties of model or coupled model predictions (prognoses), as well as to identify priorities for further investigation and use.

### 2.1.1 Uncertainty Analysis

The input parameters of models are not always known with sufficient certainty. Input uncertainties are caused by natural variations and/or uncertainties in the measurements. The uncertainty of the input parameters is often expressed in terms of the assumed probability

distributions. Further, the engineering models using these input parameters are assumed to be deterministic, which means the same output is retrieved for the same input data for any number of runs. Therefore, the uncertainty of the model prognosis stems from the propagation of the uncertainty of the input parameters through the model. It can be deduced from the above that the analysis is performed to assess the uncertainty in the model output that originates from the uncertainty of the input parameters. Uncertainties stemming from a lack of knowledge or abstractions and assumptions in building the model are yet to be included [58–60].

### 2.1.2 Sensitivity Analysis

*Saltelli* states that "sensitivity analysis (SA) is the study of how the variation in the output of a model (numerical or otherwise) can be apportioned, qualitatively or quantitatively, to different sources of variation, and how the given model depends upon the information fed into it" [61].

Sensitivity analysis aims at determining how sensitive the model output is to changes in the model input. The simplest formulation of the sensitivity analysis is the partial derivative of the output function with respect to input parameters. This sensitivity measure is computed numerically by varying the input parameters around their nominal values. Such measures that capture the local impact of input parameters on the model output are called local sensitivity indices. For complex engineering models where interactions may exist, a global sensitivity analysis is needed; sampling-based methods are developed and used for such an analysis [60, 61]. Further, the term input of a model in the sensitivity analysis stands for any quantity that can be changed in the model prior to its execution, thus, an input may be an input parameter or a module.

## 2.2 Monte Carlo Simulation

Monte Carlo (MC) methods are algorithms for solving various kinds of computational problems by using random numbers. It includes techniques of statistical sampling, which are

used to estimate solutions, e.g., mean values or variances for a model prognosis. It is a straight-forward approach for solving uncertainty analysis problems, which has been utilized for dealing with the problem of random input parameters and processes [62]. A Monte Carlo simulation is based on performing multiple model evaluations with probabilistically selected inputs. The results of these evaluations can be used to determine the uncertainty of the model output.

The sampling procedure used in this study is Latin Hypercube Sampling (LHS), which is designed to accurately recreate the input distribution through sampling in fewer iterations compared with the simple random sampling. LHS is a so-called "stratified sampling" technique, whereby random variable distributions are divided into equal probability intervals. It is equivalent to a uniform sampling from the quantiles of the distribution [63, 64].

The sampling starts by generating a normally distributed sample with a mean value of zero and a standard deviation of one, and then using its cumulative distribution function (CDF) to create the sample being sought, which is described by its distribution and probabilistic characteristics.

The main steps for obtaining the output used in the uncertainty and sensitivity analyses are:

1. For a defined model $f$ with input parameters $x_i$, $i = 1, \ldots, k$ and the output $y$. The ranges and distributions are selected for each input parameter. These $k$ distributions characterize the input uncertainties. The choice of these distributions is of significance as it may affect the results obtained from the sensitivity analysis.

2. Samples, $\mathbf{X} = X_1, X_2, \ldots, X_k$, which correspond to the distributions defined in the previous step are generated. These samples are presented in a matrix, with $k$ input parameters and $N$ samples and is expressed as

$$\mathbf{X} = \begin{bmatrix} x_{11} & x_{12} & \ldots & x_{1k} \\ x_{21} & x_{22} & \ldots & x_{2k} \\ \vdots & \vdots & \ddots & \vdots \\ x_{N1} & x_{N2} & \ldots & x_{Nk} \end{bmatrix}$$

3. The model is evaluated $N$ times, once for each row of the sample matrix, creating a mapping in the input-output space. The output produced computes the following:

$$\mathbf{Y} = f(\mathbf{X}_1, \mathbf{X}_2, \ldots, \mathbf{X}_k)$$

4. The uncertainty of the output can then be calculated as the variance, the standard deviation, or the coefficient of variation.

5. The mapping between $\mathbf{Y}$ and $\mathbf{X}$ is used for performing a sensitivity analysis using variance-based procedures to qualitatively and quantitatively study the importance and contribution of the inputs to the uncertainty of the output.

## 2.3   Probability Distribution

In this section, an elementary theory for probability distributions and essential moments are described [65]. The distributions used in this study are also briefly explained.

When studying an uncertain input parameter $x$, the cumulative distribution function $\Phi(x)$ (CDF) gives the probability $P$ that the variable $X$ will be less than or equal to $x$, which is expressed as:

$$\Phi(x) = P(X \le x)$$

The CDF is always non-decreasing with $\Phi(x) = 0$ at $x = -\infty$ and $\Phi(x) = 1$ at $x = \infty$.

The uncertainty of the input parameters is described with the probability density function (PDF). The PDF is described as the first derivative of the CDF, as shown below:

$$\phi(x) = \frac{d}{dx}\Phi(x)$$

The PDF is zero or positive since the first derivative of a non-decreasing curve is always non-negative.

The expected value of random variable $X$ is denoted either as $\mu$ or $E(X)$, the mean or average, and expressed as:

$$E(X) = \int_{-\infty}^{\infty} x\phi(x)$$

The variance of a random variable $X$ is denoted as $\sigma^2$ or $V(X)$:

$$V(X) = \int_{-\infty}^{\infty} (x - \mu)^2 \phi(x) dx$$

The positive square root of the variance is the standard deviation $\sigma$.

The above are the formulations from the continuous probability theory. In the case of discrete probability distribution, the mean and the variance are computed using the sums instead of the integration, as shown below:

$$
\begin{aligned}
E(X) &= \sum_{i=1}^{\infty} x_i f_i(x) \,, \\
V(X) &= \sum_{i=1}^{\infty} (x_i - \mu)^2 f_i(x)
\end{aligned}
$$

where $f_i(x)$ is the probability associated with the possible value $x_i$.

**Normal (Gaussian) distribution**

The normal distribution is probably the most frequent distribution used in probability theory. Its popularity comes from the fact that many natural phenomena are believed to follow a statistically normal distribution. The PDF of this distribution is presented in Figure 2.1 and is expressed as follows:

$$\phi(x) = \frac{1}{\sigma\sqrt{2\pi}} e^{-\frac{1}{2}\left(\frac{x-\mu}{\sigma}\right)^2}$$

**Log-normal distribution**

In a like manner, many natural phenomena also occur according to the log-normal distribution. This distribution is often used to model quantities or variables, which cannot be

negative. The log-normal PDF is plotted in Figure 2.1 and is evaluated as

$$\phi(x) = \frac{1}{x\sigma\sqrt{2\pi}}e^{-\frac{1}{2}\left(\frac{log(x)-\mu}{\sigma}\right)^2}$$

**Extreme value distribution**

Extreme value theory has been applied in various fields, from the environmental sciences to financial econometrics. The salient feature of the extreme value analysis is to assess the extremal behavior of random variables.

The PDF of the extreme value distribution type I, which is also known as Gumbel, is depicted in Figure 2.1 and it expressed as:

$$\phi(x) = \frac{e^{(\alpha-x)/\beta - e^{(\alpha-x)/\beta}}}{\beta},$$

where $\mu = \alpha - \gamma\beta$, $\sigma = \beta\pi/\sqrt{6}$, and $\gamma$ is Euler-Mscheroni constant.
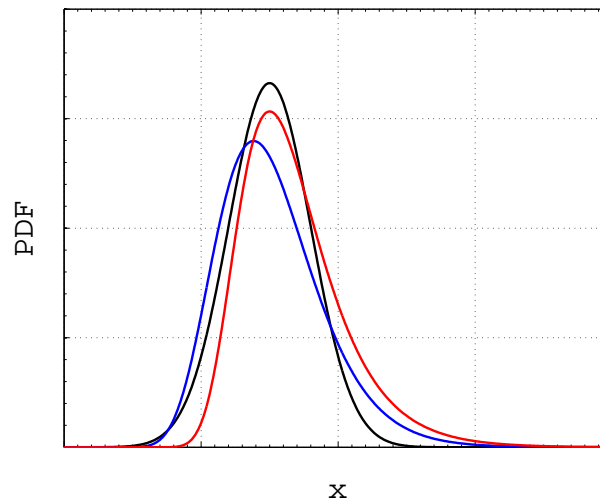


FIGURE 2.1: Probability distribution function: (—) Normal, (—) Log-Normal, (—) Extreme Value Type I

The uncertainties of the input parameters of the engineering problem examined are assumed to follow normal and log-normal distributions. The output of interest is the maximum response of the dynamic problem and thus follows an extreme value distribution type I, which is verified by its likelihood estimates.

## 2.4 Model Assessment

### 2.4.1 Variance-Based Methods for Sensitivity Analysis

As mentioned before, sensitivity analysis is the study of how uncertainties in the output of a model are apportioned to the uncertainties of the inputs. Variance-based methods have been chosen for this study since they are independent from the model investigated, the interactions between input parameters or modules can be considered, and the effects of groups or sets of input parameters may be examined. Moreover, such sensitivity analysis provides the importance ranking of the input parameters, and quantifies their contribution to the output uncertainty [61].

Only a number of input parameters are chosen for the sensitivity analysis performed. Information fed into the model, e.g., physical or mathematical constants, internal model variables (e.g., number of discretized elements or time step) are disregarded. In other words, such inputs are not allowed to vary, therefore, they do not contribute to the variation of the output. The risk that the assigned time step used in the dynamic analysis could be large enough to have a dramatic influence on the output exists and should be kept to minimum for a reliable analysis. This is why it is important to be as objective and careful as possible in the setting and choice of the input parameters for the analysis.

In general, the more variables considered in the analysis, the greater the variance of the model prediction. This could lead to a situation, in which the prediction varies so greatly that it would not be of practical use. However, this is not an absolute fact since in some cases the increasing number of input parameters does not lead to increased variance in model prediction. As key parameters (key players) dominate in the sensitivity analysis and create almost all the uncertainty of the output. Hence, if the key factors have been carefully chosen, adding further variables to the analysis contribute to its totality without increasing the variance of the output.

The main idea of variance-based methods is to estimate the amount of variance that would disappear if the true value of the input parameter $X_i$ is known. This can be described by the conditional variance of $Y$ fixing $X_i$ at its true value $V(Y|X_i)$, and is obtained by varying

over all parameters, except $X_i$. Since the true value of $X_i$ in complex engineering problems is unknown, the average of the conditional variance for all possible values of $X_i$ is used, i.e. $E(V(Y|X_i))$. Having the unconditional variance of the output $V(Y)$ and the expectation of the conditional variance $E(V(Y|X_i))$, the following relation holds:

$$V(Y) = V(E(Y|X_i)) + E(V(Y|X_i)), \tag{2.1}$$

Equation (2.1) is often known as the law of total variance and can be proved as the following: The variance $V(Y)$ can be defined as [66]:

$$V(Y) = E(Y^2) - (E(Y))^2 \tag{2.2}$$

Hence, the conditional variance $V(Y|X)$ can be written as:

$$V(Y|X) = E(Y^2|X) - (E(Y|X))^2 \tag{2.3}$$

Knowing that $E(E(Y|X)) = E(Y)$ thus $E(V(Y|X))$ can be derived as:

$$\begin{aligned} E(V(Y|X)) &= E\left(E(Y^2|X)\right) - E\left((E(Y|X))^2\right), \\ &= E(Y^2) - E\left((E(Y|X))^2\right) \end{aligned} \tag{2.4}$$

The variance of the expected value $V(E(Y|X))$ can be written following Equation (2.2) as:

$$\begin{aligned} V(E(Y|X)) &= E\left((E(Y|X))^2\right) - (E(E(Y|X)))^2, \\ &= E\left((E(Y|X))^2\right) - (E(Y))^2 \end{aligned} \tag{2.5}$$

Taking the sum of $E(V(Y|X))$ expressed in Equation (2.4) and $V(E(Y|X))$ expressed in Equation (2.5) results in $V(Y)$ as in Equation (2.1).

$$E(Y^2) - E\left((E(Y|X))^2\right) + E\left((E(Y|X))^2\right) - (E(Y))^2 = E(Y^2) - (E(Y))^2 = V(Y) \tag{2.6}$$

From Equation (2.1) the variance of the conditional expectation $V(E(Y|X_i))$ is determined. This term is often referred to as the main effect, as it estimates the main effect contribution

of the $X_i$ to the variance of the output. Normalizing the main effect by the unconditional variance $V(Y)$ results in:

$$S_i = \frac{V(E(Y|X_i))}{V(Y)} \tag{2.7}$$

The ratio $S_i$ is known as a first order sensitivity index [67], which is also known as the importance measure [68]. It is expected that the larger $V(E(Y|X_i))$ is, the more influential the input parameter $X_i$ is. The value of $S_i$ is less than 1. In addition, the sum of all first order indices corresponding to multiple input parameters is an indicator of the additivity of the model. The model is considered additive when the sum equals one (no interactions between the input parameters), and non-additive when the sum is less than one. Hence, the difference $1 - \sum S_i$ is an indicator of the presence of interactions between the input parameters. For example, the interaction between two parameters $X_i$ and $X_j$ on the output $Y$ in terms of conditional variance is expressed as:

$$V_{ij} = V(E(Y|X_i, X_j)) - V(E(Y|X_i)) - V(E(Y|X_j)), \tag{2.8}$$

where $V(E(Y|X_i, X_j))$ describes the joint effect of the pair $(X_i, X_j)$ on $Y$. This is known as a second order effect. Higher order effects can be computed in a like manner. The total effect index $S_{Ti}$ is used to represent the total contribution of the input parameter $X_i$ to the output, i.e. the first order effects, in addition to all higher order effects. A total effect index is defined as:

$$S_{Ti} = 1 - \frac{V(E(Y|X_{\sim i}))}{V(Y)}, \tag{2.9}$$

where $V(E(Y|X_{\sim i}))$ is the variance of the expected value of $Y$ when conditioning over all except for $X_i$ and $V(Y)$ is the unconditional variance of $Y$. The difference $S_{Ti} - S_i$ is a measure of how much $X_i$ interacts with other input parameters.

### 2.4.1.1 Settings for the Sensitivity Analysis

For the engineering problem at hand, different sensitivity tests can be applied depending on the goal of the analysis. Since the assessment of numerical models is the objective of this study, sensitivity analysis is used to give a better understanding of the contribution of input parameters or groups of input parameters and, consequently, of their underlying phenomena

or module to the uncertainty of the model response. The power of such an analysis can be attributed to the fact that the model itself is exercised, therefore, measurements or reference models are not needed. Furthermore, its implementation and simulation can be done regardless of the model type. As long as the input-output mapping is available, the analysis can be performed. The following settings are used for the engineering problem covered in this study:

- The first setting performs the classical sensitivity analysis for all chosen input parameters directly on the run samples of the model for all the input parameters selected [61]. The aim is to detect and rank the contribution of the input parameters in relation to the variance of the output.

- The second setting is proposed counter to the known "factor fixing" setting in variance-based methods. In "factor fixing" setting, a non-influential parameter is fixed at any value of its range of variance as this does not compromise the model prediction. The proposed setting averages the prediction over the influential processes, conducts the sensitivity analysis on the average prediction and investigates the corresponding results. This setting is used to include the influence of random stochastic processes on the dynamic response. The setting is facilitated through the introduction of sub-sampling. For a single sample of input parameters, i.e., vehicle input parameters, a set of random processes is sub-sampled. For the $(j^{th})$ sample of input parameters, $(n)$ number of processes are sub-sampled. Then an average value of the run response is attributed to the $(j^{th})$ sample, as shown below:

$$
\begin{bmatrix} X_1^j & X_2^j & \cdots & X_m^j \end{bmatrix} \rightarrow \begin{pmatrix} f_1^j(t) \\ f_2^j(t) \\ \vdots \\ f_n^j(t) \end{pmatrix}
$$

#### 2.4.1.2 Estimation of Sensitivity Indices

A sampling based numerical procedure is employed to compute first order and total effect indices for a model of $k$ input parameters [47]. This procedure is thought to be benignant

and best suited to estimate sensitivity indices that are based only on model evaluations. An explanation of the general sampling procedure has been given in Section 2.2. The following are more detailed steps in building the required input samples:

- Two matrices for $k$ random input parameters are generated and called the base samples. The number of the generated samples $N$ in each matrix can range from hundreds to thousands depending on the model studied and the level of reliability required for the results. These matrices are depicted as:

$$
\mathbf{X}^A = \begin{bmatrix}
x_{11}^A & x_{12}^A & \cdots & x_{1i}^A & \cdots & x_{1k}^A \\
x_{21}^A & x_{22}^A & \cdots & x_{2i}^A & \cdots & x_{2k}^A \\
\vdots & \vdots & \ddots & \ddots & \vdots & \vdots \\
x_{N1}^A & x_{N2}^A & \cdots & x_{Ni}^A & \cdots & x_{Nk}^A
\end{bmatrix}
$$

$$
\mathbf{X}^B = \begin{bmatrix}
x_{11}^B & x_{12}^B & \cdots & x_{1i}^B & \cdots & x_{1k}^B \\
x_{21}^B & x_{22}^B & \cdots & x_{2i}^B & \cdots & x_{2k}^B \\
\vdots & \vdots & \ddots & \ddots & \vdots & \vdots \\
x_{N1}^B & x_{N2}^B & \cdots & x_{Ni}^B & \cdots & x_{Nk}^B
\end{bmatrix}
$$

- The matrix $\mathbf{X}^{C_i}$ is built from the base matrices, where all columns are retrieved from $\mathbf{X}^A$ except for the $i^{th}$ column, which is retrieved from $\mathbf{X}^B$, as shown below:

$$
\mathbf{X}^{C_i} = \begin{bmatrix}
x_{11}^A & x_{12}^A & \cdots & x_{1i}^B & \cdots & x_{1k}^A \\
x_{21}^A & x_{22}^A & \cdots & x_{2i}^B & \cdots & x_{2k}^A \\
\vdots & \vdots & \ddots & \ddots & \vdots & \vdots \\
x_{N1}^A & x_{N2}^A & \cdots & x_{Ni}^B & \cdots & x_{Nk}^A
\end{bmatrix}
$$

- The model output for all the input values of sample matrices $\mathbf{X}^A$, $\mathbf{X}^B$ and $\mathbf{X}^{C_i}$ are run to obtain the output vectors $\mathbf{Y}_A$, $\mathbf{Y}_B$, $\mathbf{Y}_{C_i}$.

The evaluation of the sensitivity follows one of the early studies of *Sobol* [67], in which the sensitivity indices are estimated as correlation coefficients; the first order index for input

factor $x_i$ is computed as:

$$S_i = \frac{\mathbf{Y}_A^T \mathbf{Y}_{C_i} - N(\overline{Y}_A \overline{Y}_{C_i})}{\mathbf{Y}_A^T \mathbf{Y}_A - N(\overline{Y}_A)^2} \tag{2.10}$$

Furthermore, the total effect index is estimated as:

$$S_{Ti} = 1 - \frac{\mathbf{Y}_B^T \mathbf{Y}_{C_i} - N(\overline{Y}_B \overline{Y}_{C_i})}{\mathbf{Y}_B^T \mathbf{Y}_B - N(\overline{Y}_B)^2}, \tag{2.11}$$

where $\overline{Y}_{\cdots}$ is the mean value of the output.

The estimations in Equations (2.10) and (2.11) have a different second term in the numerator when compared with the estimations of the sensitivity indices documented in *Saltelli et al.* [47]. A simplification is introduced to the estimates presented by [47] assuming $\overline{Y}_A = \overline{Y}_{C_i}$ and $\overline{Y}_B = \overline{Y}_{C_i}$. This assumption is justified by running a very large number of samples for the sensitivity analysis. However, Equations (2.10) and (2.11) are more reliable in their estimates with a smaller number of samples run.

In the cases where the sensitivity analysis is performed for groups of related input parameters, the formulation of the $\mathbf{X}^{C_i}$ matrix is slightly adapted. Multiple columns corresponding to the group of the related input parameters are treated as a block and moved together when creating $\mathbf{X}^{C_i}$. The procedure to estimate the sensitivity indices is not affected and these indices indicate the effect of the group of the realted inputs on the variance of the output.

$$\mathbf{X}^{C_i} = \begin{bmatrix} x_{11}^A & x_{12}^A & \cdots & x_{1(i-1)}^B & x_{1i}^B & x_{1(i+1)}^B & \cdots & x_{1k}^A \\ x_{21}^A & x_{22}^A & \cdots & x_{2(i-1)}^B & x_{2i}^B & x_{2(i+1)}^B & \cdots & x_{2k}^A \\ \vdots & \vdots & \ddots & \vdots & \vdots & \vdots & \ddots & \vdots \\ x_{N1}^A & x_{N2}^A & \cdots & x_{N(i-1)}^B & x_{Ni}^B & x_{N(i+1)}^B & \cdots & x_{Nk}^A \end{bmatrix}$$

$$\underbrace{\qquad\qquad\qquad\qquad}_{\text{input parameters handled as one group}}$$

The main drawback of variance-based methods is the need for a large number of samples in order to get reliable results when sampling methods are used to estimate $S_i$ and $S_{Ti}$. The high computational cost of every simulation, as well as the large number of random parameters and processes may prove to be more problematic than expected for complex engineering problems. Therefore, meta-modeling is used for the input-output mapping.

## 2.4.2 Aid tool: Meta-Modeling

The meta-models presented are classified into two types depending on the nature of their input-output mapping. Polynomial regression models are treated as global approximation models, whereas moving least squares and the proposed hybrid algorithm are considered to be local approximation models. The sensitivity analysis is performed on the meta-models, therefore, attention has been given to the derivation of such models. The following is a description of the meta-models used in the analysis.

### 2.4.2.1 Polynomial Response Surface

Polynomial response surface modeling is one of the popular approximation models in engineering applications due to its simplicity and ease of implementation. Most of the engineering problems are complex in nature, therefore, they require multidimensional polynomial base functions, such linear, quadratic, and mixed terms, e.g.,

$$\mathbf{p}^T(x) = \begin{bmatrix} 1 \ x_1 \ x_2 \ x_3 \ \ldots x_1^2 \ x_2^2 \ x_3^2 \ \ldots x_1 x_2 \ x_1 x_3 \ \ldots \end{bmatrix}. \tag{2.12}$$

One mapping between the input and output can be written as follows:

$$\begin{aligned} y_i &= \beta_0 + \beta_1 x_{i1} + \beta_2 x_{i2} + \ldots + \beta_{n_t} x_{in_t} + \epsilon_i \ , \\ &= \beta_0 + \sum_{j=1}^{n_t} \beta_j x_{ij} + \epsilon_i \ , \quad i = 1, 2 \ldots, n_s \end{aligned} \tag{2.13}$$

where $y$ is the observed response, $\beta_0$, $\beta_j$, ..., and $\beta_{n_t}$ represent the unknown polynomial or regression coefficients, $\epsilon$ is a random error term, $n_s$ is the number of observations or supporting points, and $n_t$ is the number of polynomial base functions.

It is more convenient to use a matrix notation to express the mathematical relations, such as:

$$\mathbf{y} = \mathbf{X}\boldsymbol{\beta} + \boldsymbol{\epsilon}, \tag{2.14}$$

where $\mathbf{y}$ is the $(n_s \times 1)$ vector of observations, $\mathbf{X}$ represents the $(n_s \times n_t)$ input variables and their combinations, $\boldsymbol{\beta}$ is a $(n_t \times 1)$ vector of regression coefficients, and $\boldsymbol{\epsilon}$ is a $(n_s \times 1)$ vector of random errors.

The method of least squares can be used to estimate the regression coefficients, $\hat{\boldsymbol{\beta}}$, which minimizes the foloowing:

$$L = \sum_{i=1}^{n_s} \epsilon_i^2 = \boldsymbol{\epsilon}^T \boldsymbol{\epsilon} = (\mathbf{y} - \mathbf{X}\boldsymbol{\beta})^T (\mathbf{y} - \mathbf{X}\boldsymbol{\beta}) \qquad (2.15)$$

Therefore, $\hat{\boldsymbol{\beta}}$ is the solution for $\boldsymbol{\beta}$ in the following equation:

$$\frac{\partial L}{\partial \boldsymbol{\beta}} = 0 \rightharpoonup \hat{\boldsymbol{\beta}} = \left(\mathbf{X}^T\mathbf{X}\right)^{-1} \mathbf{X}^T\mathbf{y} \qquad (2.16)$$

The estimation of the polynomial coefficients $\hat{\boldsymbol{\beta}}$ involves evaluating the model output $n_s$ times, where $n_s \geq n_t$.

Once the polynomial coefficients are estimated, the response can be predicted for any set of input variables or parameters as follows:

$$\hat{\mathbf{y}}^{poly} = \mathbf{X}\hat{\boldsymbol{\beta}}, \qquad (2.17)$$

where $\hat{\mathbf{y}}^{poly}$ represents the approximated response. The polynomial response surface provides an explicit and compact functional relationship between the input and the output, which is advantageous since the meta-model is built once and used repeatedly.

### 2.4.2.2 Moving Least Squares

The moving least squares is employed because of its ability to catch localities or nonlinearities in the input-output relation. The local character of this approximation method is obtained by introducing radial weighting functions that depend on the position of the evaluated response. The prediction is strongly influenced by the neighboring response values and less influenced by those further away. Moving least squares models can be seen as an extension of the polynomial response surface models since the former assumes equal weightings for

the support points, whereas the latter introduces position-dependent weights, which enables it to capture localities in the output. The flexibility of such an approximation model is obtained at a higher computational expense. Furthermore, an explicit formulation of the meta-model cannot be attained, i.e., a new moving least squares model is built for every new set of inputs. A more detailed description of the moving least squares models and their properties can be found in [69, 70].

As mentioned before, moving least squares is an extension of the polynomial response surface model since weighted least squares solutions are obtained for the regression coefficients, $\hat{\boldsymbol{\beta}}_{MLS}$, which minimizes the following:

$$L_{MLS} = \sum_{i=1}^{n_s} \epsilon_i^2 w_i(x) = \boldsymbol{\epsilon}^T \mathbf{W}(x)\boldsymbol{\epsilon} = (\mathbf{y} - \mathbf{X}\boldsymbol{\beta}_{MLS})^T \mathbf{W}(x) (\mathbf{y} - \mathbf{X}\boldsymbol{\beta}_{MLS}) \tag{2.18}$$

And similarly, $\hat{\boldsymbol{\beta}}_{MLS}$ is the solution for $\boldsymbol{\beta}_{MLS}$ in the following equation:

$$\frac{\partial L_{MLS}}{\partial \boldsymbol{\beta}_{MLS}} = 0 \rightharpoonup \hat{\boldsymbol{\beta}}_{MLS} = \left[\mathbf{X}^T \mathbf{W}(x)\mathbf{X}\right]^{-1} \mathbf{X}^T \mathbf{W}(x)\mathbf{y}, \tag{2.19}$$

where $w_i$ is a local weighting function for each supporting point $x_i$, which depends on the position of the approximation point $x$.

The approximated values of the output can be determined by the following:

$$\hat{\mathbf{y}}^{MLS} = \mathbf{p}^T \left[\mathbf{X}^T \mathbf{W}(x)\mathbf{X}\right]^{-1} \mathbf{X}^T \mathbf{W}(x)\mathbf{y} \tag{2.20}$$

The Gaussian weighting function is used for the algorithm, which is an exponential function described as

$$w_G(s) = e^{-s^2/\alpha^2}, \tag{2.21}$$

with $\alpha$ as a shape factor and $s = \|x - x_i\| / D$, where $s$ is the normalized distance between the approximation point and the supporting point considered and $D$ is the influence radius.

### 2.4.2.3 Hybrid Algorithm

The main motivation in deriving a meta-model is to overcome the computational cost of running the numerical model directly. Nevertheless, building a meta-model requires performing a sufficient number of numerical computations to capture the input-output relation. For multi-dimensional mapping of input-output where localities depend on the model dimensions, different approximation models can be used for the different dimensions in order to capture the nature of the relation and to avoid overfitting. Therefore, a hybrid model of polynomial regression and moving least squares has been proposed for the input-output mapping in order to capture the global output with its localities without overfitting. This approximation model is based on using the moving least squares in the dimension where the polynomial response surface fails to capture, and can be expressed as:

$$
\begin{aligned}
\hat{y}^{hprd} &= \hat{y}^{poly} + \hat{y}^{MLS}(\mathbf{R}) \,, \\
\mathbf{R} &= \left[ y_1 - \hat{y}_1^{poly}, \ \ldots, \ y_i - \hat{y}_i^{poly}, \ \ldots, \ y_s - \hat{y}_s^{poly} \right]^T
\end{aligned}
\tag{2.22}
$$

Similar approaches to building meta-models can be found using variant algorithms to approximate the output, which are then used for different purposes [71, 72].

It is worth mentioning that a greater number of base terms leads to a more accurate approximation of the input-output relationship for any of the meta-models proposed. Nevertheless, the greater the number of terms also leads to a more flexible model, which could overfit the noise originating from computing the underlying response. In other words, the meta-model could be built with excessive base terms that would lead to poor generalizations, which should be avoided.

### 2.4.2.4 Coefficient of Determination

The sensitivity indices are estimated directly on the approximated model, therefore, a measure for testing the adequacy of the meta-model is required. The coefficient of determination

is often used for these purposes and is defined as:

$$R^2 \;\; = \;\; 1 - \frac{\sum_{i=1}^{n_s} (y_i - \hat{y}_i)^2}{\sum_{i=1}^{n_s} (y_i - \bar{y})^2}, \tag{2.23}$$

where $y_i$ is the model output (support points) evaluated, $\hat{y}_i$ is the approximated model output, $\bar{y}$ is the mean value of the model output evaluated, and $n_s$ is the number of support samples.

The values of the coefficient of determination ($R^2$) for the moving least squares and the hybrid meta-models depend on the influence radius ($D$) used in the meta-model, thus, the $R^2$ values cannot be reliable. Hence, a more reliable measure is the estimation of $R^2$ using cross-validation. This measure is denoted as the predictive coefficient of determination ($R_{cross}^2$) [73].

Cross-validation involves splitting the input randomly into $q$ subsets, removing one of these subsets and fitting the approximation model to the $q - 1$ remaining subsets [74]. The approximation $\hat{y}$ for all inputs is obtained by combining the output of the $q$ subsets, and Equation (2.23) is used for finding $R_{cross}^2$. This procedure is convenient in this study since a cross-validation is already carried out to obtain the optimum influence radius $D$ for the moving least squares and the hybrid models.

**Test Function**

The test function, Equation (2.24), retrieved from [71] is used to illustrate the different meta-models. Noise has been introduced into the function, Equation (2.25), in order to examine the approximation models [71]. The test function $y_s(x)$ and its noisy version $y_n(x)$ are created for $\epsilon = 1$ and $n_v = 2$ and plotted in Figure 2.2 and Figure 2.3, respectively. This test function appears quasi sinusoidal on $[-1, 1]$.

$$y_s(x) = \sum_{i=1}^{n_v} \left[ \frac{3}{10} + \sin\left(\frac{16}{15}x_i - \epsilon\right) + \sin^2\left(\frac{16}{15}x_i - \epsilon\right) \right] \tag{2.24}$$

$$y_n(x) = y_s(x) + \sum_{i=1}^{n_v} \left[ \frac{2}{100}\sin\left(40\left(\frac{16}{15}x_i - \epsilon\right)\right) \right] \tag{2.25}$$

In order to examine the performance of the meta-models, 100 uniformly distributed samples with $\mu = 0$ and $\sigma = 1$ are generated and used as support points for which the values of the test function with noise are computed following Equation (2.25). A different 40 samples are then created to be the test points, for which the meta-models are used to approximate their values using the support points. Further, the value for the shape factor $\alpha$ in Equation (2.21) is taken as 0.38. A general comparison of the different meta-models is shown in Figure 2.4, which shows that the polynomial regression surface is not capturing the localities of the function, whereas the behavior of the moving least squares and hybrid models are much better.
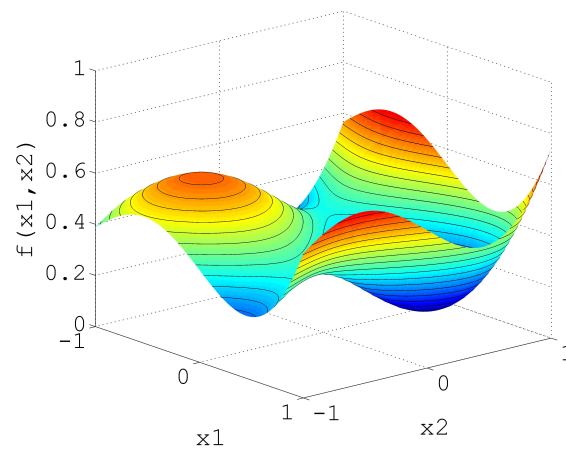


FIGURE 2.2: Two-dimensional view of the test function
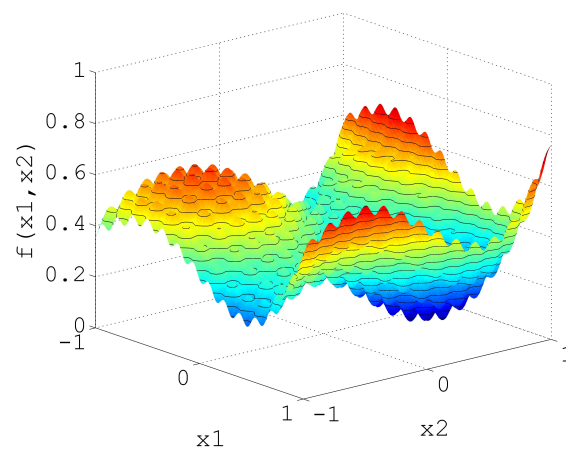


FIGURE 2.3: Two-dimensional view of the test function with noise

The quality of the meta-models is then examined. For the moving least squares and hybrid
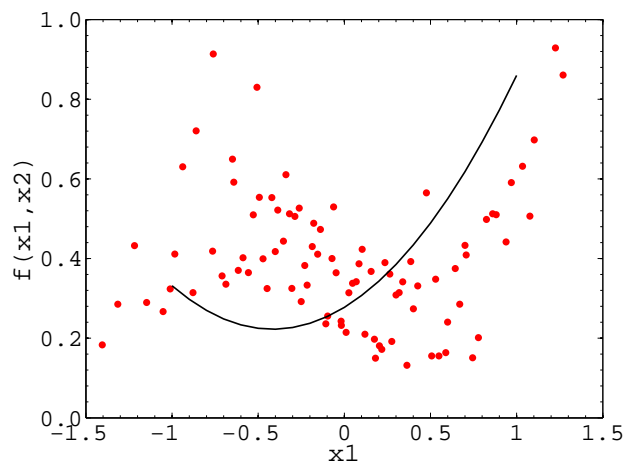
(a) Polynomial response surface
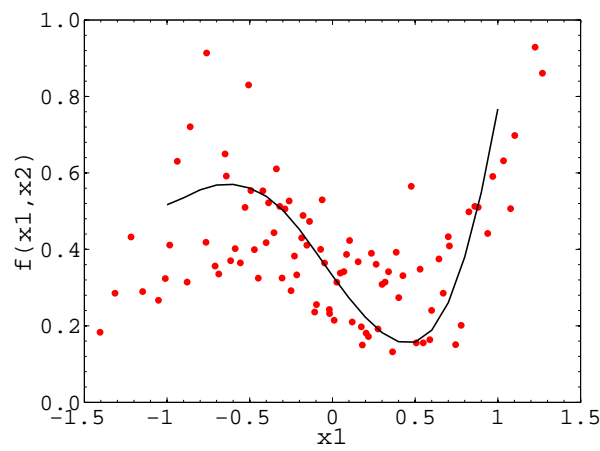


(b) Moving least squares approximation
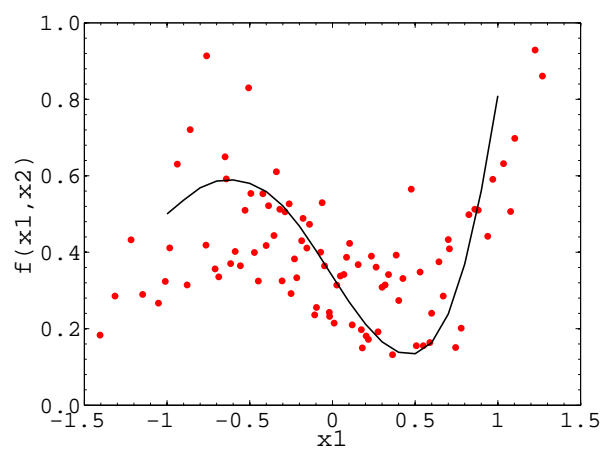


(c) Hybrid approximation

FIGURE 2.4: One-dimensional view of the approximation models: ( ● ) Support points, (—) Approximation model

models, cross-validation is needed to find the optimum influence radius $D$ and the predictive coefficient of determination $R^2_{cross}$. Each of the subsets in the cross-validation has 10 samples. The optimum influence radius $D$ is chosen as the one which gives the highest corresponding predictive coefficient of determination $R^2_{cross}$. Table 2.1 shows different influence radii with their corresponding $R^2_{cross}$. The optimum influence radius is found to be $D = 0.8$.

TABLE 2.1: Optimum Influence Radius $D$

| D | MLS $R^2_{cross}$ | Hybrid $R^2_{cross}$ |
|---|---|---|
| 0.6 | 0.91 | 0.90 |
| **0.8** | **0.94** | **0.92** |
| 1.0 | 0.93 | 0.91 |
| 1.2 | 0.91 | 0.89 |

The calculated qualities of the meta-models of the test function are presented in Table 2.2. The moving least squares and hybrid meta-models are the ones with the highest $R^2_{cross}$ for the test function data. This is to be expected as the test function shows strong localities.

TABLE 2.2: Approximation Model Quality: Coefficient of Determination

| | $R^2$ | $R^2_{cross}$ |
|---|---|---|
| Polynomial | 0.55 | 0.39 |
| MLS | 0.99 | 0.94 |
| Hybrid | 0.99 | 0.92 |

#### 2.4.2.5 Standardization of the Input

The inputs for building the meta-models could be of different scales. Thus, standardizations of their values are needed as a prior step to building the meta-models and performing the sensitivity analysis. The standardized value $x_i^s$ of the input parameter $x_i$ is computed as

$$x_i^s = \frac{x_i - \min(x)}{\max(x) - \min(x)}, \tag{2.26}$$

where $\min(\dots)$ and $\max(\dots)$ are the minimum and maximum of the samples of the input parameter examined.

## 2.4.3 Total Uncertainty

Uncertainty is the acknowledgment of existence of more possibilities. A true model does not exist, rather the model that fits the purpose of its development holds true. This is where uncertainty is inevitably involved in assessing plausible models created for a specific purpose. The general notion has been that more complex models simulate reality better, however, the higher uncertainties associated with their output cannot be ignored. An approach is presented and tested at a later time to weigh the model complexity against its uncertainty. This may help in assessing the model utility for practical applications.

Before describing the approach, it is important to define the terms used to categorize the uncertainties of a model output. The first category is called 'Model Input Uncertainty,' due to the inherent variability and randomness of the input parameters. This can be studied by propagating the variations in the input parameters through the model and examining its output variation, which is addressed in the previously described uncertainty and sensitivity analyses. The second category is 'Model Framework Uncertainty,' which is related to the implications of modeling simplification, incomplete scientific data and lack of knowledge of what is affecting the modeled system. This type of uncertainty is to be taken into account in the approach presented.

The adjustment factor approach [50] is used to propagate the model uncertainty into the prediction of the model. The prediction of a system response is represented as

$$y = y^* + E_a^*, \tag{2.27}$$

where $y^*$ is the prediction of the response by the best model, $E_a^*$ is an additive adjustment factor, and $y$ is an adjusted prediction. An additive adjustment factor $E_a^*$ is presumed to be a normal random variable.

Assuming that the predictions and probabilities of a set of models are known, [75] computed the means and the variances of both $E_a^*$ and $y$ as:

$$E\left(E_a^*\right) \;=\; \sum_{i=1}^{N_m} P(M_i)(y^{M_i} - y^*) \tag{2.28}$$

$$V\left(E_a^*\right) \;=\; \sum_{i=1}^{N_m} P(M_i)(y^{M_i} - E(y))^2 \tag{2.29}$$

$$E\left(y\right) \;=\; y^* + E\left(E_a^*\right) \tag{2.30}$$

$$V\left(y\right) \;=\; V\left(E_a^*\right) \tag{2.31}$$

where $E(\ldots)$ is the mean of a variable, $V(\ldots)$ is the variance of a variable, $y^{M_i}$ is the prediction of model $M_i$, $P(M_i)$ is the probability of $M_i$, and $N_m$ is the number of models considered. The mean and variance of $E_a^*$ are the averaged mean and the averaged variance of the difference between the prediction of the best model and those of other plausible models using model probabilities as weights. The mean of $y$ is the sum of the prediction of the best model and the mean of $E_a^*$ as described in Equation (2.30). The variance of $y$ is the same as that of $E_a^*$, as expressed in Equation (2.31).

The total uncertainty of a single plausible model is of interest. Thus, the input uncertainty is introduced to the model response, and the average prediction over the variation of the input parameters $\left(Y^{M_i}\right)$ is computed and used in the further derivation.

Since the model probabilities add up to one, the following relations hold [76]:

$$E\left(Y\right) \;=\; \sum_{i=1}^{N} P(M_i)(Y^{M_i}) \tag{2.32}$$

$$V\left(Y\right) \;=\; \sum_{i=1}^{N} P(M_i)(Y^{M_i} - E(Y))^2 \tag{2.33}$$

Thus, the single contribution of a plausible model to the total variance of the prediction can be retrieved from Equation (2.33), [76].

The variance of a single plausible model $M_i$ can be derived as follows:

$$V_{M_i}(Y) = E\left[(Y^{M_i} - E(Y))^2\right] \tag{2.34a}$$

$$= E\left[(Y^{M_i})^2 - 2Y^{M_i}E(Y) + (E(Y))^2\right] \tag{2.34b}$$

$$= E\left[(Y^{M_i})^2\right] + E\left[-2Y^{M_i}E(Y) + (E(Y))^2\right] \tag{2.34c}$$

$$= E\left[(Y^{M_i})^2 - (E(Y^{M_i}))^2 + (E(Y^{M_i}))^2\right] + E\left[-2Y^{M_i}E(Y) + (E(Y))^2\right] \tag{2.34d}$$

$$= V(Y^{M_i}) + (E(Y^{M_i}))^2 + E\left[-2Y^{M_i}E(Y) + (E(Y))^2\right] \tag{2.34e}$$

$$= V(Y^{M_i}) + (E(Y^{M_i}))^2 - 2E(Y^{M_i})E(Y) + (E(Y))^2 \tag{2.34f}$$

$$= V(Y^{M_i}) + \left[E(Y^{M_i}) - E(Y)\right]^2 \tag{2.34g}$$

The variance of the single model is composed of two parts, as shown in Equation (2.34g). The first part $V(Y^{M_i})$ originates from the propagation of input uncertainty through the models; the second part $\left[E(Y^{M_i}) - E(Y)\right]^2$ can be viewed as the additive framework uncertainty. The second part of the uncertainty is the difference between the average response of the single model and the average response of an adjusted model.

If $E(Y)$ is known, then the application of the relations above is straightforward. However, this is not the case in complex engineering problems, especially when physical measurements are lacking. Therefore, the best model $Y^{ref}$ is assumed to be a representative of the prediction $Y$. An additive error term $\epsilon^{ref}$ is assumed and introduced to account for its shortcomings and imperfections. Following Equation (2.34g), the total variance of the single model is represented as:

$$V_{M_i}(Y) = V(Y^{M_i}) + V(\epsilon_\Delta^{M_i}) + V(\epsilon^{ref}), \tag{2.35}$$

where

$$V(\epsilon_\Delta^{M_i}) = \left[E(Y^{M_i}) - E(Y^{ref})\right]^2, \tag{2.36}$$

and $V(\epsilon^{ref})$ is the uncertainty stemming from the assumption that the reference prediction is the best model.

The value of $V(\epsilon^{ref})$ is unknown, however it is assumed to take on different values, and its influence on the total uncertainty of a model prediction is examined. The model $M_i$ with the

lowest $V_{M_i}(Y)$ is assumed to be the model that is most fit since its quality of prediction is balanced against its uncertainty. The influence of tested values of $V(\epsilon^{ref})$ affects as expected the qualitative evaluations of the $V_{M_i}(Y)$, therefore, it does not affect the ranking of the single models, which is the objective for using this procedure.

It is important to mention that the assumed distribution for the additive adjustment or error term imposes a bias in the estimates for the single model, therefore, the variation of the model prediction is computed and employed in model ranking.

## 2.5 Summary

The main assessment method is based on sensitivity and uncertainty analyses. In addition to the classical approaches for performing a variance-based sensitivity analysis, a new setting is proposed that computes the averages over influential processes that have eminent effects on the response.

Variance-based approaches require a large number of samples to produce reliable estimates, therefore, to keep the performance of such approaches to a practical level, meta-models are derived. The main goal of these meta-models is to create input-output relationships, which are computationally inexpensive and sufficiently representative of the response output. A hybrid algorithm of polynomial and moving least squares models has been developed to capture localities and to avoid overfitting. The adequacy requirements of the meta-model are met by using an acceptance threshold for the value of the predictive coefficient of determination $R^2_{cross}$.

Finally, an estimate of the model uncertainty is derived based on the assumption that the uncertainty is additive and can be described as a normal variable. Furthermore, the input parameter uncertainty can also be considered. The variance of the response is used as an estimate for the model uncertainty. The models with the lower total uncertainty are assumed to be the most fit for the response studied.

# Chapter 3

# Coupled Subsystems in Bridges

The vibration of bridges caused by moving vehicles has been a subject of continuous research since the nineteenth century, as discussed in Chapter 1. In the last two decades, the dynamic problem of bridge-vehicle interaction has received even more attention from engineers and researchers, due to the considerable increase in traffic and upgrade projects for existing bridges [38]. The main focus of this chapter deals with the modeling of the vehicle, bridge and bearings, and the solution methods for the bridge-vehicle interaction. A verification example is presented to control the solutions of the numerical models.

## 3.1 Bridge-Vehicle Interaction

Researchers have utilized different methods for determining bridge-vehicle interaction. *Yang et al.* [1] and *F. Yang et al.* [19] have reviewed these methods to solve the dynamic problem with their corresponding mathematical and computational descriptions. When analyzing bridge-vehicle interaction, two sets of differential equations of motion can be written for the vehicle and the bridge. These equations are solved ensuring compatibility and equilibrium conditions at the contact points. The methods to perform the analysis can be of two types, those based on solving the uncoupled set of equations of motion, i.e., the equations of the vehicle and the bridge are solved separately, in iterative or non-iterative algorithms [19, 21, 30], and those based on solving the coupled set of equations, i.e., there is a unique matrix

for the bridge-vehicle system obtained by eliminating the contact forces appearing in the equations of motion for the vehicle and bridge [20, 77, 78].

In this sections, the systems of the vehicle and bridge examined are described. Furthermore, the solution method used for the bridge-vehicle interaction is discussed, in which the equations of motion of the bridge and the vehicle are solved separately in the time domain. An FE model to solve the interaction problem by employing contact elements is described. In addition, a validation example using the numerical and analytical solutions for the dynamic problem is presented.

### 3.1.1   Vehicle Models

Researchers have used different suspended mass models to represent heavy vehicle systems varying from single to multiple degrees of freedom depending on the level of modeling [30, 37, 79, 80]. The heavy vehicle models built and used are a two-degree-of-freedom model, also known as a "1/4 car model," and an eight-degree-of-freedom model considering the configuration of a five-axle vehicle. Both models are built in the pitch mode; the effect of rolling of the vehicle is not considered in the dynamic analysis. According to [37], the pitch plane models are usually sufficiently accurate for the global response, therefore, roll degrees of freedom can be ignored. Furthermore, the models do not consider nonlinearities in the suspension system or tire behavior nor do they consider the complexities in the sprung mass motion. The suspension system and tires are assumed to behave linearly, and modeled as linear springs with viscous damping. Further, the sprung masses are assumed rigid.
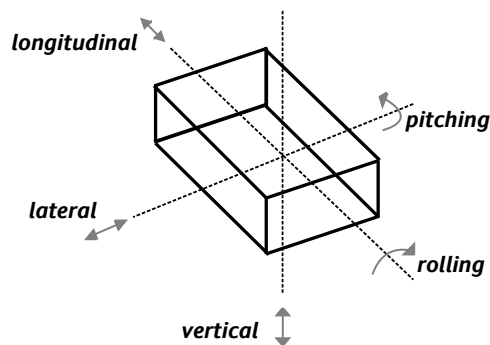


FIGURE 3.1: Motions of the vehicle

The equations of motion for the vehicle can be written in the following general form:

$$\mathbf{M}_v \ddot{\mathbf{U}}_v + \mathbf{C}_v \dot{\mathbf{U}}_v + \mathbf{K}_v \mathbf{U}_v = \mathbf{P}_v, \tag{3.1}$$

where $\mathbf{M}_v$ is the mass matrix of the vehicle, $\mathbf{C}_v$ is the damping matrix of the vehicle, $\mathbf{K}_v$ is the stiffness matrix of the vehicle, $\mathbf{P}_v$ is the dynamic force vector of the vehicle, and $\mathbf{U}_v$ is the generalized coordinate vector describing the dynamics of the vehicle model (degrees of freedom).

The generalized coordinates of the **two-degree-of-freedom vehicle model** are the sprung mass vertical displacement $y_s$ and the unsprung mass vertical displacement $y_u$. The sprung mass is the mass supported by the suspension system and the unsprung mass is the mass connected to the suspension, which is supported by the tires (Figure 3.2).

$$\mathbf{U}_v = \left\{ \begin{array}{cc} y_u & y_s \end{array} \right\}^T \tag{3.2}$$
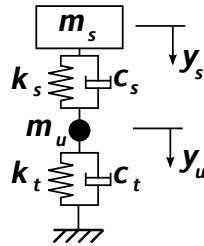


FIGURE 3.2: Schematic for the quarter car model

When the equations of motion for the vertical displacements of the sprung and the unsprung masses of the vehicle are formulated, the following system of matrices describing the dynamics of the vehicle model are written as:

$$\mathbf{M}_v = \begin{bmatrix} m_u & 0 \\ 0 & m_s \end{bmatrix} \quad \mathbf{K}_v = \begin{bmatrix} k_t + k_s & -k_s \\ -k_s & k_s \end{bmatrix} \quad \mathbf{C}_v = \begin{bmatrix} c_t + c_s & -c_s \\ -c_s & c_s \end{bmatrix}, \tag{3.3}$$

where $m_s$ is the sprung mass, $m_u$ is the unsprung mass, $k_s$ is the stiffness of the suspension system, $c_s$ is the damping of the suspension system, $k_t$ is the stiffness of the tire, and $c_t$ is the damping of the tire. The interaction force $F_i^{int}$ at the contact point $i$, which is time-variant

and depends on the interaction between the vehicle and the bridge, can be expressed as:

$$F_i^{int} = k_t \left[ y_u(t) - y_b(x_i, t) - r_i(t) \right], \tag{3.4}$$

where $y_b(x_i, t)$ and $r_i(t)$ are the displacements of the bridge and road unevenness respectively, at $i^{th}$ contact point at instant $t$.

The vibrational modes of this model are the bouncing mode of the sprung mass (main body of the vehicle) and the axle hop mode.

The **eight-degree-of-freedom vehicle model** represents the configuration of a typical heavy truck traveling on the road network of Europe [80]. The vehicle consists of a two-axle tractor and a three-axle semi-trailer linked by a hinge. The tractor and the semi-trailer are assumed to be rigid components and are characterized by their masses and moments of inertia. The vehicle model is excited at five points, which are the contact points between the tires and the roadway. It is also assumed that the three axles of the semi-trailer share the rear static load equally since load-sharing mechanisms are common in multi-axle heavy vehicle suspensions [37]. The generalized coordinates used to describe the vehicle dynamics are tractor vertical displacement $y_T$, tractor pitch angle $\theta_T$, semi-trailer vertical displacement $y_S$, semi-trailer pitch angle $\theta_S$, tractor front unsprung mass vertical displacement $y_1$, tractor rear unsprung mass vertical displacement $y_2$, and semi-trailer unsprung masses vertical displacements $y_{31}$, $y_{32}$, and $y_{33}$, as shown below:

$$\mathbf{U}_v = \left\{ \begin{array}{cccccccc} y_T & \theta_S & \theta_S & y_1 & y_2 & y_{31} & y_{32} & y_{33} \end{array} \right\}^T \tag{3.5}$$

Due to the articulation of the truck and the semi-trailer, a kinematic constraint can be written for the semi-trailer vertical displacement $y_S$, [79] as expressed below:

$$y_S = y_T + b_5 \theta_T + b_4 \theta_S \tag{3.6}$$

After fulfilling this constraint equation, the vehicle model has eight independent degrees of freedom. The equations of motion are based on the derivation provided by [79] for the ride
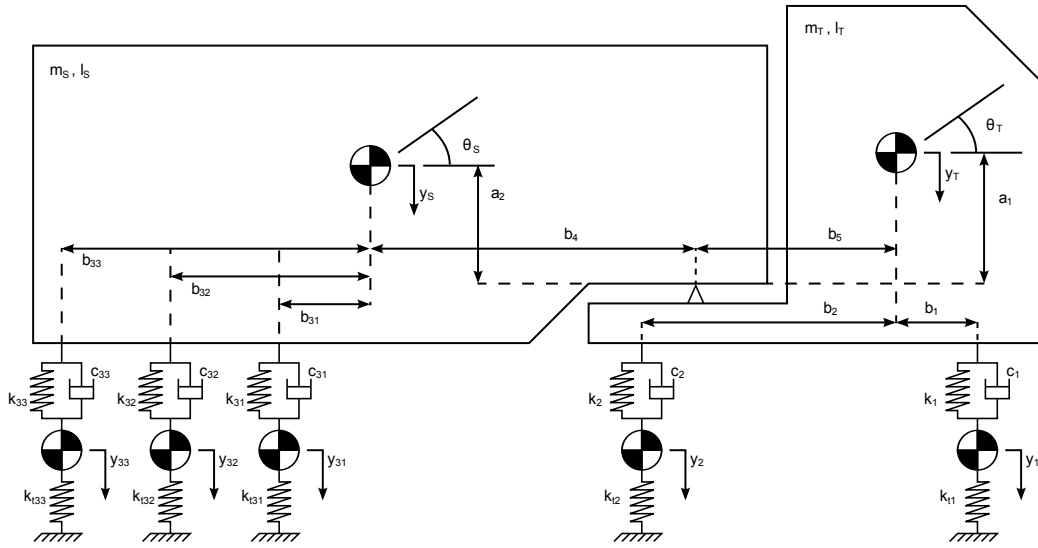
FIGURE 3.3: Schematic for the five-axle vehicle model

behavior of a three-axle tractor and semi-trailer truck. Such a formulation has also been used in other studies [80, 81]. Mass, damping, and stiffness matrices are found in Appendix 7. The interaction force $F_i^{int}$ can be expressed as:

$$F_i^{int} = k_{ti} \left[ y_i(t) - y_b(x_i, t) - r_i(t) \right], \quad i = 1, \, 2, \, 31, \, 32, \, 33 \qquad (3.7)$$

where $y_b(x_i, t)$ and $r_i(t)$ are the displacements of the bridge and road unevenness respectively, underneath the $i^{th}$ axle at instant $t$.

The vibration of such a heavy vehicle has two distinctive frequency ranges; the first range is 1.5 Hz to 4 Hz, representing the sprung mass bounce involving some pitching, and the second range is 8 Hz to 15 Hz, representing the unsprung mass bounce involving suspension pitch modes [37].

## 3.1.2 Bridge Model

The equations of motion of the bridge considering time varying forces can be expressed in the following matrix notation:

$$\mathbf{M}_b \ddot{\mathbf{U}}_b + \mathbf{C}_b \dot{\mathbf{U}}_b + \mathbf{K}_b \mathbf{U}_b = \mathbf{P}_b, \qquad (3.8)$$

with $\mathbf{M}_b$, $\mathbf{C}_b$, $\mathbf{K}_b$ are the mass, damping and stiffness matrices of the bridge, $\ddot{\mathbf{U}}_b$, $\dot{\mathbf{U}}_b$, $\mathbf{U}_b$ are the accelerations, velocities and displacements of the bridge, and $\mathbf{P}_b$ is the vector of forces acting on each bridge node at time $t$, which has two components, as shown below:

$$\mathbf{P}_b = \mathbf{F}^g + \mathbf{F}^{int} , \tag{3.9}$$

where $\mathbf{F}^g$ is the force acting on the bridge due to the weight of the vehicle, which is independent of the interaction, and $\mathbf{F}^{int}$ is the time-variant force acting on the bridge, which depends on the interaction between the bridge and the vehicle. The damping of the bridge is assumed to be viscous, which means that it is proportional to the nodal velocities. Rayleigh damping is often used to model viscous damping and is described as:

$$\mathbf{C}_b = \alpha \mathbf{M}_b + \beta \mathbf{K}_b , \tag{3.10}$$

where $\alpha$ and $\beta$ are proportionality constants which satisfy

$$\frac{\alpha}{2\omega} + \frac{\beta\omega}{2} = \xi ,$$

with $\xi$ as the damping ratio. Since there are two unknowns, a constant damping ratio is assumed over a frequency range $\omega_1$ and $\omega_2$. This gives two simultaneous equations expressed as follows:

$$\begin{aligned} \xi &= \frac{\alpha}{2\omega_1} + \frac{\beta\omega_1}{2} \\ \xi &= \frac{\alpha}{2\omega_2} + \frac{\beta\omega_2}{2} \end{aligned} \tag{3.11}$$

These equations are solved for $\alpha$ and $\beta$.

### 3.1.3  Solution of Bridge-Vehicle Interaction

The solution of the bridge-vehicle interaction is often obtained by solving the equations of motion of the bridge and the vehicle systems separately using a direct numerical integration method. The compatibility conditions and equilibrium equations at the contact between

the vehicle tires and the bridge are satisfied by iterative algorithms. The general idea of the solution procedure consists of assuming the initial displacements at the contact points and solving the vehicle equations to obtain the interaction forces, substituted into the bridge equations and improved displacements are computed. In case of iterative procedures the same steps are repeated until a certain tolerance is met.

During the passage of a vehicle across a bridge, the dynamic tire forces of a vehicle can lead to additional dynamic effects on the bridge. These effects are mainly due to the excitation of the vehicle by the dynamic deflection of the bridge and by the initial road unevenness. Models that consider bridge-vehicle interaction are often derived to consider these sources of excitation. The equations of motion for the vehicle and the bridge are written as Equation (3.1) and Equation (3.8), respectively. Assuming perfect contact, the solution of these equations is governed by satisfying the compatibility equation and imposing the equality of displacement at the contact point, as expressed below:

$$y_w(x_i, t) \quad = \quad y_b(x_i, t) + r_i(t) \, , \tag{3.12}$$

where $y_w(x_i, t)$ is the displacement of the tire of the vehicle at $i^{th}$ contact point at instant $t$. In addition, the force equilibrium conditions at the contact point $i$ must be satisfied, which can be shown as:

$$P_b^i \quad = \quad F_i^g + F_i^{int} \, , \tag{3.13}$$

where $F_i^g$ is the static weight of the $i^{th}$ axle and $F_i^{int}$ is the interaction force at the $i^{th}$ axle. The $i^{th}$ contact point usually does not coincide with the a DOF of the bridge model. Therefore, the forces $F_i^g$ and $F_i^{int}$ are converted to equivalent nodal forces associated with the bridge's DOF.

The analysis starts by assuming the initial displacements of the bridge for the time step $t$. The displacement of the vehicle's tire at the contact point is computed following the compatibility condition in Equation (3.12). The vehicle Equations (3.1) are solved using a numerical integration method for its displacements ($\mathbf{U}_v$). The determined displacements of the vehicle are replaced into Equation (3.4) or Equation (3.7), depending on the vehicle

model, to calculate the interaction forces ($F_i^{int}$). Satisfying the equilibrium conditions at the contact point as in Equation (3.13) and converting the forces to the associated DOFs of the bridge results in the equivalent bridge forces ($\mathbf{P}_b$). These forces ($\mathbf{P}_b$) are then used to solve the bridge Equations (3.8) using a numerical integration method to compute the improved displacements of the bridge ($\mathbf{U}_b$). This procedure is repeated till a tolerance assigned to the difference between the outputs is met for the analyzed time step. Then the same iterative analysis is repeated to $t + \Delta t$ till the desired period of time is reached.

An alternative, which is described as non-iterative algorithm is proposed by [21] for the above solution procedure. It is non-iterative conditioning over a sufficiently small time step. With such a time step, the force acting on the vehicle at the current time step is estimated from the previous step. According to [21], the choice of the time step should be *small enough* to capture the highest desired frequency of the bridge, the vehicle passage, and the excitation from road unevenness. Moreover a factor of $\frac{1}{10}$ is introduced into the $\Delta t$ selected to secure reasonable integration accuracy and is expressed as:

$$\Delta t \leq \frac{1}{10} \times \min \left\{ T_f = \frac{1}{f_{\max}},\ T_s = \frac{L}{v},\ T_r = v \kappa_r^{\max} \right\}, \tag{3.14}$$

where $f_{\max}$ is the upper frequency of interest for the bridge, and $\kappa_r^{\max}$ is the largest wavenumber of the road unevenness corresponding to the minimum wavelength. The numerical integration procedure used to solve the system of differential equations is the Newmark-$\beta$ method, which is described for the $k^{th}$ time step as:

$$\begin{aligned}
\dot{u}_{k+1} &= \dot{u}_k + \frac{\Delta t}{2} \left( \ddot{u}_k + \ddot{u}_{k+1} \right) \\
u_{k+1} &= u_k + \Delta t\, \dot{u}_k + \frac{1 - 2\beta}{2} \Delta t^2 \ddot{u}_k + \beta \Delta t^2 \ddot{u}_{k+1},
\end{aligned} \tag{3.15}$$

where $\beta$ is taken as $1/4$.

In general, many DOFs are involved in the FE model of the bridge system, but only the first modes of vibration make the significant contribution to the dynamic response. Therefore, the modal superposition method can be used to solve the equations of motion of the bridge, which reduces the computational effort considerably, which is regarded as advantageous [82]. The total dynamic response $y(x,t)$ is obtained by the superposition of the response obtained

for each modal coordinate as follows:

$$y(x,t) = \sum_{n=1}^{\infty} \phi_n(x) z_n(t), \tag{3.16}$$

where $\phi_n(x)$ is the mode shape of the $n^{th}$ mode and $z_n(t)$ is the modal contribution of the $n^{th}$ mode at instant $t$. Equation (3.16) can be expressed in matrix notation as:

$$\mathbf{Y} = \mathbf{\Phi Z} \tag{3.17}$$

The mode shapes are normalized such that:

$$\mathbf{\Phi}^T \mathbf{M}_b \mathbf{\Phi} = \mathbf{I} , \quad \mathbf{\Phi}^T \mathbf{K}_b \mathbf{\Phi} = \omega_n^2 \mathbf{\Phi}^T \mathbf{M}_b \mathbf{\Phi} \tag{3.18}$$

Introducing Equation (3.17) and its first and second derivative into Equation (3.8) leads to the following:

$$\mathbf{M}_b \mathbf{\Phi} \ddot{\mathbf{Z}}_b + \mathbf{C}_b \mathbf{\Phi} \dot{\mathbf{Z}}_b + \mathbf{K}_b \mathbf{\Phi} \mathbf{Z}_b = \mathbf{P}_b \tag{3.19}$$

Equation (3.19) is premultiplied by the transpose of the $n^{th}$ mode shape $\mathbf{\Phi}_n^T$, and it becomes as:

$$\mathbf{\Phi}_n^T \mathbf{M}_b \mathbf{\Phi} \ddot{\mathbf{Z}}_b + \mathbf{\Phi}_n^T \mathbf{C}_b \mathbf{\Phi} \dot{\mathbf{Z}}_b + \mathbf{\Phi}_n^T \mathbf{K}_b \mathbf{\Phi} \mathbf{Z}_b = \Phi_n^T \mathbf{P}_b \tag{3.20}$$

Following the mode shape orthogonality properties, in which all terms except the $n^{th}$ will vanish, thus the result is as:

$$\mathbf{\Phi}_n^T \mathbf{M}_b \mathbf{\Phi}_n \ddot{\mathbf{Z}}_b^n + \mathbf{\Phi}_n^T \mathbf{C}_b \mathbf{\Phi}_n \dot{\mathbf{Z}}_b^n + \mathbf{\Phi}_n^T \mathbf{K}_b \mathbf{\Phi}_n \mathbf{Z}_b^n = \mathbf{\Phi}_n^T \mathbf{P}_b \tag{3.21}$$

From Equation (3.21), the following can be attributed as the normal-coordinate generalized

mass, generalized damping, generalized stiffness, and generalized load for mode $n$, respectively and expressed as:

$$
\begin{aligned}
M_b^n &= \boldsymbol{\Phi}_n^T \mathbf{M}_b \boldsymbol{\Phi}_n \\
C_b^n &= \boldsymbol{\Phi}_n^T \mathbf{C}_b \boldsymbol{\Phi}_n \\
K_b^n &= \boldsymbol{\Phi}_n^T \mathbf{K}_b \boldsymbol{\Phi}_n \\
P_b^n &= \boldsymbol{\Phi}_n^T \mathbf{P}_b
\end{aligned}
\tag{3.22}
$$

If Equation (3.21) is divided by the $M_b^n$, this modal equation of motion may be expressed as:

$$
\ddot{Z}_b^n + 2\xi_n \omega_n \dot{Z}_b^n + \omega_n^2 Z_b^n = \frac{P_b^n}{M_b^n},
\tag{3.23}
$$

where $\xi_n$ is the modal viscous damping ratio, as shown below:

$$
\xi_n = \frac{C_b^n}{2\omega_n M_b^n}
\tag{3.24}
$$

with $n = 1,\ 2,\ 3,\ldots N_{mode}$, where $N_{mode}$ is the number of the considered modes. Each of Equation (3.23) is an independent single DOF equation of motion that is solved in the time domain using time integration method, e.g. Newmark-$\beta$. The total response is then obtained by solving $N_{mode}$ uncoupled modal equations and superposing their output following Equation (3.17)

## FE Model of BVI

An FE model of the vehicle and the bridge and their interaction are constructed based on the built-in code of FE package ANSYS. Contact elements moving with the vehicle have been used to couple the systems of the vehicle and the bridge. The solution of the contact problem is based on the Augmented Lagrange Multiplier. The use of contact algorithm allows penetrations between the vehicle and the bridge models, which may affect the numerical results obtained from the dynamic analysis. Therefore, the contact stiffness is chosen to induce penetrations, which are negligible compared with the dynamic displacements due to

the passage of a heavy vehicle over the bridge. Mass and spring-damper elements are utilized to model the vehicle, and beam elements are used to model the bridge.

The road unevenness is accounted for in the FE model by conditioning over the contact points using constraint equations. These constraint equations are updated at every time step to consider the corresponding road unevenness. The modeling process needs the FE model to run the analysis, as well as an external code to control the generation of samples, the execution of the dynamic analysis, and the analysis of the output. The software packages Matlab [83] and ANSYS [84] have been coupled successfully to perform the aforementioned tasks. Matlab provides the controlling environment and ANSYS provides the analysis environment.

### 3.1.4 Road Unevenness

As the vehicle traverses over the bridge, it is excited by the roadway conditions at the contact points. These conditions can be characterized by global road roughness (unevenness) and local roughness (bumps or pot holes). Only the global road unevenness is considered in the dynamic analysis, which is often described as a random Gaussian process. Therefore, this subsection includes a general introduction to random Gaussian processes with their stochastic characteristics, a description of roadway profiles as a random process, as well as an illustration of models for the realizations of roadway profiles.

In general, for a Gaussian stochastic process $f_0(t)$ with an autocorrelation function $R_{f_0 f_0}(\tau)$ and a two-sided power spectral density function $S_{f_0 f_0}(\omega)$, the following relations hold [45]:

$$E\left[f_0(t)\right] = 0 \tag{3.25}$$

$$E\left[f_0(t+\tau)f_0(t)\right] = R_{f_0 f_0}(\tau) \tag{3.26}$$

$$S_{f_0 f_0}(\omega) = \frac{1}{2\pi}\int_{-\infty}^{\infty} R_{f_0 f_0}(\tau)e^{-i\omega\tau}d\tau \tag{3.27}$$

$$R_{f_0 f_0}(\tau) = \int_{-\infty}^{\infty} S_{f_0 f_0}(\omega)e^{-i\omega\tau}d\omega \tag{3.28}$$

where $\omega$ is the temporal frequency.

Road unevenness is often obtained by measuring existing roadways, which is a laborious procedure. Therefore, [26] suggested a simplified way of describing the road surfaces. The authors handle the treatment of road unevenness as a realization of a stationary Gaussian homogeneous random process described by its power spectral density function in the space domain $S_{f_0 f_0}(\kappa)$ with $\kappa$ as the wavenumber. However, the dynamic analysis is performed in the time domain, hence, a description of the road unevenness in the time domain is needed. Therefore, the temporal power spectral density function $S_{f_0 f_0}(\omega)$ is to be computed. Assuming a constant speed for the vehicle $v$, the relationship between $S_{f_0 f_0}(\omega)$ and $S_{f_0 f_0}(\kappa)$ can be derived as follows:

- Since the vehicle is traveling at a constant speed of $v$, any instant of the travel time $\tau$ can be expressed in terms of the distance traveled $x$ as:

$$\tau = \frac{x}{v} \tag{3.29}$$

- A cycle of wavelength $\lambda = 2\pi/\kappa$ is covered in period $T$ as:

$$T = \frac{\lambda}{v}, \tag{3.30}$$

therefore, the temporal frequency can be written as:

$$\omega = \frac{2\pi}{T} = v\frac{2\pi}{\lambda} = v\kappa \tag{3.31}$$

- Substituting the above Equations (3.29), (3.30), and (3.31) in Equation (3.27) results in the following:

$$\begin{align} S_{f_0 f_0}(\omega = v\kappa) &= \frac{1}{2\pi} \int_{-\infty}^{\infty} R_{f_0 f_0}\left(\tau = \frac{x}{v}\right) e^{-i(\omega = v\kappa)\left(\tau = \frac{x}{v}\right)} \frac{1}{v} dx \tag{3.32} \\ &= \frac{1}{v} \cdot \frac{1}{2\pi} \int_{-\infty}^{\infty} R_{f_0 f_0}(x) e^{-i\kappa x} dx \tag{3.33} \\ &= \frac{1}{v} S_{f_0 f_0}(\kappa) \tag{3.34} \end{align}$$

With this relationship, the temporal spectral density function $S_{f_0 f_0}(\omega)$ can be obtained from the spatial spectral density function $S_{f_0 f_0}(\kappa)$. When performing the analysis in the

time domain, one can deduce that the excitation of the vehicle due to road unevenness can be described as non-stationary when the vehicle speed is time dependent [85]. Even when the speed is constant and the vehicle excitation is stationary, the dynamic responses of the bridge are non-stationary due to the movement of the vehicle [41]. This observation is of importance in deriving the stochastic characteristics when the dynamic problem is solved in the frequency domain.

In most engineering applications, the one-sided spectral density function $S_{FF}(\kappa)$ is derived from measurements for which the following relation holds:

$$S_{FF}(\kappa) = 2S_{ff}(\kappa) \tag{3.35}$$

There are two main models for generating realizations of random processes that are based on the work of Rice and Shinozuka [45, 86]. One consists of a series of sines and cosines with random amplitudes and the other consists of a series of cosine terms with random phase angles. The latter is often adopted for the realization of road profiles, as shown in Equation (3.36) below:

$$
\begin{aligned}
f(t) &= \sum_{k=0}^{N_d-1} \left[ C_k \cos(\omega_k t + \Phi_k) \right] , \\
\omega_k &= \omega_l + k\Delta\omega , \\
k &= 0, 1, 2, \ldots, N_d - 1 ,
\end{aligned}
\tag{3.36}
$$

where $\Phi_k$s are independent random phase angles uniformly distributed in the range $[0, 2\pi]$ and $C_k$s are defined as $\sqrt{S_{FF}(\omega_k)\Delta\omega}$. $S_{FF}$ is the one-sided power spectral density function (PSD) used to describe the road unevenness. Further, the road surfaces realized reflect the prescribed probabilistic characteristics of the random process accurately as the number $N_d$ gets larger.

Equation (3.36) shows that the PSD is discretized into temporal frequency bands of a width of $\Delta\omega$, and the corresponding discretized frequencies are used in the realization of the stochastic process (Figure 3.4). However, the entire frequency domain of the PSD cannot be used in the realization due to mathematical and physical reasons [45]. Cut-off frequencies
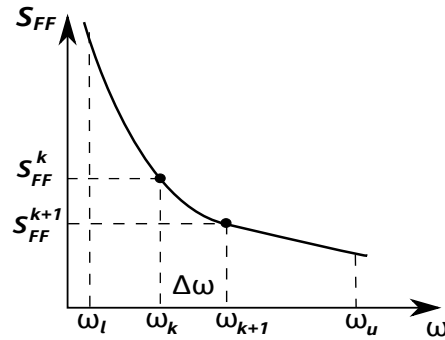
FIGURE 3.4: Discretized one-sided power spectral density function

are needed for the realizations of road surfaces. The discretizing frequency band is defined as:

$$\Delta\omega = (\omega_u - \omega_l)/N_d , \tag{3.37}$$

with $\omega_u$ and $\omega_l$ (rad/s) as the upper and lower cut-off frequencies. The long wavelength irregularities correspond to low frequency components in the time domain and short wavelength irregularities correspond to high frequency components [87]. The different wavelengths and their corresponding temporal frequencies excite different vibrational modes of the heavy vehicle; the bouncing mode of the sprung mass is more of a low frequency mode while the axle hop and pitching modes are of higher frequencies [37]. Furthermore, when the wavelengths of the irregularities are too small compared with the dimensions of the contact patch between the tire and the roadway, the tire absorbs these irregularities due to its flexibility. This phenomenon is referred to as tire envelopment, which reduces the excitations of the axle of the vehicle. Therefore, filtering or smoothing algorithms are recommended [88] depending on the dimension of the contact patch. Often a moving averaging filter is used for such purposes [89]. However, the effects of tire envelopment of short wavelengths irregularities can be neglected for normal highway speeds, whereas for low speeds tire envelopment becomes important and more detailed models for the contact patches may be significant [37, 90].

### 3.1.5 Numerical Verification

The response of a bridge due to the passage of a heavy vehicle is investigated for the numerical verification. The vehicle is a 40-ton truck modeled as a two-degree-of-freedom vehicle

model [37]. The sprung mass of the vehicle $m_s = 36000$ kg is supported by the suspension system modeled as a spring-damper element with a spring stiffness of $k_s = 18$ MN/m and a damping constant of $c_s = 1.4$ MNs/m. The unsprung mass of the vehicle $m_u = 4000$ kg is supported by the tires modeled as a spring-damper element with a spring stiffness of $k_t = 72$MN/m and a damping constant of $c_t = 1.4$ MNs/m. The vehicle has two modes, a bouncing mode of the sprung mass with a natural frequency of 3.18 Hz and an axle hop mode with a natural frequency of 23.9 Hz. The bridge model is a single-span simply supported beam model for the Pirton Lane Highway bridge in Gloucester (United Kingdom) [37]. The bridge's length $L = 40$m, an estimated mass per unit length of $m = 12000$ kg/m and a bending stiffness of EI $= 1.26 \times 10^5$ MNm$^2$. The bridge's first natural frequency is $f_1 = 3.20$ Hz with a modal damping ratio of $\zeta_1 = 0.02$.
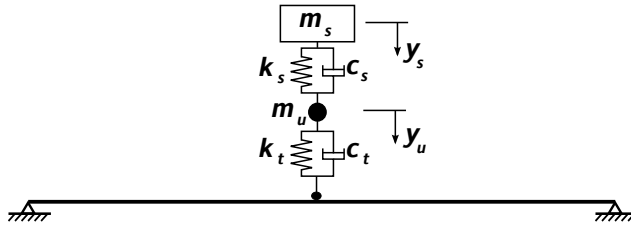


FIGURE 3.5: Schematic of the verification example

The numerical solutions presented in Section 3.1.3 are used to obtain the vertical displacement at mid-span during the passage of the 40-ton truck at a speed of $v = 90$ km/h, which is depicted in Figure 3.6. The numerical solutions are compared with an analytical solution that is derived in frequency domain, in which the dynamic interaction force is computed from the total compliance of the vehicle and the bridge [42]. The aim of this example is to verify the numerical solutions and establish a reference case for the analysis of more complex applications.

- Solution I is the FEM solution

- Solution II is the loosely coupled non-iterative solution [21]

- Solution III is the closed form solution [42]

The displacement vector of the two-degree-of-freedom vehicle model is $\mathbf{Y}_v = \{y_u, y_s\}^T$, where $Y_u$ is the displacement of the unsprung mass and $y_s$ is the displacement of sprung

mass. The mass, damping, and stiffness matrices of the vehicle are computed according to Equation (3.3).

A comparison of the different solutions of the bridge-vehicle interaction is depicted in Figure 3.6, which shows that a good agreement exists between the different solutions. Furthermore, upper fiber flexural strains and accelerations have been compared for Solution I and Solution II in Figures 3.7 and 3.8. A good agreement between the responses has also been observed. Solution I and Solution II are more suitable for sophisticated bridge and vehicle models. Solution II is only appropriate assuming linear systems, whereas, Solution I is more general and applies to linear and nonlinear systems. However, in terms of computation, Solution I is more expensive compared to Solutions II and III.

The computational cost is a decisive factor in this study since what is being proposed and applied is a probabilistic study, which means that a long computational time would render the study to be rather difficult and impractical. Hence, Solution II has been adopted as the solution for the dynamic problem. Furthermore, Solution III is used to control the solutions of the two numerical solutions (Solution I and Solution II) and to check the minimum number of road profile samples analyzed when running the Monte Carlo simulation. Solution I has been used to control the results of the numerical solution for variant responses and more complex subsystems.
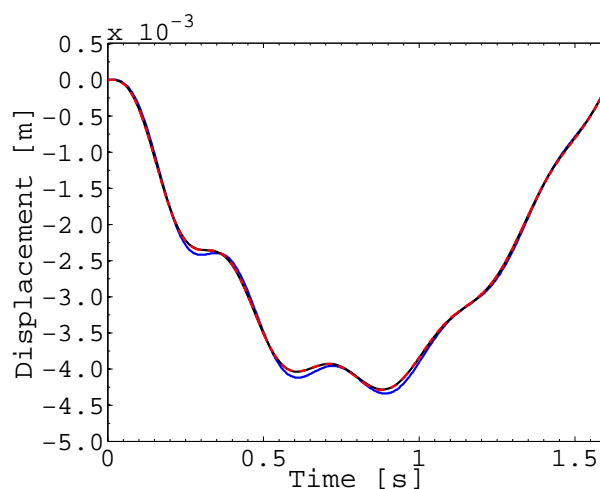


FIGURE 3.6: Time history of mid-span displacements: (——) Solution I, (– –) Solution II, (——) Solution III
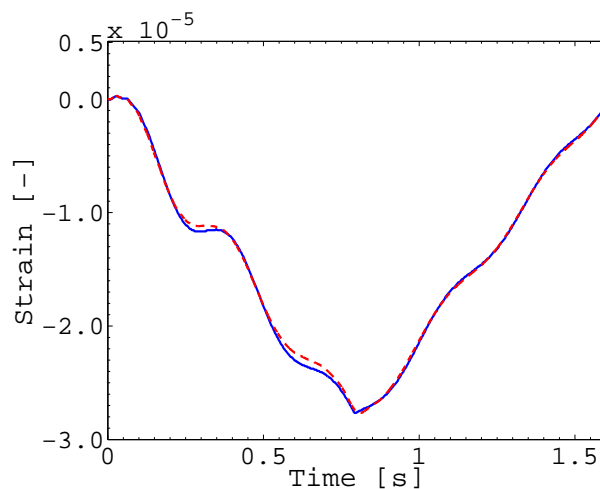
FIGURE 3.7: Time history of mid-span strains: (——) Solution I, (– –) Solution II
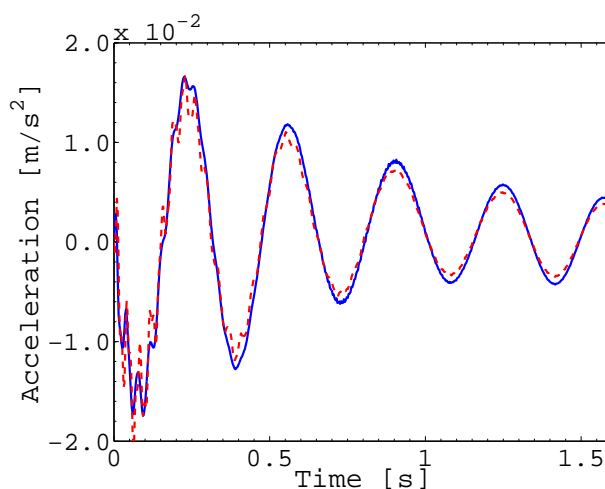


FIGURE 3.8: Time history of mid-span accelerations: (——) Solution I, (– –) Solution II

## 3.2 Superstructure-Substructure Coupling: Elastomeric Bearings

It has already been mentioned that highway beam bridges are the examined systems in this study. The superstructure of these bridges is often supported by elastomeric bearings. Bearings, in general, can be viewed as a coupling element between the superstructure and the substructure of the bridge; they accommodate the movements and transfer the forces between the two subsystems. There are different types of bearings depending on their material and the mechanism used to accommodate movements. Elastomeric bearings are one

type of bearings characterized as deformation bearings due to the fact that they accommodate the relative movements between the superstructure and the substructure through the deformation of the elastomer. While they are effective in supporting the superstructure of the bridge, they may also prevent bridge vibrations that are induced by moving vehicles from transmitting downward, which results in accumulated or amplified responses [34].

The material used for the elastomer is a rubber elastic material, which is created from vulcanized natural or synthetic caoutchouc. The elasticity of the elastomer is time and temperature dependent. However, for short-term loading, e.g., shocks or vibrations, the material may react elastically. Furthermore, the dynamic characteristics of the elastomer is frequency dependent. This behavior is of significance when the elastomeric bearings are used as isolators in earthquake-prone areas [91]. Elastomeric bearings are, in general, vertically stiff and horizontally flexible, which may affect the period of vibration of the bridge, thereby influencing the inertia forces that develop in the superstructure when running a dynamic analysis.

Most researchers study the elastomeric bearing as an element of its own [32, 33]. Only a few researchers have focused on the behavior of elastomeric bearings when integrated in the bridge structure. Several of them investigated the use of elastomeric bearings as an isolation element for traffic induced vibrations [6, 92], or as an isolation element for earthquake-proofed bridges [1]. In contrast, others have studied the effects of traffic vibrations on the degradation of elastomeric bearings [93].

A three-dimensional analysis for the dynamic response of bridges due to moving vehicles has been performed by [92] in order to examine the influence on the dynamic response when steel bearings are replaced with elastomeric bearings. The authors noticed that the use and modeling of elastomeric bearings for the bridge system studied did not change the system's resonant frequencies significantly. Moreover, the inclusion of bearings in the dynamic analysis resulted in larger displacements, especially the horizontal displacements in the direction of the bridge's main axis. The vibration of a two-girder steel bridge supported by elastomeric bearings was run by [6]. The authors concluded that the traffic-induced accelerations and the dynamic reaction forces when considering the elastomeric bearings were greater than those of the bridge with pin bearings. Furthermore, in [34] it was illustrated that inserting

elastomeric bearings at the supports of the single-span beam to isolate earthquake forces may adversely amplify the dynamic response of the beam to moving loads. It was observed that this conclusion depended on the vehicle's speed. In the aforementioned studies, the elastomeric bearings were modeled as independent linear springs in the vertical, horizontal, and lateral directions depending on the dimensionality of the bridge model.

The objective of modeling the bearings is to investigate the dynamic behavior of elastically supported bridges. A simple model for the elastomeric bearings is used; they are represented by a linear spring with constant stiffness properties considering only their vertical and rotational degrees of freedom.

The vertical (compression) stiffness of an elastomeric bearing according to EN1337-3 [94] is defined as:

$$K_V^{br} = \frac{A}{T\left(\frac{1}{5GS^2} + \frac{1}{E_b}\right)}, \tag{3.38}$$

where $A$ is the total plan area of the bearing, $T$ is the total thickness of elastomer in shear, $G$ is the shear modulus of the bearing, $E_b$ is the bulk modulus, and $S$ is a shape factor. This factor $S$ is defined as the ratio of the loaded area to the total force-free surface area:

$$S = \frac{A_1}{l_p t_e}, \tag{3.39}$$

where $A_1$ is the effective plan area of the bearing, $l_p$ is the force-free perimeter of the bearing, and $t_e$ is the effective thickness of an individual elastomer layer in compression. In case of rectangular bearings without holes, $A_1 = a'b'$, $l_p = 2(a' + b')$ with $a'$ as the effective width (i.e., the width of the reinforcing plates), and $b'$ as the effective length (i.e., the length of the reinforcing plates). The rotational stiffness of a rectangular elastomeric bearing is computed according to EN1337-3 [94] as follows:

$$K_R^{br} = G\frac{a'^5 b'}{n t_i^3 K_s}, \tag{3.40}$$

where $t_i$ is the thickness of an individual layer of elastomer, $n$ is the number of the elastomer layers, and $K_s$ is a restoring moment factor given in EN1337-3 [94].
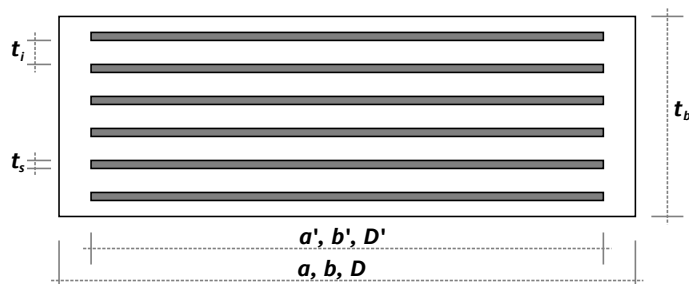
FIGURE 3.9: Cross section of an elastomeric bearing

The treatment of the bearings as spring elements has been integrated in the bridge structure and modeled in the FE model. The mode shapes that take the bearings into account have been extracted for Solution II of the dynamic problem, and the same solution algorithm for the dynamic analysis is used.

## 3.3   Summary

The vehicle and bridge models examined in this study have been discussed. The vehicle models are suspended mass models and their degrees of freedom depend on the level of modeling. Two-degree-of-freedom and eight-degree-of-freedom vehicle models are used in the dynamic analysis.

The numerical solutions for the bridge-vehicle interaction have been presented. The computational cost of one run of the dynamic solution is a decisive factor with regard to a probabilistic analysis. Thus, a long computation time would be impractical for the study. Therefore, the numerical solution based on solving the modal equations of motion using a time integration algorithm (Solution II) is adopted for the solution of the dynamic problem. However, the FEM solution (Solution I) and the analytical solution (Solution III) of the interaction are used to verify and control the dynamic solutions and their stochastic characteristics. A verification example is illustrated for a single-span bridge system, in which the three solutions show very good agreement for the dynamic responses. Moreover, the elastomeric bearings are treated as spring elements supporting the bridge structure.

It is important to set the premises of the dynamic solution since it is built on the assumption that the modeled subsystems of the vehicle, bridge, and bearings, do not show nonlinearities in their behavior. Furthermore, the vehicle models do not consider the complexities in the movement of the vehicle body, thus, the representative suspended masses are assumed to be rigid. It is assumed that there is perfect contact between the vehicle and the bridge while the vehicle is traveling at a constant speed. Moreover, the analysis is run in the pitch mode, and rolling effects are excluded.

# Chapter 4

# General Analysis of the Coupled Subsystems

## 4.1 Introduction

The modeling of the bridge-vehicle interaction has previously been discussed in Chapter 3. A general dynamic analysis aiming for a better and a more thorough examinations of the responses is performed. The constituents of the dynamic responses and their responsive behavior to different sources of excitation are investigated. Further, critical frequency ratios are derived to enable drawing generalized conclusions for the dynamic responses.

## 4.2 Bridge-Vehicle Interaction

The main influence of the bridge-vehicle interaction on the dynamic response is evident for short to medium bridges [15, 95, 96]. Therefore, most of the analyses of the dynamic responses are examined for this category of bridges. However, the response of a continuous system has been presented in order to obtain a more comprehensive investigation. The target vehicle is a heavy truck of approximately 40 tons of mass.

## 4.2.1 Bridge Systems

The systems are existing highway bridges. Their first natural bending frequency is close to the body bouncing frequency of heavy vehicles, thus, the interaction is expected to have a significant influence on the bridge response.

The first bridge is the single-span Pirton Lane highway beam bridge in Gloucester (United Kingdom) [37], Figure 4.1a. The main description of the bridge and its physical properties can be found in Section 3.1.5. The eigenfrequencies of the single-span bridge are shown in Table 4.1.

TABLE 4.1: Eigenfrequencies of the single-span bridge

| Bridge mode | Natural freq. [Hz] |
|:---:|:---:|
| $1^{st}$ | 3.18 |
| $2^{nd}$ | 12.73 |
| $3^{rd}$ | 28.65 |

The second bridge is the three-span Deibüel continuous beam bridge (Switzerland) [96], Figure 4.1c. It is a prestressed concrete box girder bridge with spans that are 37 m, 41 m, and 32 m. The structural system presented in [96] is slightly modified assuming a constant cross-sectional area and inertia over the spans. This has an effect on the values of the natural frequencies of the bridge, however, these differences are small. The bridge has an estimated mass per unit length of m $= 14225$ kg/m and a bending stiffness of EI $= 0.95 \times 10^5$ MNm$^2$. The bridge's first natural bending circular frequency is $\omega_1 = 2\pi \times 2.70$ rad/s with a presumed modal damping ratio of $\zeta_1 = 0.02$.

TABLE 4.2: Eigenfrequencies of the multi-span continuous bridge

| Bridge mode | Natural freq. [Hz] |
|:---:|:---:|
| $1^{st}$ | 2.70 |
| $2^{nd}$ | 3.98 |
| $3^{rd}$ | 5.41 |
| $4^{rd}$ | 10.82 |
| $5^{rd}$ | 13.68 |

As mentioned previously in Section 3.2, elastomeric bearings are modeled as linear springs. The spring constants are computed as $2 \times 10^9$ N/m for the vertical movement and $1 \times 10^6$ Nm/rad

for the in-plane rotational movement. Schematics of the bridge systems with elastic supports are depicted in Figures 4.1b and 4.1d.



a. single-span

b. single-span elastically supported

c. three-span continuous system

d. three-span continuous elastically supported
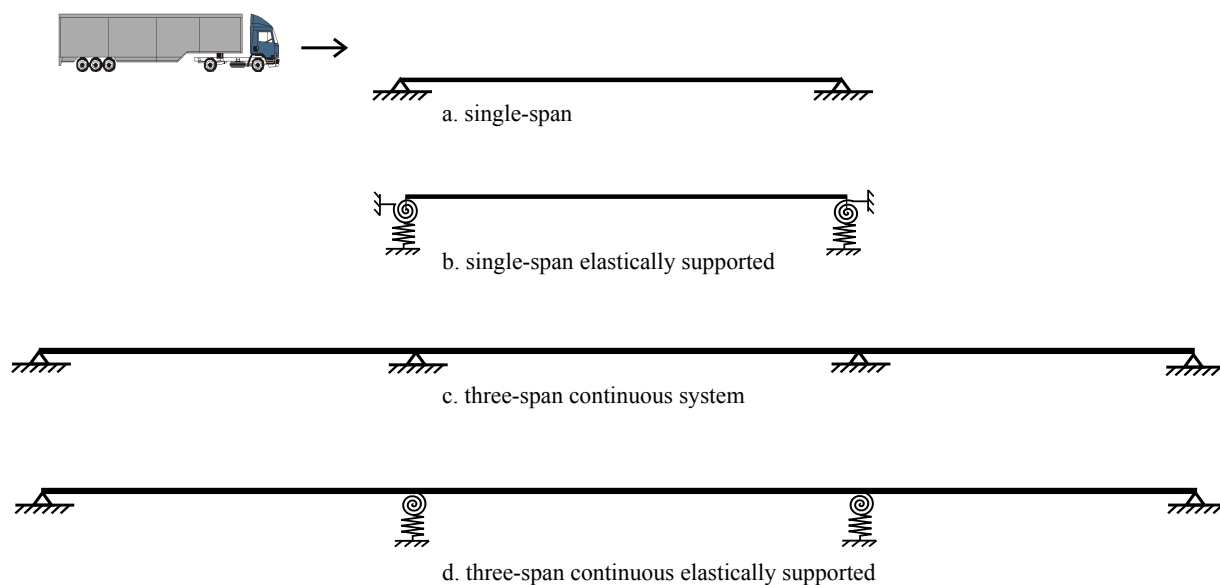
FIGURE 4.1: Schematic for the bridge systems: single-span and multi-span continuous systems

## 4.2.2 Vehicle Models

The common models for vehicles are suspended mass models for which the level of modeling defines the degrees of freedom considered. There are different models for heavy vehicles found in the literature, some of which have been discussed in Section 3.1.1.

### 4.2.2.1 Vehicle Model: 2DOF

The vehicle is modeled as a two-degree-of-freedom model (2DOF model). The dynamic characteristics and matrices of this model are presented in Section 3.1.1. This type of model considers the bouncing of the body mass and the axle hop vibrational modes, which are essential for the dynamic response of the bridge. The bouncing mode is particularly important because it is often within the range of the first natural frequency of most highway beam bridges. The characteristics of the vehicle and its modal information are presented in Tables 4.3 and 4.4

TABLE 4.3: Vehicle parameters (2DOF)
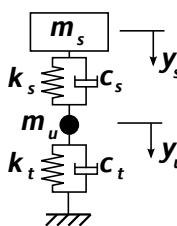


Body mass $(m_s) = 36\,\text{ton}$
Axle mass $(m_u) = 4\,\text{ton}$
Suspension stiffness $(k_s) = 1.8 \times 10^7\,\text{N/m}$
Tire stiffness $(k_t) = 7.2 \times 10^7\,\text{N/m}$
Suspension damping $(c_s) = 14.4 \times 10^5\,\text{Ns/m}$
Tire damping $(c_t) = 14.4 \times 10^5\,\text{Ns/m}$

TABLE 4.4: Eigenfrequencies of the (2DOF) vehicle

| Vehicle mode | Natural freq. [Hz] |
|---|---|
| Bouncing of body mass | 3.18 |
| Axle hop | 23.85 |

### 4.2.2.2  Vehicle Model: 8DOF

A more realistic model for a five-axle heavy vehicle is also described in Section 3.1.1. The vehicle is composed of a two-axle tractor and a three-axle semi-trailer connected with a hinge. The effect of vehicle roll on bridge dynamics is not considered, and the analysis is performed in the pitch plane only.

The characteristics of the vehicle are obtained from [80] and are presented in Figure 4.2. The eigenmodes with their corresponding eigenfrequencies are computed and presented in Table 4.5. It can be observed that the heavy vehicle has two ranges of vibrational frequencies, the first range is from 1.5 Hz to 5 Hz, representing the sprung mass bounce involving pitching and axle hop movements; the second range is 8 Hz to 12 Hz, representing the axle hop involving slight suspension pitch modes.

TABLE 4.5: Eigenmodes and eigenfrequencies of the (8DOF) vehicle

| Vehicle mode | Freq. [Hz] | Mode shape | | | | | | | |
|---|---|---|---|---|---|---|---|---|---|
| | | $y_t$ | $\theta_t$ | $\theta_s$ | $y_1$ | $y_2$ | $y_{31}$ | $y_{32}$ | $y_{33}$ |
| Bounce of body mass | 1.4 | 1.00 | -0.21 | -0.02 | 0.21 | 0.11 | 0.07 | 0.06 | 0.05 |
| Bounce and pitch | 1.6 | 1.00 | -0.61 | 0.02 | 0.25 | -0.12 | -0.07 | -0.8 | -0.09 |
| Pitch, axle hop, and bounce | 4.6 | 0.34 | 1.00 | -0.62 | -0.04 | 0.79 | 0.18 | 0.32 | 0.46 |
| Axle hop (tractor front) | 8.9 | -0.03 | 0.01 | 0.00 | 1.00 | 0.01 | 0.00 | 0.00 | 0.00 |
| Axle hop (tractor rear) | 10.4 | -0.02 | -0.07 | 0.04 | 0.00 | 1.00 | 0.03 | 0.06 | 0.09 |
| Axle hop (tridem middle) | 12.0 | 0.00 | 0.00 | 0.00 | 0.00 | 0.00 | -0.50 | 1.00 | -0.50 |
| Axle hop (tridem front) | 12.0 | 0.00 | 0.00 | 0.00 | 0.00 | 0.00 | 1.00 | 0.21 | -0.58 |
| Axle hop (tridem rear) | 12.1 | 0.00 | 0.00 | 0.00 | 0.00 | 0.00 | 0.50 | -0.58 | 1.00 |
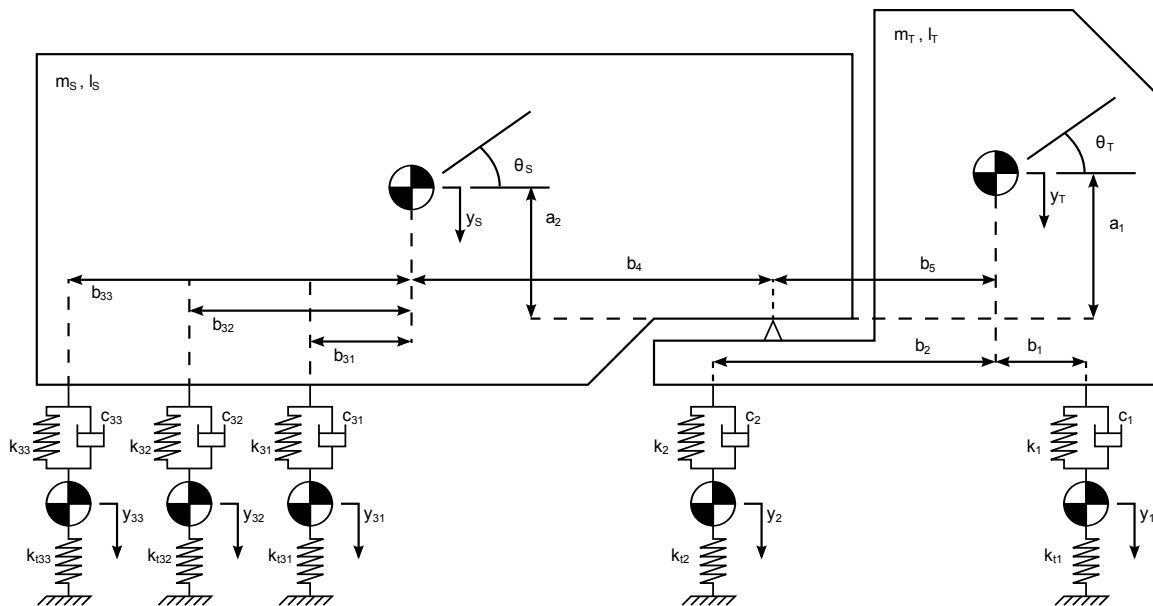
(a) Sketch of a truck model

| Dimensional data (m) | | |
|---|---|---|
| $a_1$ = -0.13 | $b_4$ = 2.40 | |
| $a_2$ = 1.10 | $b_5$ = 3.50 | |
| $b_1$ = 0.50 | $b_6$ = 4.15 | |
| $b_2$ = 2.50 | $b_7$ = 2.15 | |
| $b_3$ = 1.30 | | |

| Mass parameters (kg) | |
|---|---|
| Tractor sprung mass ($m_t$) | 4500 |
| Semi-trailer sprung mass ($m_s$) | 31450 |
| Tractor front axle mass ($m_1$) | 700 |
| Tractor rear axle mass ($m_2$) | 1100 |
| Semi-trailer tridem mass ($m_{31}$, $m_{32}$, $m_{33}$) | 750 |

| Inertia parameters (kg m$^2$) | |
|---|---|
| Tractor pitch moment of inertia ($I_t$) | 4604 |
| Semi-trailer pitch moment of inertia ($I_s$) | 16302 |

| Suspension parameters (kN/m) | |
|---|---|
| Tractor front axle ($k_1$) | 400 |
| Tractor rear axle ($k_2$) | 1000 |
| Semi-trailer tridem axle ($k_{31}$, $k_{32}$, $k_{33}$) | 750 |

| Damping parameters (kNs/m) | |
|---|---|
| Tractor front axle ($c_1$) | 10 |
| Tractor rear axle ($c_2$) | 10 |
| Semi-trailer tridem axle ($c_{31}$, $c_{32}$, $c_{33}$) | 10 |

| Tire stiffness (kN/m) | |
|---|---|
| Tractor front axle ($k_{t1}$) | 1750 |
| Tractor rear axle ($k_{t2}$) | 3500 |
| Semi-trailer tridem axle ($k_{t31}$, $k_{t32}$, $k_{t33}$) | 3500 |

(b) Vehicle parameters (8DOF)

FIGURE 4.2: Vehicle parameters (8DOF)

### 4.2.3 Road Unevenness

Road unevenness is often obtained by measuring existing roadways using profilometers, which is a laborious time-consuming procedure. Therefore, [26] suggested a simplified way of representing road surfaces. The authors describe road unevenness as a Gaussian random process characterized by a spatial power spectral density function (PSD), which was explained earlier in Section 3.1.4. The work of [26] has served as the basis for ISO 8608 [27] which classify the roadway profiles according to their degree of roughness. In order to generate artificial road profiles, a description of the PSD is provided by the ISO 8608 [27], which is represented as:

$$S_{FF}(\kappa) \quad = \quad S_{FF}(\kappa_0) \left( \frac{\kappa}{\kappa_0} \right)^{-a},$$

where $\kappa$ is the unevenness wavenumber, $a$ is taken as 2, and the value of $S_{FF}(\kappa_0)$ depends on the road condition class. Some of these classes are given in Table 4.6. The dynamic analysis is performed in the time domain, therefore, a description of the road unevenness in the time domain is needed. Consequently, the temporal power spectral function $S_{FF}(\omega)$ is required with $\omega$ as the temporal frequency. Equation (3.34) illustrates the relationship between $S_{FF}(\kappa)$ and $S_{FF}(\omega)$, which has been used in the realization of road unevenness. The cut-off temporal frequencies used in the road profile realizations are chosen to bound the ranges of frequencies of the road unevenness to those that coincide with the frequencies of vibration of the vehicle models. Each realization of road profiles follows Equation (3.36) where $\omega_l = 1.74$ rad/s and $\omega_u = 34.90$ rad/s for the two-degree-of-freedom vehicle model, and $\omega_l = 1.74$ rad/s and $\omega_u = 75.54$ rad/s for the eight-degree-of-freedom vehicle model with $\Delta\omega = 0.104$ rad/s. The road profiles generated are passed through a moving average filter to take the tire envelopment of road unevenness into account, [89]. Two examples of road profiles of class A generated are depicted in Figure 4.3(a) and their computed PSDs are shown in Figure 4.3(b). The upper and the lower cut-off wavenumbers corresponding to the cut-off temporal frequencies according to Equations (3.31) and (3.37) can be seen in Figure 4.3(b). Well-maintained highway roads are assumed to have very good to good road conditions [40]. Therefore, these road classes are adopted for the realizations of road profiles, which are used in the dynamic analysis.

TABLE 4.6: ISO 8608 road profile classifications

| Class | $S_{FF}(\kappa_0)[\times 10^{-6}\,\mathrm{m}^3/\mathrm{cycle}]$ | | |
| | Min. | Mean | Max. |
| --- | --- | --- | --- |
| A | 0 | 1 | 2 |
| B | 2 | 4 | 8 |
| C | 8 | 16 | 32 |
| D | 32 | 64 | 128 |
| E | 128 | 256 | 512 |
| F | 512 | 1024 | 2048 |
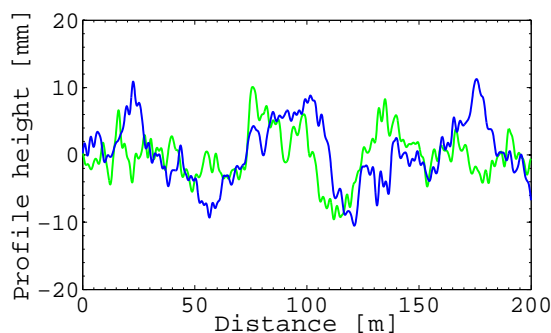


(a) Artificial road profiles of Class A
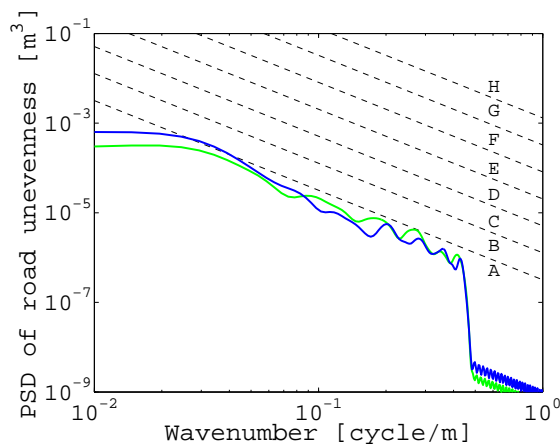


(b) Computed PSD for the artificial road profiles and the PSD specified by ISO 8608

FIGURE 4.3: Artificial road profiles of Class A and their PSDs

## 4.3 Dynamic Analysis

The dynamic analysis is performed using a non-iterative algorithm to solve the differential equations of the bridge and the vehicle systems using the Newmark-$\beta$ time integration method [21]. This solution algorithm allows reasonable computational time for the systems used in the analysis.

## 4.3.1 General Analysis

Many experimental studies that have investigated and quantified the dynamic response of bridges due to traveling vehicles have showed inconsistent results, especially when different response measures have been used as mentioned in [16, 46, 96, 97]. Therefore, three responses are considered for this analysis: displacements as a structural serviceability measure, strains as a structural design measure, and accelerations as a vibrational serviceability measure. The numerical estimates used to quantify these measures are the Dynamic Incremental Factor for the displacements ($\mathrm{DIF}_u$) and strains ($\mathrm{DIF}_\varepsilon$), and the maximum accelerations. The Dynamic Incremental Factor is defined as the ratio of a maximum dynamic response to the corresponding static one within a cycle of the dynamic response [98]. Furthermore, the maximum accelerations are normalized by the gravitational acceleration. The aforementioned numerical estimates for quantifying the dynamic response are determined at the mid-span of the single system and the middle of the first span of the continuous system as these locations are critical for the static response.

For the eight-degree-of-freedom vehicle model, the maximum dynamic response when studying its time history depends on the position of the axle of the vehicle. Figure 4.4 depicts the response at the contact point of every axle of the eight-degree-of-freedom vehicle model as it moves over the single-span bridge system. The maximum displacements and strains are attained as the rear axle of the semi-trailer reaches the mid-span as shown in Figures 4.4(a) and 4.4(b). The accelerations attain their maximum values when the tractor's axles pass the mid-span, Figure 4.4(c). The same observations are made for the continuous system, Figure 4.5. The maximum displacements and strains occur when the semi-trailer's tridem axles travel over the middle of the first span, Figures 4.5(a) and 4.5(b). Whereas the accelerations are more sensitive to the movement of the tractor axles, Figure 4.5(c). In order to calculate the Dynamic Incremental Factor, the static response for the eight-degree-of-freedom vehicle model is computed when the rear axle of the semi-trailer is at the location chosen for the single-span and continuous bridge systems.

A common assumption in the analysis of beam bridges is that the support conditions are perfect pin supports. The influence of the bridge's bearings, i.e., elastomeric bearings, has

(a) Displacements



(b) Strains



(c) Accelerations
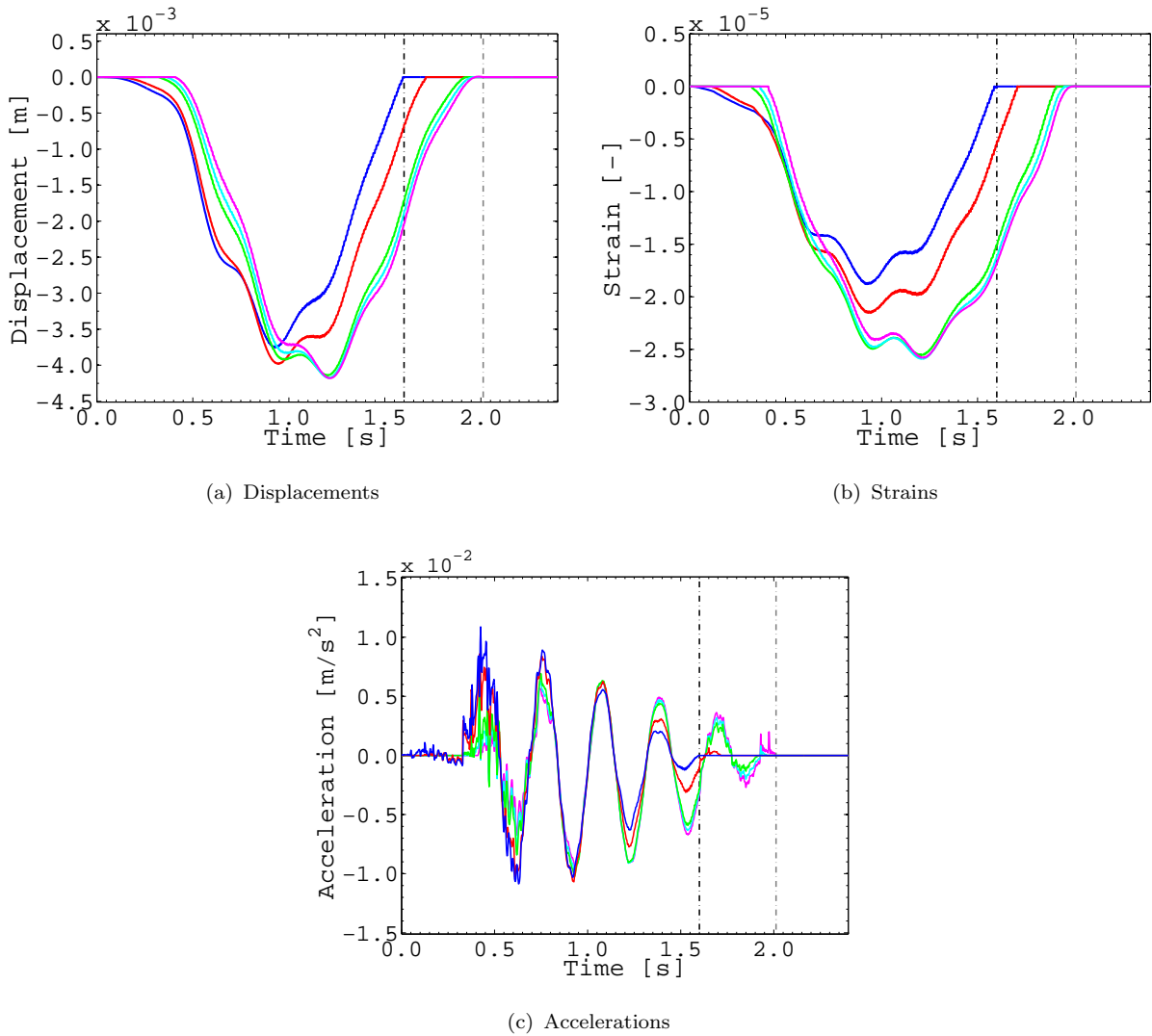
FIGURE 4.4: Dynamic responses of the single-span system at the contact points of the (8DOF) vehicle: (—) Tractor front axle, (—) Tractor rear axle, (—) Semi-trailer front axle, (—) Semi-trailer middle axle, (—) Semi-trailer rear axle

been addressed in a number of studies [1, 6, 92]. These studies examine the effects of including the elastomeric bearings in the bridge model on global or local, as well as in or out of the plane displacements and/or rotations of the bridge. It was found that the inclusion of bearings in the dynamic analysis resulted in larger displacements, especially the horizontal ones [92]. Furthermore, the traffic-induced accelerations of the bridge when considering the elastomeric bearings were greater than those of the bridge with pin bearings [6]. Figures 4.6 and 4.7 depict the effect of elastomeric bearings (ignoring road unevenness) for the single-span and continuous bridge systems, respectively. In addition, the dynamic response retrieved from the two-degree-of-freedom and eight-degree-of-freedom vehicle models

(a) Displacements

(b) Strains

(c) Accelerations
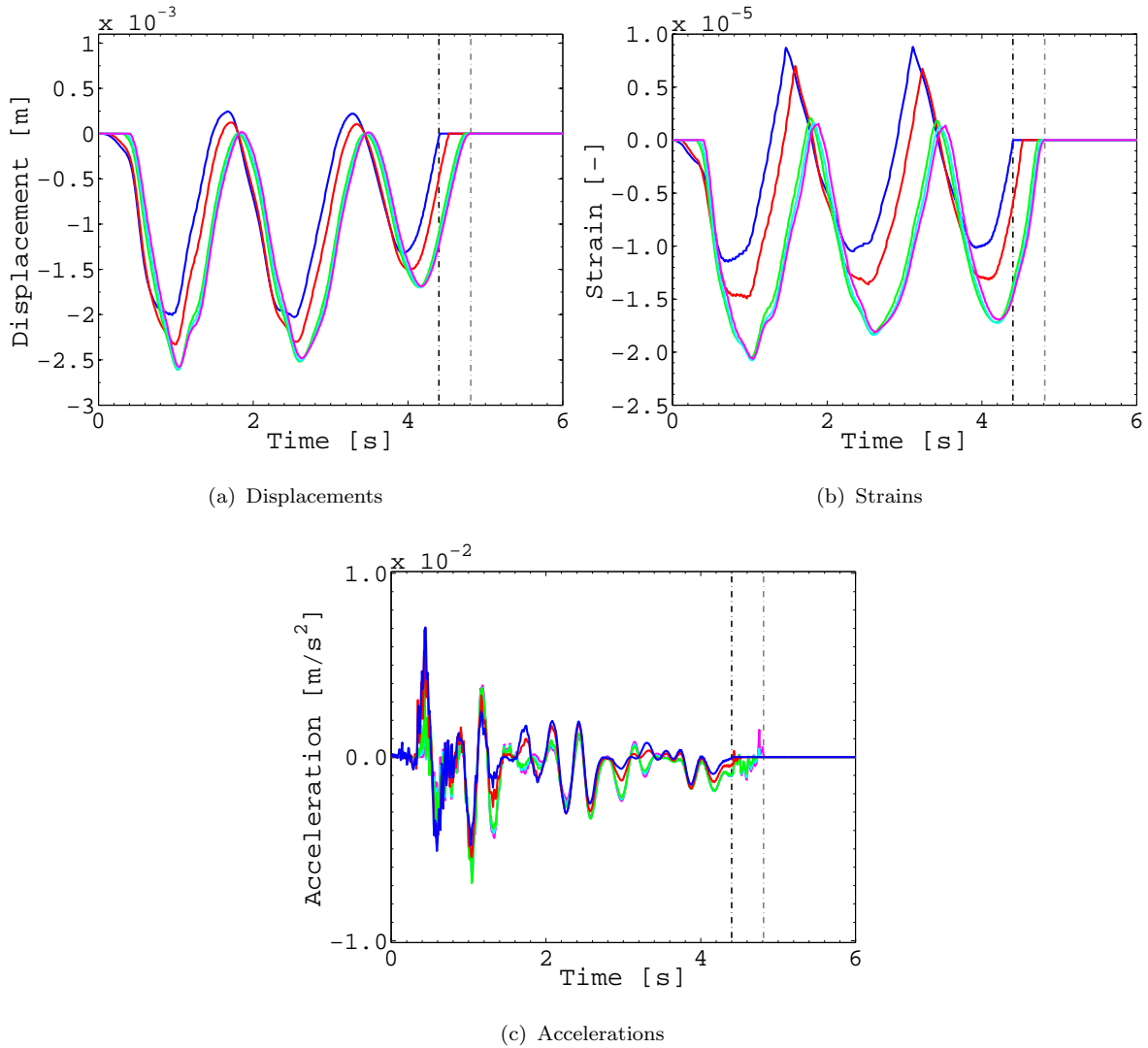
FIGURE 4.5: Dynamic responses of the continuous system at the contact points of the (8DOF) vehicle: (—) Tractor front axle, (—) Tractor rear axle, (—) Semi-trailer front axle, (—) Semi-trailer middle axle, (—) Semi-trailer rear axle

are also compared in Figures 4.6 and 4.7. For the single-span system (Figure 4.6), the main difference in the response stems from the vehicle model used in the analysis. The two-degree-of-freedom vehicle model is rather conservative, which is understandable as it assumes a concentrated mass, whereas the total mass of the eight-degree-of-freedom vehicle model is distributed according to its axles. The dynamic response of the bridge obtained with the eight-degree-of-freedom vehicle model is less than the response obtained with the two-degree-of-freedom vehicle model. The difference between the responses of the two models is 5% for the displacements, 6% for the strains, and 57% for the max. accelerations. The second difference in the response stems from the influence of considering the bearings

in the bridge model, which is evident for the accelerations as shown in Figure 4.6(c), less apparent for the displacements as shown in Figure 4.6(a), and insignificant for the strains as shown in Figure 4.6(b). The same results are obtained for the continuous system, as seen in Figure 4.7. It can be observed from Figure 4.7 that the main differences of the responses of the continuous system are also a result of the type of vehicle model used, i.e., the dynamic response of the bridge resulting from the eight-degree-of-freedom vehicle model is less than the response resulting from the two-degree-of-freedom vehicle model, which is broken down as follows: 6% for the displacements, 9% for the strains, and 86% for the max. accelerations. A time shift can be seen in Figures 4.6 and 4.7 between the maximum response due to the two-degree-of-freedom and the eight-degree-of-freedom vehicle model. This time shift is the time needed for the rear axle of the semi-trailer to reach the critical location for obtaining the maximum dynamic response.

The worst cases of the dynamic responses are to be selected for more detailed analysis. Therefore, the dynamic estimates are compared for four cases, which are listed below and shown in Figure 4.8:

- Single-span system traversed by the two-degree-of-freedom vehicle model (Case 1)

- Single-span system traversed by the eight-degree-of-freedom vehicle model (Case 2)

- Continuous system traversed by the two-degree-of-freedom vehicle model (Case 3)

- Continuous system traversed by the eight-degree-of-freedom vehicle model (Case 4)

It can be observed from Figure 4.8 that the $\text{DIF}_u$ and $\text{DIF}_\varepsilon$ are dependent on the speed of the vehicle, which will be explained in Section 4.3.5. Further, the maximum accelerations are generally positively proportional to the speed. The dynamic response of Cases 1 and 2 (using the single-span system) have produced the highest values for the dynamic response estimates as depicted in Figure 4.8, therefore, they been selected as the worst cases of the dynamic response, which will be used for the further analyses.

A detailed analysis is performed for the dynamic responses, in which their constituents and frequency contents are examined. Such a study helps to develop a better understanding
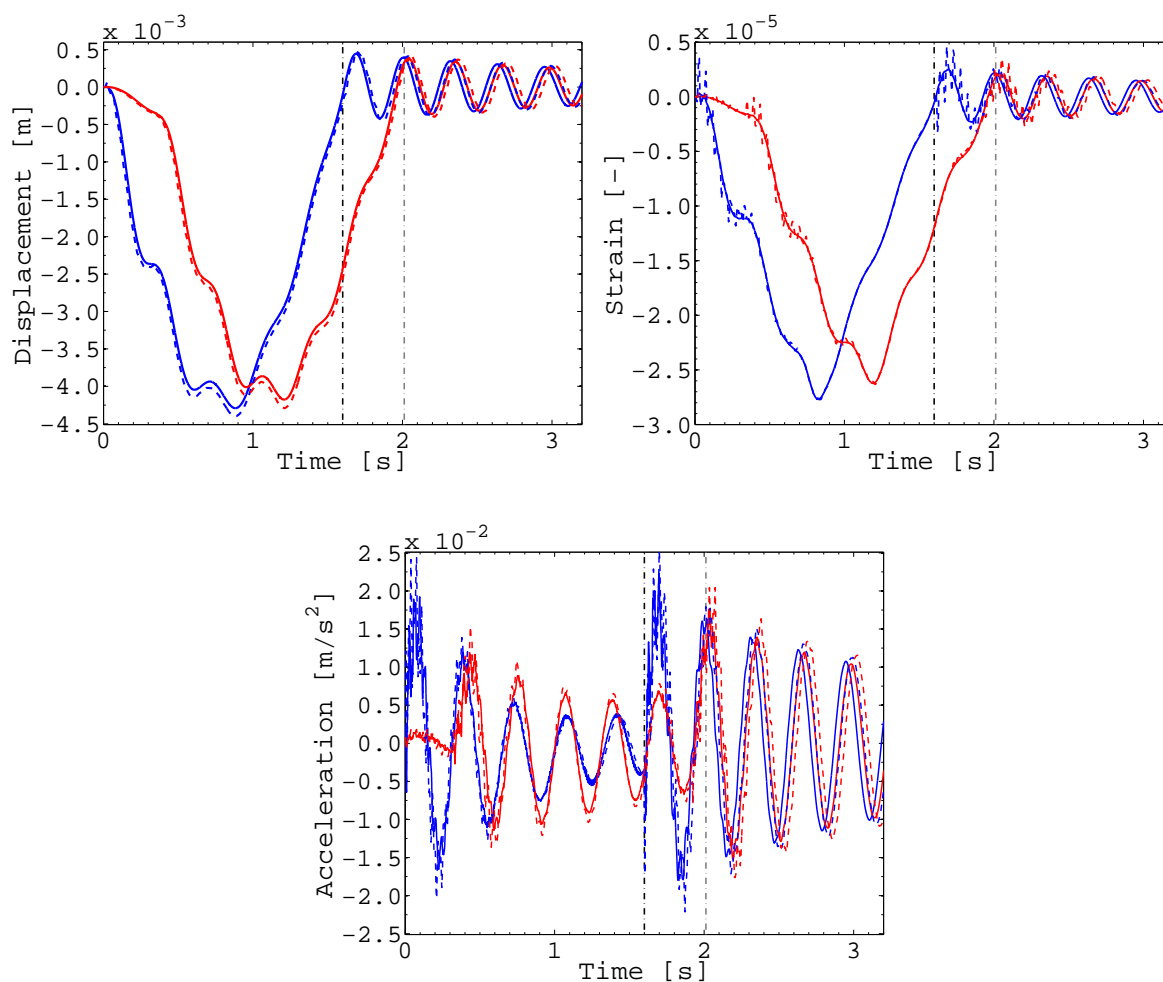
FIGURE 4.6: Dynamic responses of the single-span system at mid-span: (—) Response for the 2DOF vehicle model assuming pin supports, (- -) Response for the 2DOF vehicle model assuming elastic spring supports, (—) Response for the 8DOF vehicle model assuming pin supports, (- -) Response for the 8DOF vehicle model assuming elastic spring supports

of the dynamic problem and also explains the tendencies that arise when the probabilistic study is introduced and applied.

## 4.3.2   Mode Contributions to the Dynamic Responses

The first step is to assess the contribution of the vibrational modes to the dynamic responses. Figure 4.9 depicts the contribution of either the first mode or multi-mode (up to the fiftieth) solution to the dynamic response of the single-span bridge system when the two-degree-of-freedom vehicle model travels over it at a speed of $25\,\mathrm{m/s}$ ($90\,\mathrm{km/h}$). The number of vibrational modes considered and the degree to which they influence the quality
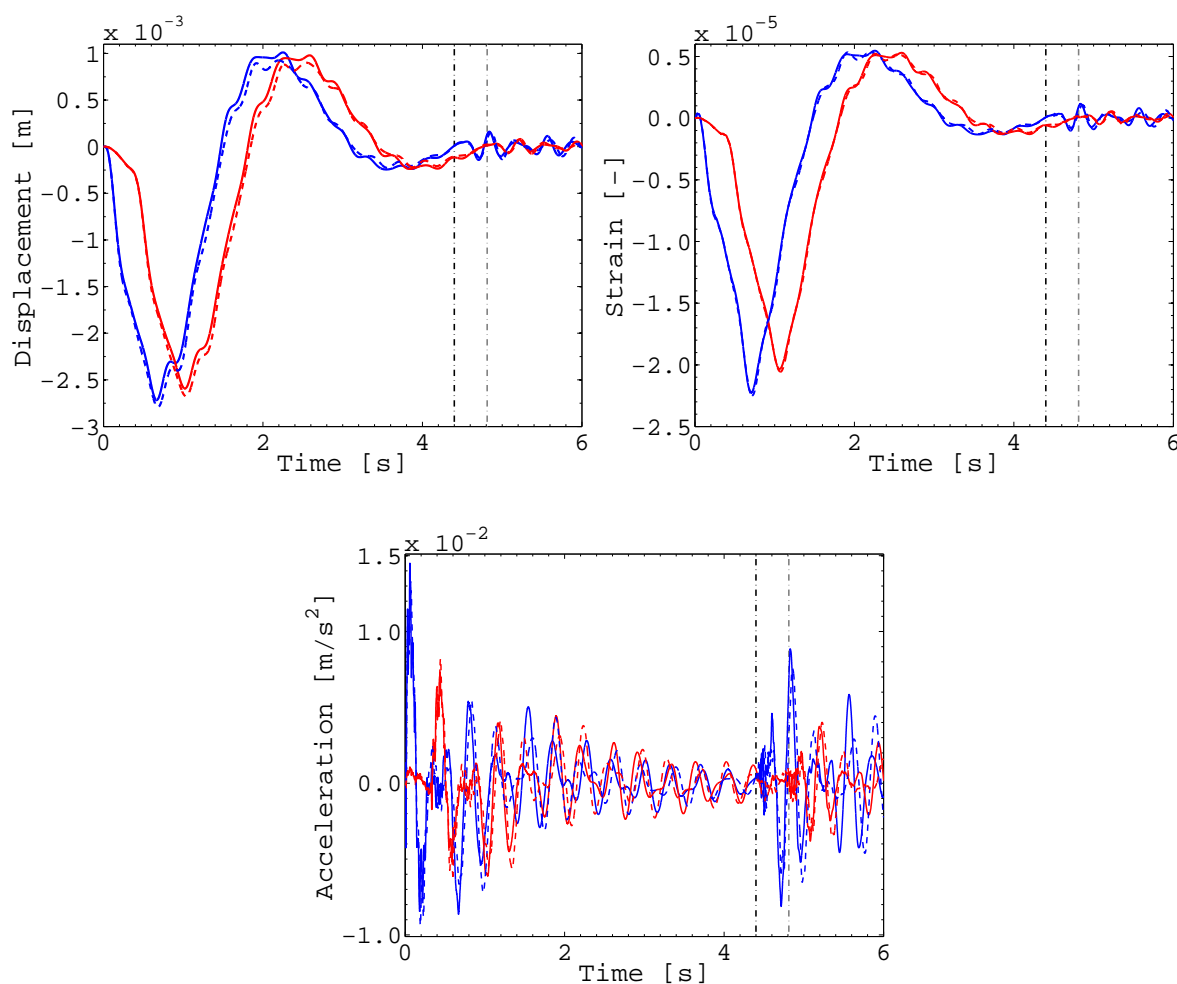
FIGURE 4.7: Dynamic responses of the continuous system at the middle of the first span: (—) Response for the 2DOF vehicle model assuming pin supports, (- -) Response for the 2DOF vehicle model assuming elastic spring supports, (—) Response for the 8DOF vehicle model assuming pin supports, (- -) Response for the 8DOF vehicle model assuming elastic spring supports

of the dynamic estimate depends on the response studied. This dependency is illustrated in Table 4.7, where each entry represents the ratio between the maximum dynamic response obtained after performing the dynamic analysis up to an assigned vibrational mode and the response of the multi-mode solution. At 98.7%, the first mode is almost enough to describe the displacements appropriately, whereas strains and accelerations require higher modes to obtain estimates with the same degree of accuracy as the displacements. The same observation is made when the eight-degree-of-freedom vehicle model is used in the dynamic analysis. The dependency of the response on the number of mode shapes analyzed may explain the inconsistency in quantifying the dynamic response when different response estimates are
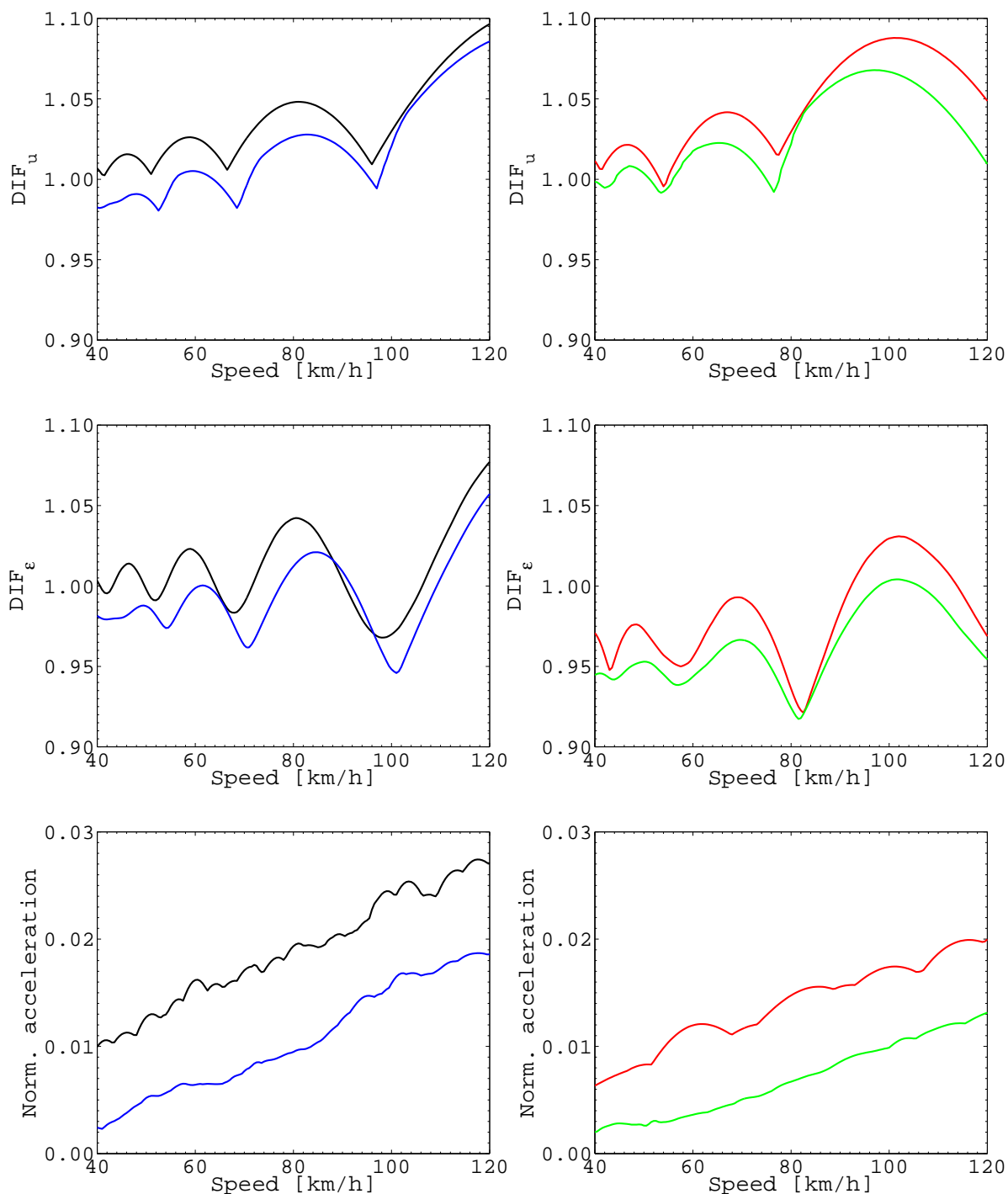
FIGURE 4.8: The dynamic response estimates against the speed of the vehicle: (—) Case 1, (—) Case 2, (—) Case 3, (—) Case 4

obtained from experimental studies.

TABLE 4.7: Ratios of the mode contribution to the dynamic response

| up to | Displacement | | Strain | | Acceleration | |
|---|---|---|---|---|---|---|
| | 2DOF | 8DOF | 2DOF | 8DOF | 2DOF | 8DOF |
| $1^{st}$ | 0.987 | 0.992 | 0.850 | 0.877 | 0.792 | 0.846 |
| $2^{nd}$ | 0.988 | 0.992 | 0.851 | 0.877 | 0.792 | 0.846 |
| $3^{rd}$ | 0.999 | 0.999 | 0.934 | 0.948 | 0.977 | 0.944 |
| $\vdots$ | $\vdots$ | $\vdots$ | $\vdots$ | $\vdots$ | $\vdots$ | $\vdots$ |
| $11^{th}$ | 0.999 | 0.983 | 0.975 | 0.983 | 0.994 | 0.973 |
| $\vdots$ | $\vdots$ | $\vdots$ | $\vdots$ | $\vdots$ | $\vdots$ | $\vdots$ |
| $21^{st}$ | 0.999 | 0.999 | 0.991 | 0.997 | 0.998 | 0.995 |
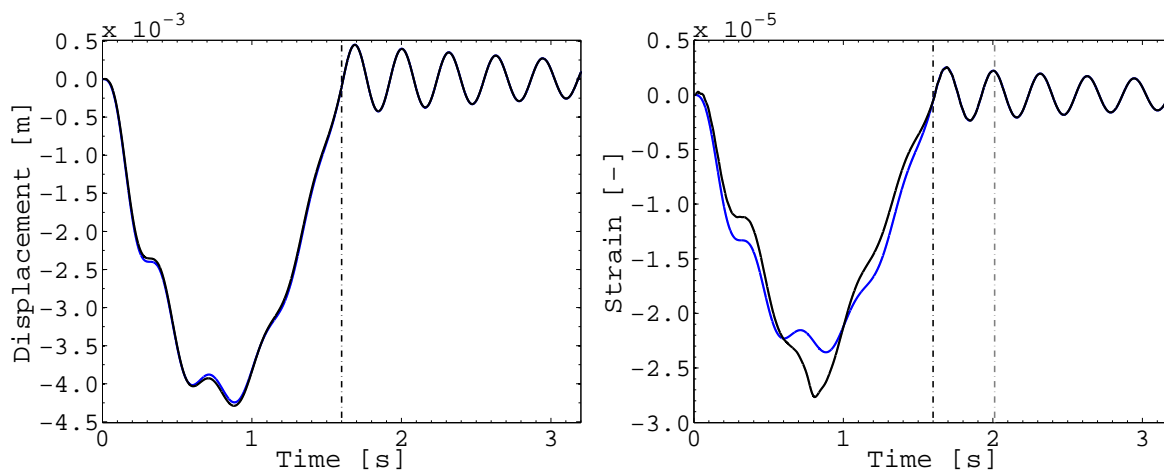


FIGURE 4.9: Vibrational mode contributions to different responses: (—) First mode solution, (—) Multi-mode solution

### 4.3.3 Sources of Excitation and their Interactions

The focus of the dynamic problem studied is the interaction between the bridge and vehicle when road unevenness is considered. As the vehicle travels over the bridge, its dynamic tire forces introduce dynamic effects on the bridge. These effects are mainly due to the excitation of the vehicle caused by the dynamic deflection of the bridge (*Source I*) and the initial road unevenness (*Source II*). The combination of these two excitations describes the dynamic effect of the coupling of the vehicle and bridge on the response of interest. Figure 4.10 depicts the mid-span displacements of the single-span system, i.e., the total response and its constituents due to the two-degree-of-freedom vehicle models traveling at a speed of $25\,\mathrm{m/s}$ ($90\,\mathrm{km/h}$). The total response is the moving weight solution combined with the interaction of the two sources of excitation. The interactions between the excitations caused by the

dynamic deflection of the bridge and road unevenness vary, thereby having different effects on the moving weight solution. In addition, the amplitudes of the excitations due to road unevenness have a great influence on the additional dynamic effects caused by bridge-vehicle interaction as these excitations may render the ones due to the dynamic deflection of the bridge to secondary. Figure 4.10 depicts two examples for the two-degree-of-freedom vehicle model excited by two different road profiles while traveling over the bridge. Figure 4.10(a) shows the excitations to be significant enough to amplify the dynamic response. This case is attributed as "greatly amplified". Whereas, Figure 4.10(b) shows the excitations being out-of-phase with approximately equal amplitudes to cancel each other, thereby having no significant effect on the moving weight solution. This case is attributed as "slightly amplified". This observation depends on the interaction between the excitations due to the dynamic deflection of the bridge and road unevenness as well as the internal interaction between the excitations caused by the frequencies constituting the road unevenness.

The interaction forces corresponding to the displacements in Figure 4.10 are retrieved and plotted for both cases in Figure 4.11. It can be seen that the maximum of the interaction forces for the greatly amplified case is larger by a factor of 1.95 when compared to the slightly amplified case as shown in Figure 4.11(a). In studying the amplitude spectra shown in Figure 4.11(b), it is observed that the amplitudes around the bouncing frequency of the vehicle and the bridge's first natural frequency (3.2 Hz) are higher for the greatly amplified case.

The realization of road profiles is described in Section 3.1.4 as a summation of cosine waves with random phase angles. Hence, the main difference between a realization and another is the randomly selected phase angles, which are introduced to ensure the randomness of the generated road profiles. Therefore, it is logical to assume that these phase angles are the reason behind the variation of the effects caused by road unevenness on the dynamic response. In order to examine this, the interaction forces caused by a single harmonic excitation related to one of the frequencies describing the road unevenness are determined and shown in Figure 4.12. The frequencies are selected around the bouncing frequency of the vehicle, and the same set of data employed in the realizations of the road profiles for the analyses in Figure 4.10 are used. It can be seen from Figure 4.12, that the interaction forces caused by single harmonic excitations vary from being in-phase and out-phase. Therefore,

the forces in Figure 4.12 may amplify or cancel each other depending on the phase angles assigned to the exciting frequencies of the road profile. Also in Figure 4.12, the sum of the interaction forces due to the single harmonic excitations is computed to show the amplification (Figure 4.12(b)) or the cancellation (Figure 4.12(b)) of the output; the sum holds as linear systems are assumed. The same analysis can be performed for all frequencies of the road profile and this amplification or cancellation of the exciting forces would explain the difference in the total contact forces observed in Figure 4.11 and in the responses in Figure 4.10. The above are only examples of what can be expected when performing the dynamic analysis considering road unevenness, which may explain the output of the dynamic analysis and its scatter when a probabilistic analysis is run.



(a) greatly amplified          (b) slightly amplified
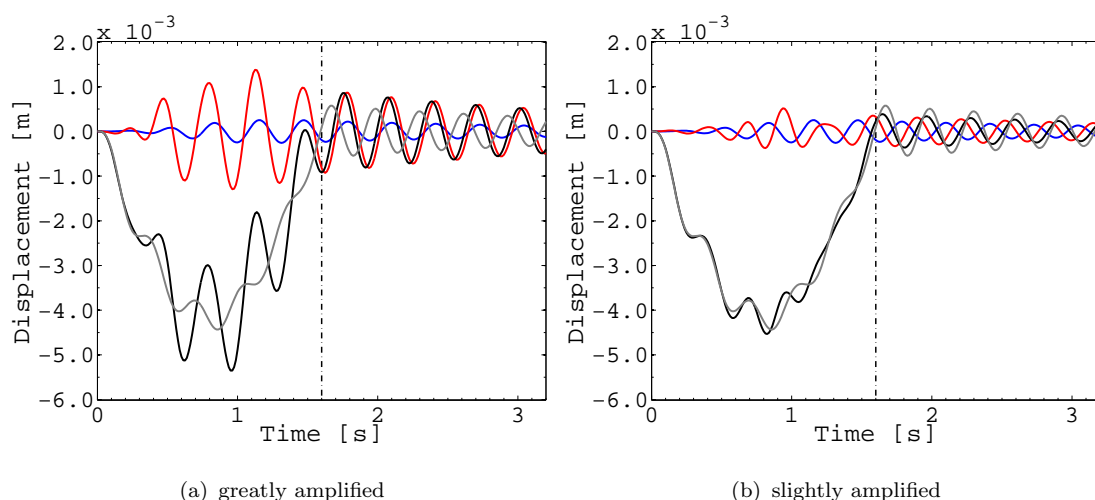
FIGURE 4.10: Decomposition of the mid-span displacement of the single-span system: (—) Source I, (—) Source II, (—) Total coupled response, (—) Moving weight

## 4.3.4   Frequency Content of the Dynamic Responses

The frequency content of the dynamic responses is examined as it gives an idea of their responsive behavior in relation to the sources of excitation. The amplitude spectra of the dynamic responses of the single-span system with the two-degree-of-freedom vehicle traveling over it are shown in Figure 4.13. It can be seen that the displacement and strain amplitude spectra show the same pattern compared with the spectrum for the acceleration. In general the response due to the moving weight is of a low frequency content. However, in looking at the bridge-vehicle interaction, another peak appears around the first bending natural

(a) Interaction forces

(b) Amplitude spectra of interaction forces
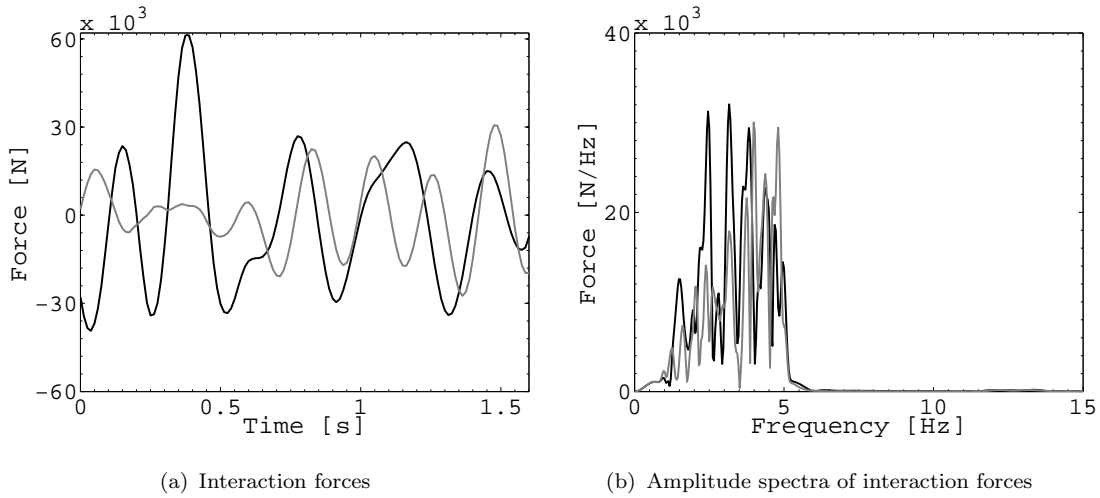
FIGURE 4.11: Contact forces between 2DOF vehicle model and the bridge considering road unevenness: (—) greatly amplified, (—) slightly amplified



(a) greatly amplified: In-Phase excitations

(b) slightly amplified: Out-of-Phase excitations
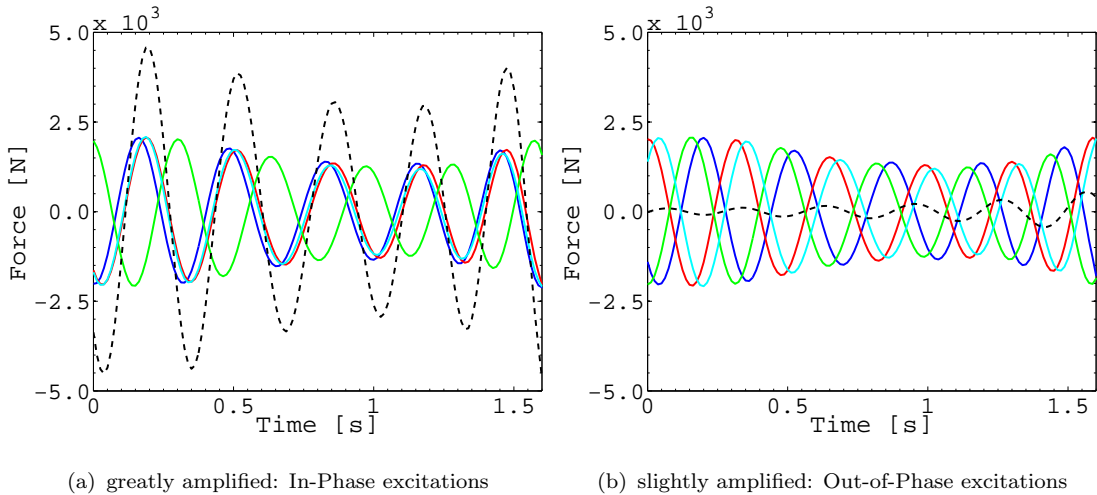
FIGURE 4.12: Contact forces due to single excitations of road unevenness temporal frequencies: (—) $\omega_1 = 19.87$ rad/s, (—) $\omega_2 = 19.94$ rad/s, (—) $\omega_3 = 20.03$ rad/s, (—) $\omega_4 = 20.11$ rad/s, (- - -) Sum

frequency of the bridge system (3.2 Hz), which coincides with the bouncing frequency of the vehicle. Furthermore, when road unevenness is considered the main additional contribution to the response amplitude is at 3.2 Hz. This additional contribution is only obtained when the bridge-vehicle interaction is considered. Again, estimates of the response studied react differently to the excitation caused by road unevenness because the response's amplitudes increase in varying degrees around the bridge's natural frequency, i.e., the displacement's amplitude increases by a factor of 3.33, the strain's amplitude by 1.66, and the acceleration's

amplitude by 3.27. The same examination is carried out for the eight-degree-of-freedom vehicle model traveling over the bridge system and depicted in Figure 4.14. Similar observations are made for the displacements and strains, however, their responsive behavior to the excitation caused by the road unevenness is not as strong as when the two-degree-of-freedom vehicle model is used in the analysis. The response amplitudes increase around the bridge's natural frequency by a factor of 1.67 for the displacements and by 1.51 for the strains. In studying the accelerations, it can be seen that the amplitude spectrum has several peaks; the main peak is around the bridge's first natural frequency and the other peaks, which are of smaller magnitude, appear around the axle hop frequencies of the tractor and the semi-trailer. The response amplitude of the accelerations increases by a factor of 1.55 around the bridge's first natural frequency.

The conclusion that can be drawn after investigating the amplitude spectra of the responses is that the estimate of the displacements and accelerations are highly influenced by the coupled model considering road unevenness, followed by the strains. Furthermore, these results depend on the vehicle model used in the dynamic analysis, e.g., the two-degree-of-freedom vehicle model shows higher sensitivity to road unevenness in comparison with the eight-degree-of-freedom vehicle model.

In short, the above analyses show the response constituents and their responsive behavior when road unevenness is considered. This is of great help when examining the output of the probabilistic analysis. The magnitude and scatter of the responses of the coupled subsystems when road unevenness is considered rely on the main contributing frequencies and their corresponding amplitudes.

## 4.3.5   Critical Ratios

The results for the dynamic responses studied in the previous subsections depend on the frequencies of the bridge, the vehicle and the driving speed used in the analysis. The influence of these frequencies and their interaction on the dynamic response is evident. A number of studies have focused on the relation between the dynamic response and speed. In the study done by [11], it was found that a unique function for the maximum dynamic response
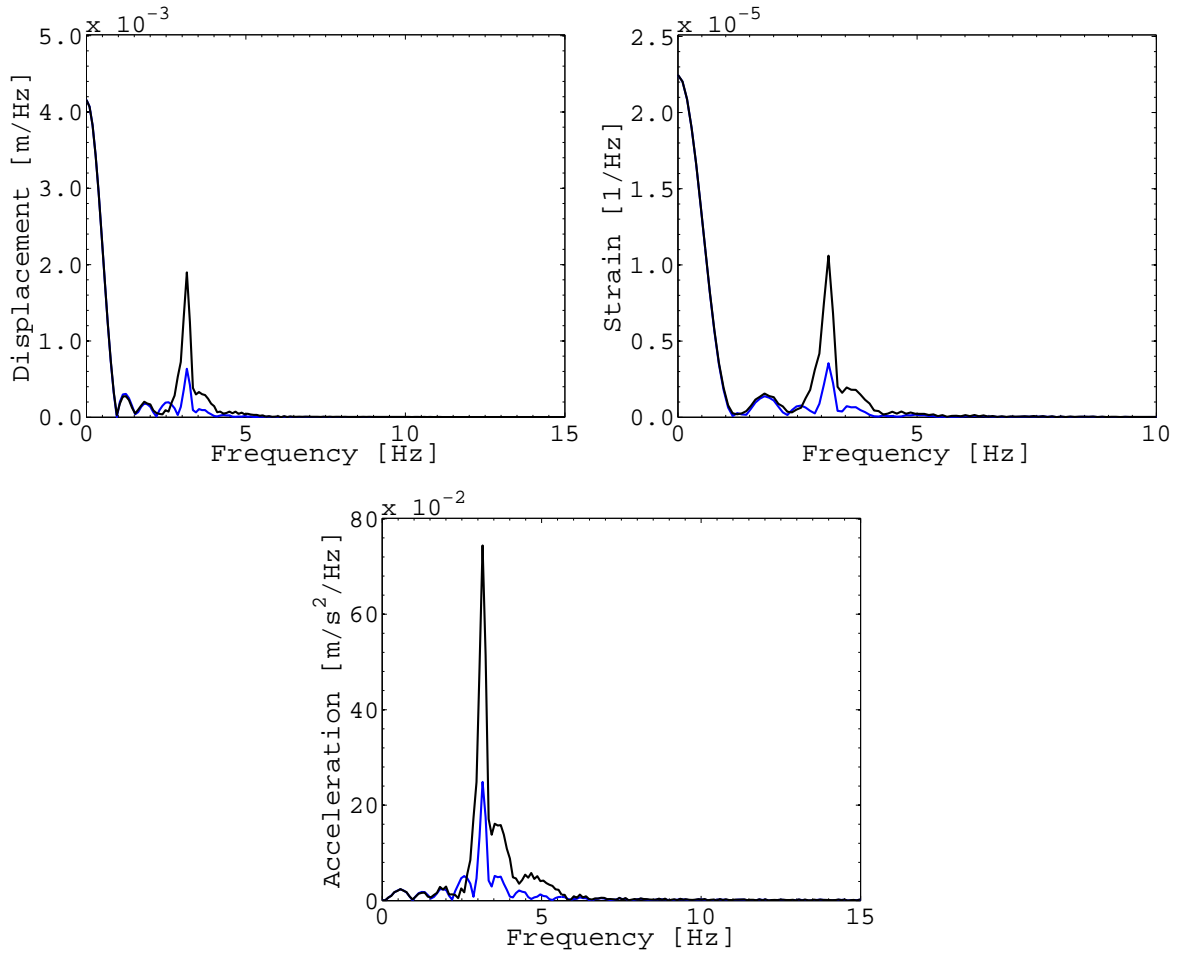
FIGURE 4.13: Amplitude spectra of the dynamic response due to excitation of the 2DOF vehicle: (—) Amplitude spectrum for the dynamic response ignoring road unevenness, (—) Amplitude spectrum for the dynamic response considering road unevenness

and the speed exists. This was calculated analytically for a simply supported beam using a moving weight model, in which the first beam mode was considered. Furthermore, [95] studied critical speeds in relation to the frequency of the bridge system; the examination was also done for a moving weight model on single-span bridges.

The relationship between the speed and first natural frequency of the bridge is examined here when the interaction between the bridge and the vehicle is considered. Figure 4.15 depicts the dynamic response estimates due to the two-degree-of-freedom vehicle model in relation to the speed circular frequency $\omega_s$ and the bridge first natural frequency $\omega_b$. The speed circular frequency $\omega_s$ is defined as:

$$\omega_s = \frac{\pi v}{L}, \tag{4.1}$$
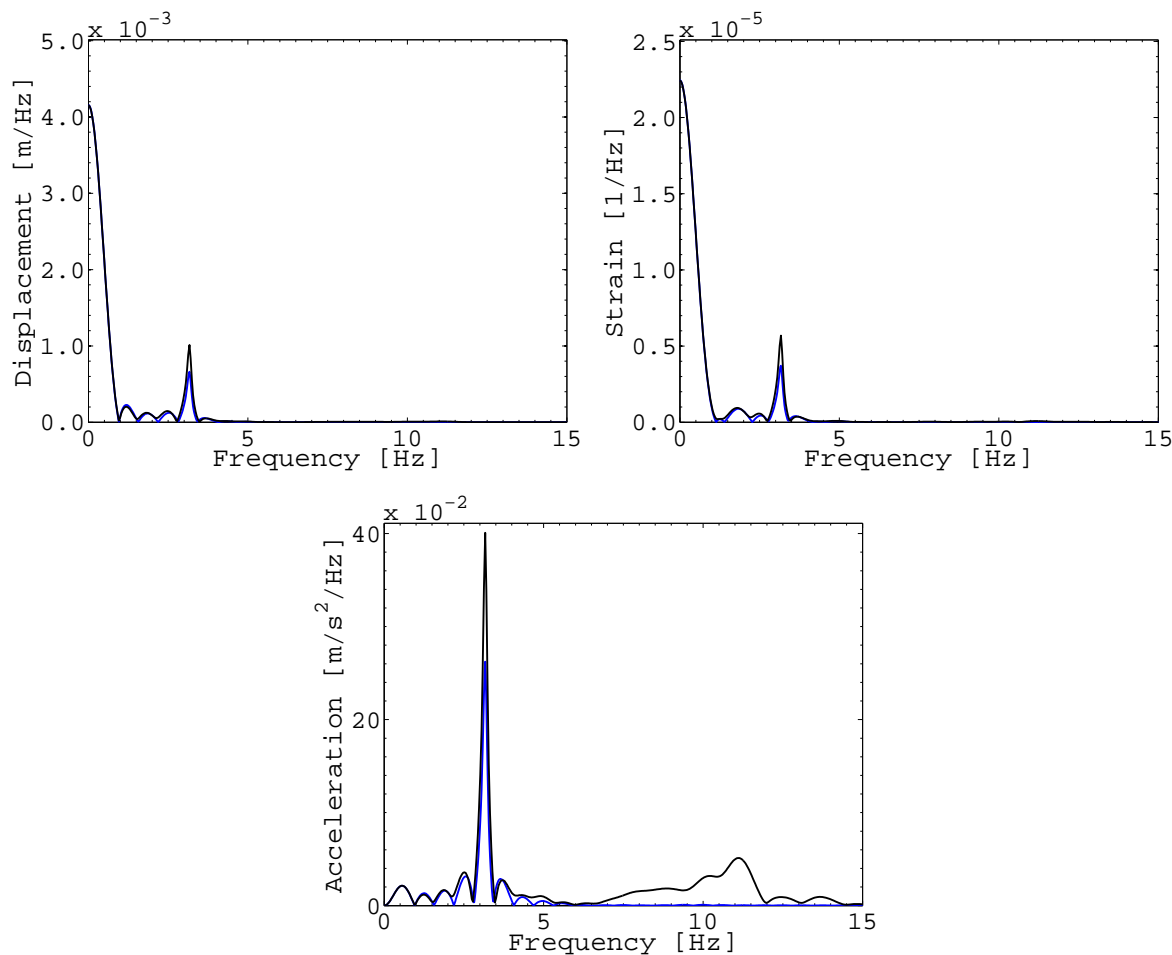
FIGURE 4.14: Amplitude spectra of the dynamic response due to excitation of the 8DOF vehicle: (——) Amplitude spectrum for the dynamic response ignoring road unevenness, (——) Amplitude spectrum for the dynamic response considering road unevenness

where $v$ is the speed of the vehicle [m/s] and $L$ is the span of the bridge [m].

The pattern for the displacements and the strains is clear and similar, whereas the accelerations show a slightly different trend since they tend to increase positively in relation to the speed circular frequency with no distinguishable pattern, as shown in Figure 4.15. The same relationship is plotted in Figure 4.16 for the dynamic response estimates due to the eight-degree-of-freedom vehicle model. The patterns between the response estimates are similar to the ones from the two-degree-of-freedom vehicle model. However, the values of the dynamic response estimates are smaller for the eight-degree-of-freedom vehicle model.

Diagonal lines are drawn to envelop the local peaks of the dynamic response relations in Figures 4.15 and 4.16. The slopes of these lines represent the critical ratios relating to the frequencies of the speed and bridge that envelop the maximum dynamic response estimate,
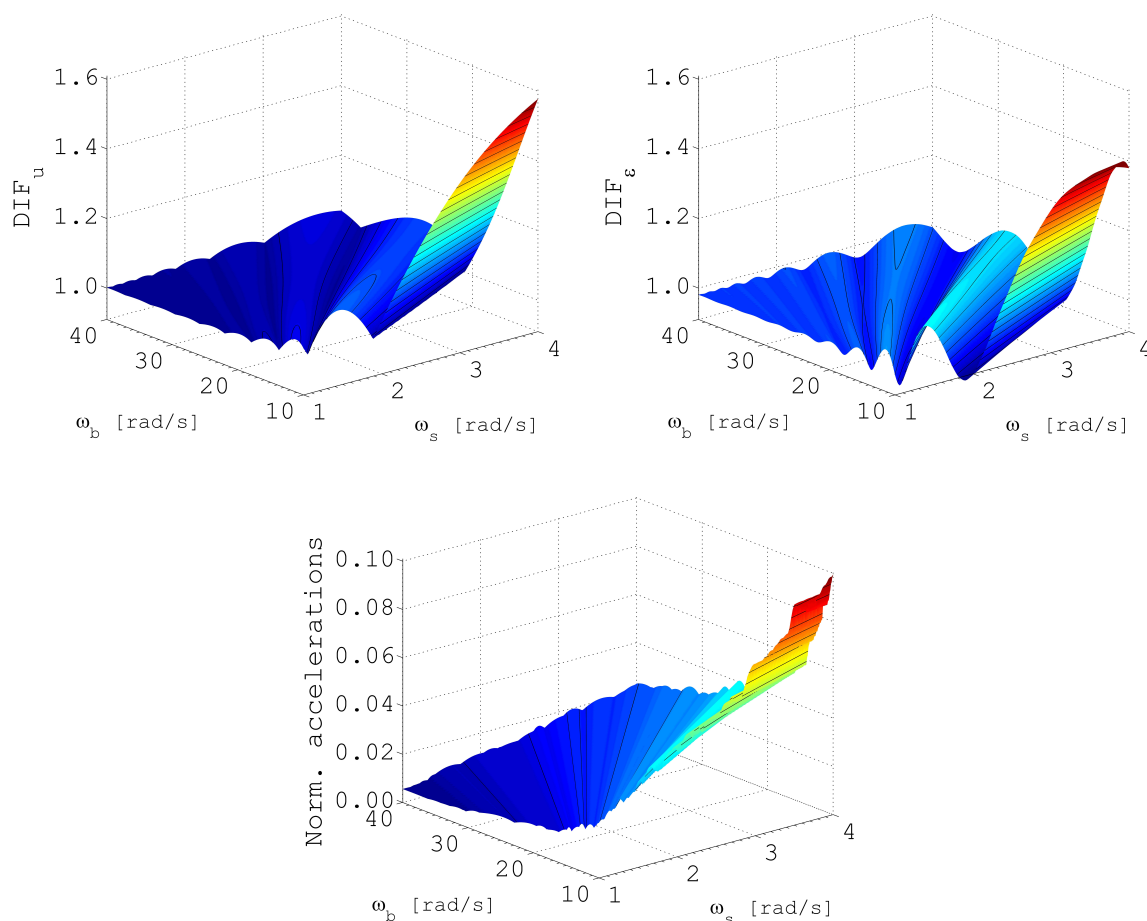
FIGURE 4.15: The Dynamic Incremental Factor versus the bridge's first natural frequency and the speed circular frequency for the 2DOF vehicle model

which is represented as:

$$FR_c = \frac{\omega_s}{\omega_b} \tag{4.2}$$

Some of these critical frequency ratios $FR_c$ are computed and presented in Table 4.8. The ratios apply to short and medium bridges that have a range of first bending natural frequencies of between $10\,\text{rad/s}$ and $40\,\text{rad/s}$ (1.6 Hz to 6.4 Hz) and to vehicle speeds that range from $40\,\text{km/h}$ to $130\,\text{km/h}$ (10 m/s to 36 m/s). The critical ratios for the $\text{DIF}_u$ and $\text{DIF}_\varepsilon$ obtained with the two-degree-of-freedom and the eight-degree-of-freedom are approximately the same. The ratios for the accelerations are not computed since they increase positively in relation to the speed circular frequency and there are no clear enveloping slopes for the response.

For the ratios presented in Table 4.8, the critical speeds for the bridge system studied are
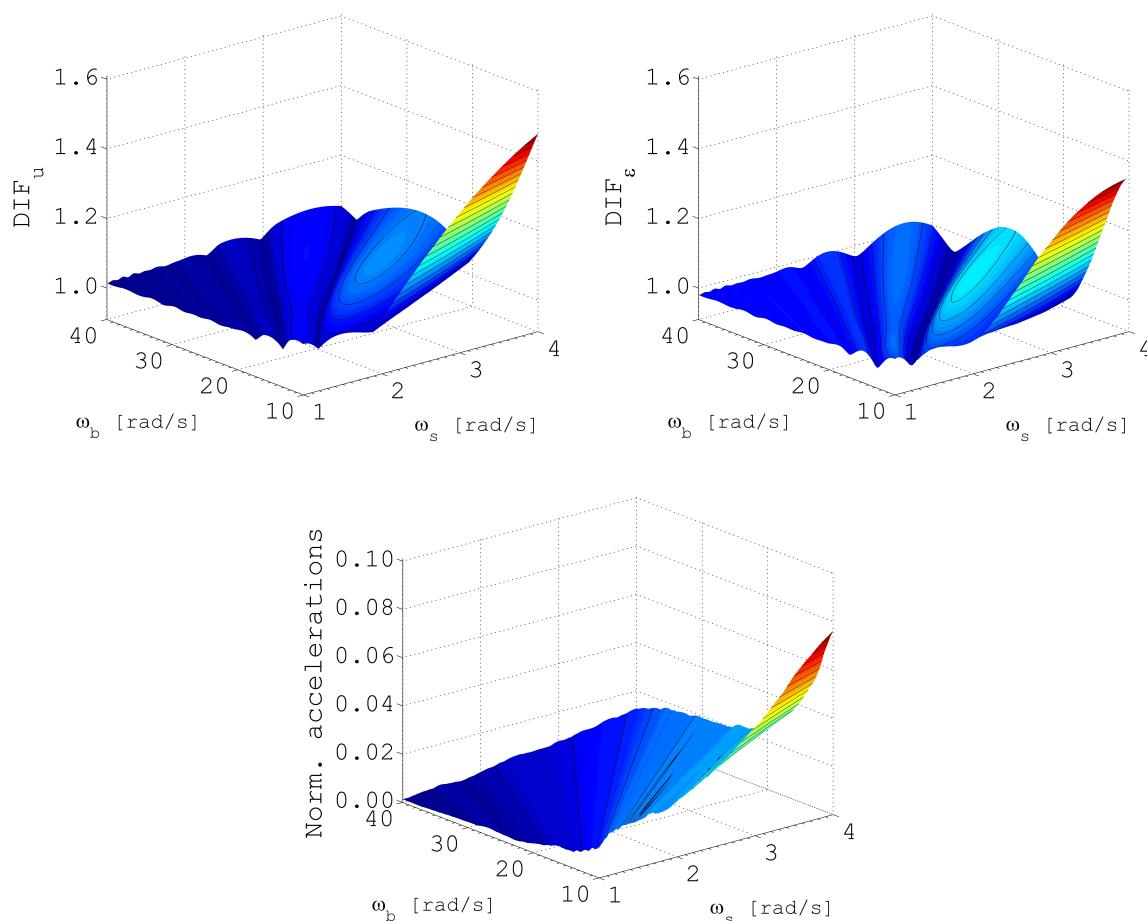
FIGURE 4.16: Dynamic responses versus the bridge's first natural frequency and the speed circular frequency for the 8DOF vehicle model

84 km/h and 130 km/h. An equivalent way to represent the frequency ratios $\omega_s/\omega_b$ is $t_d/T_n$, with $t_d$ as the time it takes the vehicle to cross the bridge and $T_n$ represents the period of the bridge that corresponds to its first natural frequency. For instance, $t_d/T_n = 5.5$ is equivalent to $\omega_s/\omega_b = 0.090$. The ratio $t_d/T_n$ is used only for convenience as a way to explain the pattern observed between the maximum dynamic responses and the speed.

TABLE 4.8: Critical frequency ratios ($FR_c$)

| $DIF_u$ | | $DIF_\varepsilon$ | |
|---|---|---|---|
| 2DOF | 8DOF | 2DOF | 8DOF |
| 0.088 | 0.090 | 0.089 | 0.092 |
| 0.143 | 0.144 | 0.145 | 0.146 |

The time histories for the displacements of the simply supported system due to the two-degree-of-freedom vehicle model traveling at different speeds are plotted in Figure 4.17. It

can be seen that the nature of the response varies when the speed is changed. Also shown in Figure 4.17 is the static solution. The difference between the two curves is an indication of the dynamic effects, which are seen to be relatively small for moderate speeds. This implies that the forces of the vehicle vary slowly relative to the natural period of the bridge. The number of local maxima or peaks that develop depends also on the $t_d/\mathrm{T}_n$ ratio. A longer duration $t_d$ or lower speed leads to more local peaks. In addition, the location of the local maxima depends on the ratio $t_d/\mathrm{T}_n$ which is important in determining the maximum dynamic response and may explain the trend in Figures 4.15 and 4.16. For example, the derived critical ratios for the maximum dynamic response in Table 4.8 for the two-degree-of-freedom vehicle model correspond to the dynamic responses depicted in Figures 4.17(b) and 4.17(d). Whereas, in Figures 4.17(a) and 4.17(c) the local maxima occur in positions where the absolute maximum of the dynamic response is not greatly affected by these local maxima. This observation depends on the exciting frequency of the speed and the first natural bending frequency of the bridge.

Further analysis is performed studying the number and the magnitude of the local peaks that appear in the dynamic response in relation to the different $t_d/T_n$ ratios, Figure 4.18. The vehicle model is crossing the bridge at different speeds for which the full time history of the bridge response is examined. The local maxima (peaks) is plotted as a function of $t_d/\mathrm{T}_n$ in Figure 4.18 with $n$ as the number of peaks appearing in the time history of the response. If $0.50 \leq t_d/T_n \leq 1.60$, only one peak occurs. A second peak develops if $t_d/T_n \geq 1.60$, but it is smaller than the first peak when $0.50 \leq t_d/T_n \leq 2.65$. A third peak develops if $t_d/T_n \geq 2.60$. The second peak is larger than the first and third peaks when $2.65 \leq t_d/T_n \leq 4.75$ and so on. The maximum response is sought and represented as a solid line in Figure 4.18. A dependency is depicted in Figure 4.18 the same as the one in Figure 4.15 but with respect to the ratio $t_d/T_n$ which is equivalent to $\omega_s/\omega_b$.

The local maxima due to the eight-degree-of-freedom vehicle model is plotted as a function of $t_d/\mathrm{T}_n$ in Figure 4.19. If $0.50 \leq t_d/\mathrm{T}_n \leq 1.55$, only one peak occurs. A second peak develops if $t_d/T_n \geq 1.55$, but it is smaller than the first peak when $0.50 \leq t_d/T_n \leq 2.55$. A third peak develops if $t_d/T_n \geq 2.60$. The second peak is larger than the first and third peaks when $2.55 \leq t_d/T_n \leq 4.80$ and so on. The maximum response is represented as a solid line in Figure 4.19. Again the same trend is depicted as in Figure 4.16.

(a) $t_d/T_n$=6.65, $v$=69 km/h

(b) $t_d/T_n$=5.50, $v$=84 km/h

(c) $t_d/T_n$=4.75, $v$=97 km/h

(d) $t_d/T_n$=3.55, $v$=130 km/h
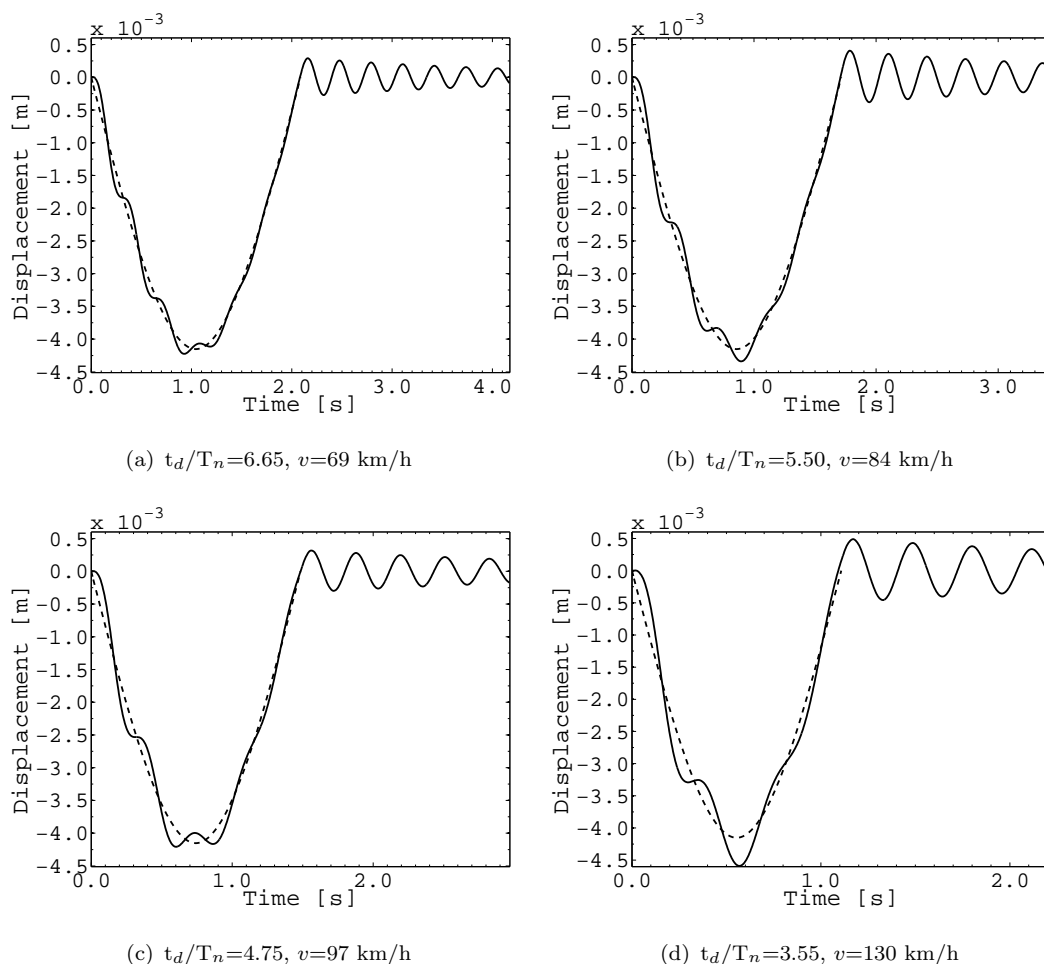
FIGURE 4.17: Dynamic response of the single-span system due to the 2DOF vehicle moving at different speeds: (—) Dynamic response (– –) Static response

As mentioned before, the relations plotted in Figures 4.18 and 4.19 mainly depend on the speed and the bridge's first bending frequency. Further, the vehicle model mainly influences the value of the dynamic amplification of the response rather than the critical ratios. Therefore, similar patterns are observed for the vehicle models for the same bridge system.

## 4.4 Conclusions

It is evident that compared to the continuous system, the single-span bridge system representing short to medium bridges offers the highest dynamic amplifications in the responses
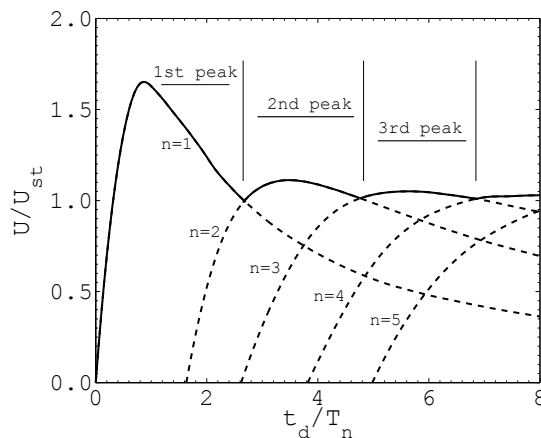
FIGURE 4.18: Response maxima due to the 2DOF vehicle traveling on the bridge
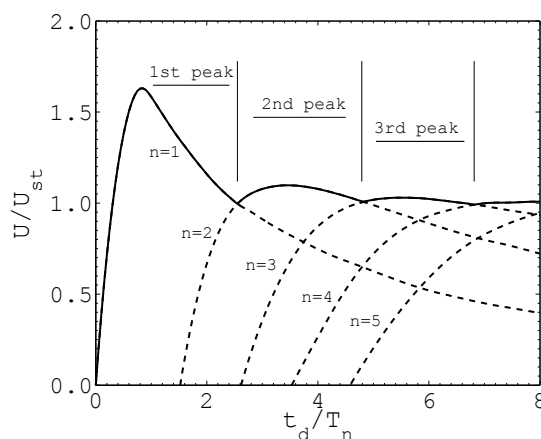


FIGURE 4.19: Response maxima due to the 8DOF vehicle traveling on the bridge

resulting from a traveling heavy vehicle. The responses obtained from the simplified two-degree-of-freedom vehicle model are rather conservative compared with the responses obtained from the more realistic model of the eight-degree-of-freedom model.

The response obtained with the moving weight is of a low frequency content and when considering the bridge-vehicle interaction, other peaks appear, and their magnitudes and positions depend on the natural frequencies of the bridge system and vehicle. Furthermore, the response amplitudes increase in variant portions around the bridge's natural frequency depending on the response examined. It is expected that the estimate of the displacements and the accelerations are highly dependent on the bridge-vehicle interaction considering road unevenness. It is worth mentioning that these conclusions depend on the vehicle model used in the dynamic analysis as the response resulting from the two-degree-of-freedom vehicle

model shows higher sensitivity to road unevenness when compared with the one resulting from the eight-degree-of-freedom vehicle model.

For the dynamic responses studied critical ratios can be derived that make up the maximum dynamic response. These ratios are used to calculate the critical speeds for the bridge system studied, for which the estimates of the additional dynamic effects caused by modeling bridge-vehicle interaction are determined.

The worst cases concerning the dynamic response are found for a single-span bridge system, which is used for further analyses in the next chapter.

# Chapter 5

# Assessment of the Coupled Subsystems

## 5.1 Introduction

In the previous Chapter, a deterministic analysis was performed, in which one realization of the input parameters and/or the road profiles is used. In studying the effects of a class of road unevenness, an interest is developed in running a full probabilistic analysis for the dynamic response estimates. This Chapter aims to use probabilistic analysis to assess the output of the coupled subsystems of the bridge and the vehicle. The assessment is performed in two parts; the first part is based on performing a sensitivity analysis to quantify the influence of the uncertainty of the vehicle dynamics and bridge bearings on the variance of the dynamic response, thereby assessing the model's quality from its input parameters. The second part is based on using the total uncertainty of the model to rank its plausible descriptions and determining their fitness in studying the dynamic response of interest at critical speeds, thereby supporting the level of complexity in deriving the model.

## 5.2   Coupled Subsystems

The probabilistic analysis is performed for the cases, which were identified as the worst cases for the dynamic responses presented earlier in Section 4.3.1. Hence, the responses of the single-span bridge system described in 4.2.1 caused by the movement of the two-degree-of-freedom described in Section 4.2.2.1 and the eight-degree-of-freedom vehicle models described in Section 4.2.2.2 are the objective outputs retrieved from the probabilistic analysis, which are used later in the assessment. The problem of the bridge-vehicle interaction is analyzed in the time domain, its solution method has been explained and presented in Section 3.1.3. Road unevenness is considered in the analysis, which is characterized as a Gaussian random process. A description of the process and its realization can be found in Section 3.1.4.

## 5.3   Probabilistic Analysis

The vehicle dynamics, bearings stiffness and road profiles are treated as random input parameters and processes. The former is described by means of probability distribution functions, while the latter is described by means of power spectral density function, which is explained in Section 4.2.3. The standard deviations and distribution types of the input parameters of the two-degree-of-freedom vehicle model are presented in Table 5.1(a). The distribution types and the standard deviations are retrieved from [36]. The mean values, standard deviations and distribution types of the eight-degree-of-freedom vehicle model are adopted from the studies of [40, 99], and presented in Table 5.1(b). In addition, the rotational and vertical stiffness of the bearings are allowed a variation of an order of 20% following the recommendations of [100]; the mean values, standard deviations, and distribution types of the stiffness of bearings are presented in Table 5.1(c). Latin Hypercube sampling is used to generate the samples of the input parameters, which are assumed to be uncorrelated.

Another important point in this probabilistic analysis is that a sufficient number of road profiles need to be used to describe appropriately the dynamic response caused by the excitation of the vehicle by road unevenness. For the simply supported single-span system,

TABLE 5.1: Input parameters used in the probabilistic analysis

(a) Vehicle parameters (2DOF)

| Parameter | Mean | Standard deviation | Distribution type |
|---|---|---|---|
| Suspension stiffness (N/m) | $1.8 \times 10^7$ | $0.18 \times 10^7$ | Normal |
| Tire stiffness (N/m) | $7.2 \times 10^7$ | $0.72 \times 10^7$ | Normal |
| Suspension viscous damping (Ns/m) | $14.4 \times 10^5$ | $1.44 \times 10^5$ | Normal |
| Tire viscous damping (Ns/m) | $14.4 \times 10^5$ | $1.44 \times 10^5$ | Normal |
| Speed (km/h) | 80 | 12 | Normal |

(b) Vehicle parameters (8DOF)

| Parameter | Mean | Standard deviation | Min | Max | Distribution |
|---|---|---|---|---|---|
| Tractor front axle suspension stiffness (N/m) | $4 \times 10^5$ | $0.92 \times 10^5$ | $2 \times 10^5$ | $8 \times 10^5$ | Normal |
| Tractor rear axle suspension stiffness (N/m) | $10 \times 10^5$ | $3 \times 10^5$ | $6 \times 10^5$ | $14 \times 10^5$ | Normal |
| Semi-trailer axle suspension stiffness (N/m) | $7.5 \times 10^5$ | $1.2 \times 10^5$ | $4 \times 10^5$ | $10 \times 10^5$ | Normal |
| Suspension viscous damping (Ns/m) | $10 \times 10^3$ | $4 \times 10^3$ | $4 \times 10^3$ | $12 \times 10^3$ | Normal |
| Tractor front axle tire stiffness (N/m) | $17.5 \times 10^5$ | $4.5 \times 10^5$ | $9 \times 10^5$ | $21 \times 10^5$ | Normal |
| Tractor rear axle tire stiffness (N/m) | $35 \times 10^5$ | $8.75 \times 10^5$ | $28 \times 10^5$ | $40 \times 10^5$ | Normal |
| Semi-trailer axle tire stiffness (N/m) | $35 \times 10^5$ | $9 \times 10^5$ | $28 \times 10^5$ | $40 \times 10^5$ | Normal |
| Speed (km/h) | 80 | 12 | 40 | 140 | Normal |

(c) Elastomeric bearings parameters

| Parameter | Mean | Standard deviation | Distribution type |
|---|---|---|---|
| Vertical stiffness (N/m) | $2.0 \times 10^9$ | $0.4 \times 10^9$ | Log-normal |
| Rotational stiffness (Nm/rad) | $1.0 \times 10^6$ | $0.2 \times 10^6$ | Log-normal |

an analytical solution for quantifying the statistical characteristics of the dynamic response due to the bridge-vehicle interaction when considering random road unevenness is available by [42], which can be used to check the minimum number of samples needed for the dynamic analysis. The influence of the number of samples of road profiles on the variance of the dynamic response $\text{DIF}_u$ of the bridge traversed by the two-degree-of-freedom vehicle model at a speed of $90\,\text{km/h}$ ($25\,\text{m/s}$) is depicted with the convergence limit according to the solution of [42] in Figure 5.1. The number of sub-samples considered appropriate and adopted for this vehicle model is 1000. The same check for the eight-degree-of-freedom vehicle model is done and plotted in Figure 5.2, which shows that the standard deviation of the dynamic response is converging to a limit. The number of sub-samples considered appropriate and adopted for this vehicle model is also 1000. Similar plots for the minimum number of samples are made for the $\text{DIF}_\varepsilon$ and the normalized accelerations for both vehicle models and can be found in Appendix .1. The number of sub-samples selected for all response estimates examined is 1000.
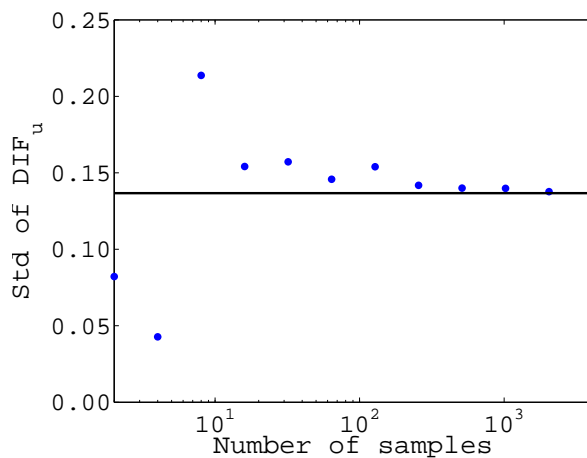
FIGURE 5.1: Effect of number of samples on the deviation of the dynamic response estimate $\text{DIF}_u$ due to the excitation of 2DOF vehicle: ($\bullet$) Monte Carlo Simulation, (—) Convergence limit
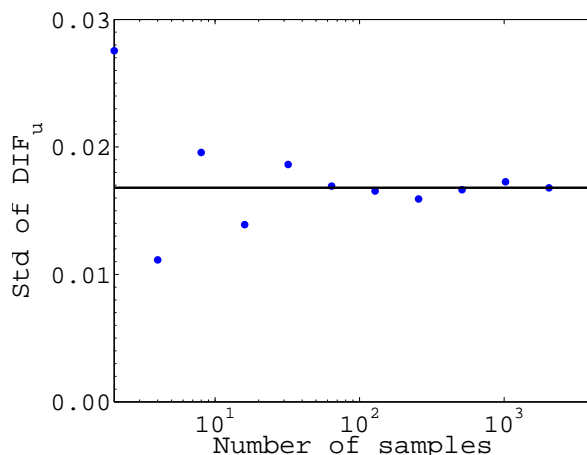


FIGURE 5.2: Effect of number of samples on the deviation of the dynamic response estimate $\text{DIF}_u$ due to the excitation of 8DOF vehicle: ($\bullet$) Monte Carlo Simulation, (—) Converging limit

The number of road profiles identified earlier is run for every sample of the vehicle's input parameters and speed. This is contributed as sub-sampling and has been explained in Section 2.4.1.1. For example, Figure 5.3 depicts the histogram of the $\text{DIF}_\varepsilon$ values when analyzing 1000 sub-samples of road profiles for one set of vehicle input parameters and speed. In other words, the strains are retrieved for the same vehicle crossing the bridge at the same speed, but assuming a different road profile every time. A number of different distributions are tested to fit the output values, the most appropriate of which is the extreme value distribution type I as it gives the largest log-likelihood estimate. The mean value and the value of the 95% quantile are retrieved for the output of the sub-samples and assigned

to the corresponding sample of vehicle input parameters and speed.
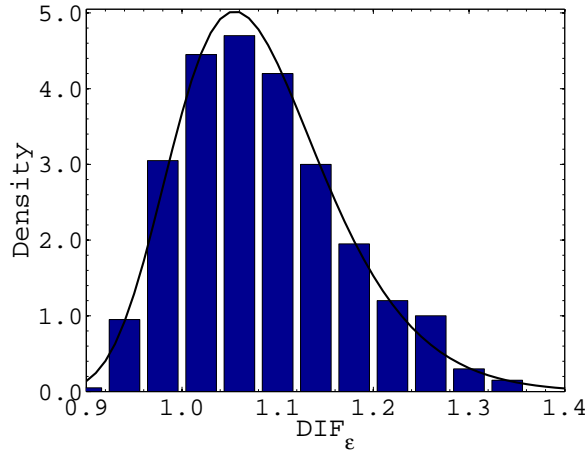


(a) Histogram of $DIF_\varepsilon$

| Normal | Log-normal | Extreme value |
| --- | --- | --- |
| 493.32 | 501.18 | 507.31 |

(b) Log-likelihood estimates

FIGURE 5.3: Histogram of the analyzed samples of the $DIF_\varepsilon$ with a fitted distribution and log-likelihood estimates: (—) Extreme value distribution

After obtaining the output from the sub-sampling and repeating the analysis for all the samples of the vehicle dynamics and speed, an approximation algorithm is used to map the input-output relation before running the sensitivity analysis. A total number of $1000 \times 1000$ samples of input parameters and processes are used in the dynamic analysis for every case study. These analyzed samples act as the support samples for the approximation model. The proposed approximation algorithm is a hybrid between the global polynomial regression models and the moving least squares as explained in Section 2.4.2.3.

The input-output mapping is used because of the large number of samples required for the sensitivity analysis; despite the fact that the numerical simulations are quite fast, they can require an enormous amount of time, which the study cannot afford. Therefore, the meta-model acts as a preliminary step to the sensitivity analysis. The reason behind using the hybrid algorithm for the developed meta-model is the clear distinctive dependency of the dynamic responses on the speed. This dependency can only be captured accurately using approximation models that can capture localities such as the moving least squares. Whereas,

the output can be mapped efficiently with respect to the other input parameters using global polynomial regression surfaces. The base functions for the approximation models consist of linear, quadratic and mixed terms as explained in Section 2.4.2.

The predictive coefficient of determination $R^2_{cross}$ is used to check the quality of the approximation model. An acceptance limit for the $R^2_{cross}$ values is set at 0.85. Figure 5.4 depicts an example for the approximation of the $DIF_\varepsilon$ comparing the analyzed samples with the approximated ones. The optimum radius for the moving least squares and the corresponding $R^2_{cross}$ is computed using cross-validation as described in Section 2.4.2.4. Table 5.2 presents the selected values of influence radius $D$ and the computed values of the $R^2_{cross}$ when the dynamic responses of the single-span system assuming perfect pin supports are approximated, and Table 5.3 presents $D$ and the computed $R^2_{cross}$ when the dynamic responses of the single-span system assuming elastic supports are approximated. The shape factor $\alpha$ in Equation (2.21) is taken as 0.38.

TABLE 5.2: Optimum $D$ and $R^2_{cross}$ values for the hybrid meta-model of responses considering pin supports

| | $D$ | | $R^2_{cross}$ | |
| | 2DOF | 8DOF | 2DOF | 8DOF |
| --- | --- | --- | --- | --- |
| $DIF_u$ | 0.15 | 0.15 | 0.89 | 0.95 |
| $DIF_\varepsilon$ | 0.10 | 0.10 | 0.91 | 0.98 |
| Norm. acceleration | 0.30 | 0.20 | 0.92 | 0.91 |

TABLE 5.3: Optimum $D$ and $R^2_{cross}$ values for the hybrid meta-model of responses considering elastic spring supports

| | $D$ | | $R^2_{cross}$ | |
| | 2DOF | 8DOF | 2DOF | 8DOF |
| --- | --- | --- | --- | --- |
| $DIF_u$ | 0.15 | 0.15 | 0.89 | 0.96 |
| $DIF_\varepsilon$ | 0.10 | 0.10 | 0.90 | 0.97 |
| Norm. acceleration | 0.25 | 0.20 | 0.92 | 0.89 |

## 5.4 Sensitivity Analysis

Within the Monte Carlo framework, the input uncertainties are propagated through the output. Sensitivity analysis is used to apportion the output uncertainty to its inputs, which
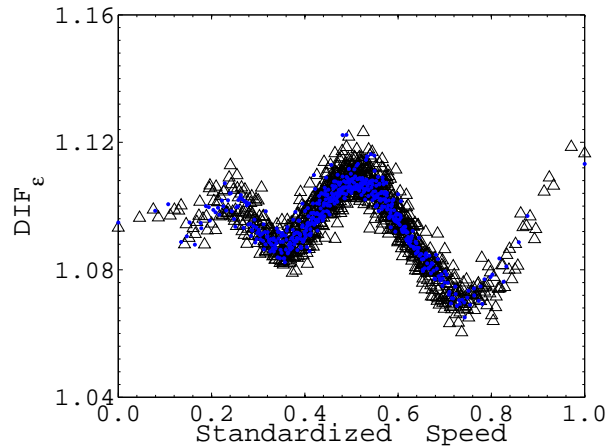
FIGURE 5.4: The analyzed samples with the approximated ones; the $R^2_{cross}$ is 0.91: ($\triangle$) Analyzed values, ($\bullet$) Approximated values

might be useful in detecting the relative important inputs in determining the output. The mathematical measures of the relative importance are the sensitivity indices. The first order indices are represented as $S_i$ and the total order indices are represented as $S_{Ti}$. The value of the sensitivity index reflects the amount of the output's uncertainty reduced if the true values of the input parameters are known. Therefore, a high value for the sensitivity index indicates that the input parameter influences the output significantly, whereas a very low value indicates that the input parameter has a negligible influence. This might help the modeler or engineer to investigate the influential inputs and their underlying subsystems in greater detail since ignoring the effect of these influential inputs would influence the reliability of the output. Such an analysis utilizes the model itself without the need for measurements or reference solutions and assesses the model's output using its input. This analysis is used here to investigate how much the vehicle dynamics, bridge bearings, and road unevenness contributes to the variance of the dynamic output. The following are the computed indices for running a general sensitivity analysis of the coupled subsystems in bridges.

## 5.4.1 Sensitivity Analysis for the Vehicle Dynamics

The study of the dynamic response constituents in Section 4.3.3 is extended by identifying the main parameters that influence each constituent. The two constituents of the dynamic

response examined are: the dynamic response due to the excitation of the vehicle caused by the dynamic deflection of the bridge (Source I) and the dynamic response due to the excitation of the vehicle caused by road unevenness (Source II). First order indices $S_i$ and total order indices $S_{Ti}$ are computed for the responses due to the two-degree-of-freedom vehicle model and illustrated in Tables 5.4-5.6. In studying the sensitivity indices $S_{Ti}$ of the input parameters for the first source of excitation (Source I), it can be seen that the speed is the dominating factor for the variance of the dynamic responses of the displacements, strains, and accelerations. The speed contribution is approximately the same for the different responses, however, $S_{Ti}$ of the speed has the highest value of 0.99 for the accelerations. Moreover, the contribution of the variance of the vehicle dynamics is not that significant to the variance of the output when considering this source of excitation (Source I). The same cannot be said for the response due to the excitation by road unevenness (Source II) since the contribution of the variance of the vehicle dynamics, mainly suspension stiffness, becomes a significant factor. The highest contribution of suspension stiffness obtained is 0.31 for the accelerations followed by the displacements and strains with a value of 0.19. Speed is still the dominating factor, however, its contribution is getting smaller.

TABLE 5.4: Sensitivity indices for the displacement response estimate $\text{DIF}_u$ due to excitation of the (2DOF) vehicle

| Parameter | Source I | | Source II | |
|---|---|---|---|---|
| | $S_i$ | $S_{Ti}$ | $S_i$ | $S_{Ti}$ |
| Suspension damping | 0.00 | 0.01 | 0.03 | 0.04 |
| Tire damping | 0.00 | 0.01 | 0.03 | 0.03 |
| Suspension stiffness | 0.02 | 0.02 | 0.17 | 0.19 |
| Tire stiffness | 0.00 | 0.01 | 0.01 | 0.01 |
| Speed | 0.97 | 0.98 | 0.75 | 0.76 |

TABLE 5.5: Sensitivity indices for the strain response estimate $\text{DIF}_\varepsilon$ due to excitation of the (2DOF) vehicle

| Parameter | Source I | | Source II | |
|---|---|---|---|---|
| | $S_i$ | $S_{Ti}$ | $S_i$ | $S_{Ti}$ |
| Suspension damping | 0.00 | 0.01 | 0.03 | 0.05 |
| Tire damping | 0.00 | 0.01 | 0.03 | 0.03 |
| Suspension stiffness | 0.02 | 0.03 | 0.17 | 0.19 |
| Tire stiffness | 0.00 | 0.00 | 0.00 | 0.00 |
| Speed | 0.96 | 0.97 | 0.75 | 0.75 |

TABLE 5.6: Sensitivity indices for the normalized acceleration response due to excitation of the (2DOF) vehicle

| Parameter | Source I | | Source II | |
|---|---|---|---|---|
| | $S_i$ | $S_{Ti}$ | $S_i$ | $S_{Ti}$ |
| Suspension damping | 0.00 | 0.01 | 0.00 | 0.00 |
| Tire damping | 0.00 | 0.01 | 0.08 | 0.10 |
| Suspension stiffness | 0.01 | 0.02 | 0.31 | 0.31 |
| Tire stiffness | 0.00 | 0.01 | 0.03 | 0.03 |
| Speed | 0.99 | 0.99 | 0.56 | 0.58 |

The dynamic response is the result of the interaction between the considered sources of excitation combined with the moving weight solution. The speed is the only input parameter that influences the moving weight solution when fixing the weight of the vehicle, which is done throughout the investigation. Therefore, when the bridge-vehicle interaction is considered in the analysis, the values of the computed sensitivity indices are a compromise between the results obtained from the moving weight and the results obtained from the other sources of excitation. These indices are computed for the mean value and the 95% quantile and shown in Tables 5.7-5.9. In studying the mean value of the dynamic response, the speed is the main contributor, however, the vehicle dynamics, which is still mainly represented by the stiffness of the suspension system ($k_s$) have a relatively significant attribution.

The higher the contribution of the variance of the vehicle dynamics to the variance of the dynamic response, the more the bridge-vehicle interaction influences the response's quality. This contribution that is indicated by the sensitivity index attributes the amount of uncertainty, which cuts out from the output if the true values of vehicle characteristics are known, thereby obtaining a better quality of the output. From the above, one can conclude that the displacements with $S_{Ti}^{k_s} = 0.21$ and the accelerations with $S_{Ti}^{k_s} = 0.16$ are strongly influenced by the variance of the inputs of vehicle when road unevenness is considered. Furthermore, one can also conclude that the strains are more resilient to the effects of the excitation caused by road unevenness since they are influenced by the variance of the stiffness of the suspension system, however at a much lower contribution ($S_{Ti}^{k_s} = 0.07$ ). This can be explained by the different responsive behavior of the dynamic estimates in relation to the sources of excitation explained in Section 4.3.4. The same can be observed when the analysis is run for the 95% quantile.

Moreover, the difference $S_{Ti} - S_i$ indicates an interaction between the input parameters in relation to the output studied. The results in Tables 5.7-5.9 show weak interactions between the speed and stiffness of the suspension system.

TABLE 5.7: Sensitivity indices for the displacement response estimate $\text{DIF}_u$ due to excitation of the (2DOF) vehicle

| Parameter | Mean | | 95% quantile | |
|---|---|---|---|---|
| | $S_i$ | $S_{Ti}$ | $S_i$ | $S_{Ti}$ |
| Suspension damping | 0.03 | 0.04 | 0.02 | 0.03 |
| Tire damping | 0.02 | 0.03 | 0.02 | 0.02 |
| Suspension stiffness | 0.18 | 0.21 | 0.14 | 0.15 |
| Tire stiffness | 0.00 | 0.00 | 0.00 | 0.00 |
| Speed | 0.73 | 0.76 | 0.79 | 0.81 |

TABLE 5.8: Sensitivity indices for the strain response estimate $\text{DIF}_\varepsilon$ due to excitation of the (2DOF) vehicle

| Parameter | Mean | | 95% quantile | |
|---|---|---|---|---|
| | $S_i$ | $S_{Ti}$ | $S_i$ | $S_{Ti}$ |
| Suspension damping | 0.00 | 0.01 | 0.02 | 0.02 |
| Tire damping | 0.00 | 0.01 | 0.01 | 0.01 |
| Suspension stiffness | 0.04 | 0.07 | 0.07 | 0.08 |
| Tire stiffness | 0.00 | 0.00 | 0.00 | 0.01 |
| Speed | 0.93 | 0.94 | 0.89 | 0.91 |

TABLE 5.9: Sensitivity indices for the normalized acceleration response due to excitation of the (2DOF) vehicle

| Parameter | Mean | | 95% quantile | |
|---|---|---|---|---|
| | $S_i$ | $S_{Ti}$ | $S_i$ | $S_{Ti}$ |
| Suspension damping | 0.00 | 0.00 | 0.00 | 0.00 |
| Tire damping | 0.05 | 0.06 | 0.03 | 0.03 |
| Suspension stiffness | 0.14 | 0.16 | 0.12 | 0.12 |
| Tire stiffness | 0.02 | 0.02 | 0.01 | 0.02 |
| Speed | 0.77 | 0.80 | 0.83 | 0.84 |

The second example shows the sensitivity indices for the response due to the passage of the eight-degree-of-freedom vehicle model. Not only are the vehicle dynamics tested, but the effect of the class of road unevenness class on the results is also examined. Tables 5.10-5.12 show the sensitivity indices of the vehicle dynamics and the speed when considering Class A and Class B roadways. In studying the indices for both classes of road unevenness, it is clear that the indices are highly influenced by the degree of roughness introduced in the

dynamic analysis. The $S_{Ti}$s of the speed are 0.98 and 0.88 for the displacements when considering Class A and Class B roadways, respectively. In addition, $S_{Ti}$s of the stiffness of the suspension of the tractor's rear axle are 0.02 and 0.09 when considering Class A and Class B roadways, respectively. The conclusion drawn from these results is that when roadways are rougher, the contribution of the speed is lower and that of the vehicle dynamics is higher. In other words the influence of bridge-vehicle interaction on the variance of the dynamic response is more evident since the uncertainties in vehicle dynamics contribute more to the output uncertainty when rougher roadways are considered. The same tendency has been observed for strains. For the acceleration, the contribution of the speed changes from 0.831 to 0.506 when the road class changes from Class A to Class B, which highlights the strong influence of the level of excitation due to road unevenness on the variance of accelerations. The observations above show an increased influence of bridge-vehicle interaction on the quality of the output with rougher roadways. The fact that the additional dynamic effects due to bridge-vehicle interaction are greater with rougher surfaces is true, but one must consider the uncertainties accompanying the response since it affects the output's quality.

A comparison between the indices for the different responses in Tables 5.10-5.12 leads to the following observation: the second highest $S_{Ti}$ for the displacements and strains is the stiffness of the suspension system of the tractor, whereas for the accelerations, it is the damping of the suspension system. In short, the sensitivity indices for the displacements and strains have a similar trend, which is different from the one of the accelerations. This may be explained by the similar frequency content between the displacements and the strains, which is different from the one of the accelerations as depicted in Section 4.3.4.

In addition, the difference $S_{Ti} - S_i$, is small, still offers larger values when compared with the differences obtained for the two-degree-of-freedom vehicle model. This indicates stronger interactions between the vehicle dynamics and the speed for the eight-degree-of-freedom vehicle model.

TABLE 5.10: Sensitivity indices for the displacement response estimate $\text{DIF}_u$ due to excitation of the (8DOF) vehicle

| Parameter | Class A | | Class B | |
|---|---|---|---|---|
| | $S_i$ | $S_{Ti}$ | $S_i$ | $S_{Ti}$ |
| Suspension system stiffness | | | | |
| Tractor front axle | 0.00 | 0.01 | 0.01 | 0.02 |
| Tractor rear axle | 0.01 | 0.02 | 0.08 | 0.09 |
| Semi-trailer tridem axle | 0.01 | 0.02 | 0.03 | 0.04 |
| Suspension system damping | | | | |
| Trailer and semi-trailer | 0.00 | 0.01 | 0.01 | 0.02 |
| Tire stiffness | | | | |
| Tractor front tire | 0.00 | 0.00 | 0.00 | 0.01 |
| Tractor rear tire | 0.00 | 0.00 | 0.00 | 0.01 |
| Semi-trailer tridem tire | 0.00 | 0.00 | 0.00 | 0.00 |
| Speed | 0.96 | 0.98 | 0.84 | 0.88 |

TABLE 5.11: Sensitivity indices for the strain response estimate $\text{DIF}_\varepsilon$ due to excitation of the (8DOF) vehicle

| Parameter | Class A | | Class B | |
|---|---|---|---|---|
| | $S_i$ | $S_{Ti}$ | $S_i$ | $S_{Ti}$ |
| Suspension system stiffness | | | | |
| Tractor front axle | 0.00 | 0.00 | 0.01 | 0.02 |
| Tractor rear axle | 0.01 | 0.01 | 0.08 | 0.09 |
| Semi-trailer tridem axle | 0.00 | 0.01 | 0.03 | 0.04 |
| Suspension system damping | | | | |
| Trailer and semi-trailer | 0.00 | 0.00 | 0.01 | 0.01 |
| Tire stiffness stiffness | | | | |
| Tractor front tire | 0.00 | 0.01 | 0.00 | 0.01 |
| Tractor rear tire | 0.00 | 0.00 | 0.00 | 0.01 |
| Semi-trailer tridem tire | 0.00 | 0.00 | 0.00 | 0.00 |
| Speed | 0.98 | 0.98 | 0.84 | 0.87 |

## 5.4.2 Sensitivity Analysis for the Bearings

The elastomeric bearings supporting the bridge system can have an influence on the variance of the dynamic response. A quantitative measure of this influence is the objective of this subsection. Therefore, instead of investigating the single input parameters of the modeled subsystems, they have been grouped. The parameters related to the bearings (i.e. rotational and vertical stiffness) are treated as the bearing group, and the vehicle inputs are considered

TABLE 5.12: Sensitivity indices for the normalized acceleration response due to excitation of the (8DOF) vehicle

| Parameter | Class A | | Class B | |
|---|---|---|---|---|
| | $S_i$ | $S_{Ti}$ | $S_i$ | $S_{Ti}$ |
| Suspension system stiffness | | | | |
| Tractor front axle | 0.00 | 0.00 | 0.00 | 0.01 |
| Tractor rear axle | 0.00 | 0.00 | 0.02 | 0.03 |
| Semi-trailer tridem axle | 0.00 | 0.00 | 0.02 | 0.02 |
| Suspension system damping | | | | |
| Trailer and semitrailer | 0.10 | 0.11 | 0.31 | 0.32 |
| Tire stiffness stiffness | | | | |
| Tractor front tire | 0.00 | 0.00 | 0.01 | 0.01 |
| Tractor rear tire | 0.05 | 0.06 | 0.12 | 0.13 |
| Semi-trailer tridem tire | 0.00 | 0.01 | 0.01 | 0.01 |
| Speed | 0.80 | 0.83 | 0.46 | 0.52 |

as the vehicle group. The sensitivity indices are calculated for the bearing, the vehicle groups and the speed. The computed sensitivity indices for the response due to the two-degree-of-freedom and the eight-degree-of-freedom vehicle models traveling on the single-span bridge system are computed and presented in Table 5.13. The output investigated in the sensitivity analysis is the mean value of the sub-samples analyzed. Each of these sensitivity indices can be used to assess the significance of the underlying subsystem. For example, $S_{Ti}$ for the bearings when examining the displacements due to the two-degree-of-freedom vehicle model is 0.05. This is the highest contribution to the variance of the dynamic responses form the stiffness of bearings. The expectation here is that the accelerations would show the highest dependency on the bearings since they are the most affected when the bearings are introduced to the bridge system assuming a straight road profile, as shown in Figure 4.6(c). However, road unevenness effects, when considered, dominate and the variance of the accelerations is more dependent on the vehicle dynamics and speed. The fact that strains are resilient to the effects of road unevenness has already been established; they are also weakly affected by the uncertainties in the bearing's stiffness with an $S_{Ti}$ of 0.03. Similar results are obtained when the eight-degree-of-freedom vehicle model is used in the dynamic analysis. Moreover, for the eight-degree-of-freedom vehicle model, the sensitivity indices for the displacements and the strains are similar, for instance, the $S_{Ti}$ of the vehicle dynamics for the eight-degree-of-freedom model is 0.10 for the displacements and 0.08 for

the strains. On the other hand, $S_{Ti}$ of the vehicle dynamics for the two-degree-of-freedom model is 0.20 for the displacements and 0.09 for the strains. The results obtained support the significance of the vehicle model used.

TABLE 5.13: Sensitivity indices considering bridge bearings

|  | 2DOF | 8DOF |
|---|---|---|
| **Displacements** | | |
| Bridge Bearings | 0.05 | 0.03 |
| Vehicle Dynamics | 0.20 | 0.09 |
| Speed | 0.78 | 0.92 |
| | | |
| **Strains** | | |
| Bridge Bearings | 0.03 | 0.02 |
| Vehicle Dynamics | 0.10 | 0.08 |
| Speed | 0.92 | 0.95 |
| | | |
| **Normalized accelerations** | | |
| Bridge Bearings | 0.02 | 0.01 |
| Vehicle Dynamics | 0.18 | 0.22 |
| Speed | 0.82 | 0.79 |

In short, the sensitivity analysis investigates the contributions of the inputs of the subsystems when coupled to the variance of the dynamic response. These contributions are quantified by the mathematical estimates of $S_i$ and $S_{Ti}$. The higher they are, the more influential their corresponding coupling is on the output's quality. Based on the analyses above, the quality of displacements and accelerations show more dependency on bridge-vehicle interaction and this can be observed to a greater extent when considering rougher roadways.

## 5.4.3 Sensitivity Analysis for Temporal Frequencies of Road Unevenness

Sensitivity analysis has been used for the purpose of assessing the dynamic output. However, in this investigation it is used to identify the temporal frequencies of road unevenness, which influence a dynamic output the most. A recent study attempted to identify the wavelengths of irregularities that affect the dynamic response at different speeds [101]. The study considered the irregularity as a sinusoidal wave corresponding to one wavelength and ran the dynamic analysis for variant speeds. Then the authors repeated the procedure for

the different wavelengths. Such a procedure overlooked the realistic and random nature of unevenness.

The randomness of the realized road profiles has been considered in this investigation, and the dynamic response is also determined for different speeds. Hence, the speed and corresponding temporal frequencies of road unevenness are used for the sensitivity analysis.

The description of the road profiles following Equation (3.36) is modified by assuming random amplitudes, which would enable the application of the sensitivity analysis. This modified model can be found in [39, 102]. Road unevenness is modeled as:

$$f(x) = \sum_{k=0}^{N_d} [C_k cos(\omega_k x + \Phi_k)] \ , \tag{5.1}$$

where $C_k$ is a random variable following Rayleigh distribution with a mean value of $\beta_k \sqrt{\frac{\pi}{2}}$ and a variance of $\beta_k^2 (2 - \frac{\pi}{2})$ taking $\beta_k$ as $\sqrt{S_{FF}(\omega_k)\Delta\omega}$.

The sensitivity analysis is run directly on the model output since overfitting cannot be avoided for any meta-model built for mapping the input-output relationship. The problem of overfitting arises from the large number of inputs that result from the discretized temporal frequencies of road unevenness. Furthermore, grouping the frequencies of road unevenness allows efficient application of the analysis. The general scheme for running the sensitivity analysis is as follows:

1. One set of random phase angles is generated $\Phi$ $(1 \times N_d)$ with $N_d$ as the number of discretized frequencies.

2. Random samples of the amplitudes are generated $\mathbf{C}$ $(N_s \times N_d)$ with $N_s$ as the number of samples.

3. The road profiles are generated according to Equation (5.1) assuming the same set of phase angles for every realization.

4. The dynamic analysis is performed considering the samples of road profiles generated and the dynamic output is obtained.

5. The sensitivity analysis is applied and the sensitivity indices for the speed and the ranges of road frequencies studied are estimated.

6. All steps (1-6) are repeated in order to consider different random sets of phase angles and the average value of the sensitivity indices are calculated.

The analysis is preformed in such a way to overcome the challenge imposed by considering the random phase angles in the realization of road profiles.

The numerical example is illustrated for the dynamic response due to the eight-degree-of-freedom vehicle model traveling at different speeds considering road unevenness. The sensitivity indices $S_i$ and $S_{Ti}$ are given in Table 5.14. These indices provide quantitative measures for the influence of frequency ranges of road profiles on the variance of the dynamic response. The ranges of the frequencies of road profiles are chosen in the ranges of the eigenfrequencies of the eight-degree-of-freedom vehicle model. The first range (0.2 Hz to 4.6 Hz) corresponds to the bouncing of the tractor and the semi-trailer masses with some pitching modes; the second range (4.6 Hz to 10.5 Hz) corresponds to the axle hop of the tractor axles; and the third range (10.5 Hz to 12.5 Hz) corresponds to the axle hop of the semi-trailer axles. It can be observed from the indices in Table 5.14 as expected that the displacements and strains are mainly affected by the temporal frequencies of road profiles, which coincide with the bouncing mode of the tractor and the semi-trailer, whereas the accelerations are affected by the ones that coincide with the bouncing modes and the axle hop modes, especially the ones of the semi-trailer axles. The corresponding wavelengths of road unevenness can be calculated for the different speeds.

## 5.5 Total Uncertainty

Most of the studies concerning the dynamic analysis of bridges focus on obtaining the dynamic response without questioning the necessity of the complex modeling and of performing the dynamic analysis. Attempts have been made by [15, 25], as well as others, to investigate the cases where the interaction between the vehicle and the bridge is needed. These studies have often been performed using a standard parametric study and in some cases defining a

TABLE 5.14: Identification of the frequencies of road unevenness with the greatest impact on dynamic response

|  | $S_i$ | $S_{Ti}$ |
|---|---|---|
| **Displacements** | | |
| Road temporal frequency range | | |
| 0.2 to 4.6 [Hz] | 0.19 | **0.28** |
| 4.6 to 10.5 [Hz] | 0.00 | 0.00 |
| 10.5 to 12.5 [Hz] | 0.00 | 0.00 |
| Speed | 0.71 | **0.81** |
| | | |
| **Strains** | | |
| Road temporal frequency range | | |
| 0.2 to 4.6 [Hz] | 0.11 | **0.18** |
| 4.6 to 10.5 [Hz] | 0.00 | 0.00 |
| 10.5 to 12.5 [Hz] | 0.00 | 0.00 |
| Speed | 0.81 | **0.89** |
| | | |
| **Normalized accelerations** | | |
| Road temporal frequency range | | |
| 0.2 to 4.6 [Hz] | 0.08 | **0.11** |
| 4.6 to 10.5 [Hz] | 0.02 | 0.04 |
| 10.5 to 12.5 [Hz] | 0.04 | **0.08** |
| Speed | 0.78 | **0.84** |

threshold to accept the shortcomings in cases where the interaction is ignored [15]. Recent studies computed the inherent uncertainty of the dynamic response when road unevenness is introduced in the analysis [42, 44, 103]. However, the issue of judging whether the improved value of the dynamic response is worth the added computational cost and the accompanying uncertainty is rarely addressed. In this section, the total uncertainty of a model stemming from the input parameters "Model Input Uncertainty" and the implications of modeling simplifications and assumptions "Model Framework Uncertainty" are computed. The total uncertainties are used to rank the coupled models according to their appropriateness for a dynamic response at critical speeds.

Total uncertainty seems to be an attractive option for assessing and ranking a set of plausible models. The evaluation of the total model uncertainty has been explained in Section 2.4.3. The uncertainty is measured by the variance of the model output as follows:

$$V_{M_i}(Y) = V(Y^{M_i}) + V(\epsilon_\Delta^{M_i}) + V(\epsilon^{ref}), \tag{5.2}$$

where $V(\epsilon_\Delta^{M_i})$ is defined as:

$$V(\epsilon_\Delta^{M_i}) = \left[E(Y^{M_i}) - E(Y^{ref})\right]^2,$$ (5.3)

and $V(\epsilon^{ref})$ is the uncertainty originating from the assumption that the adjusted model is the reference model. The term $\left[V(\epsilon_\Delta^{M_i}) + V\left(\epsilon^{ref}\right)\right]$ is the additive framework uncertainty. The plausible models tested in this section are as follows:

- The decoupled model of a moving weight (Model 1)

- The coupled model of the bridge and the vehicle without considering random vibrations (Model 2)

- The coupled model of the bridge and the vehicle considering random vibrations (Model 3)

- The coupled model of the bridge and the vehicle considering random vibrations with elastic supports (Model 4)

The model which gives the lowest total uncertainty may be recommended for the examined response as previously explained.

The critical ratios for the dynamic response are derived in Section 4.3.5. These ratios combined with the natural frequency of the bridge give the critical speeds that envelop the maximum dynamic response. The bridge system used in the investigation has a first natural bending circular frequency of $20\,\text{rad/s}$. The critical frequency ratios considered are 0.090 and 0.144, thus, the critical speeds are computed according to Equation (4.1) and are $84\,\text{km/h}$ and $130\,\text{km/h}$, respectively. The investigation is carried out for the two-degree-of-freedom and the eight-degree-of-freedom vehicle models traveling at the derived critical speeds over Class A and Class B roadways. The results are expressed using the standard deviation $Std(\ldots) = \sqrt{V(\ldots)}$.

Since a probabilistic analysis is performed, $E\left(Y^{M_i}\right)$ and $V\left(Y^{M_i}\right)$ for the response measures ($\text{DIF}_u$, $\text{DIF}_\epsilon$ and Norm. Acceleration) are estimated considering random input parameters and processes and are shown in Tables 5.15 and 5.16. In studying the results presented in the

tables, it can be seen that the dynamic response obtained with the two-degree-of-freedom vehicle model traveling at a speed of 84 km/h increases by a maximum of 37% for the displacements and of 24% for the strains. The dynamic response obtained with the eight-degree-of-freedom vehicle model traveling at a speed of 84 km/h increases by a maximum of 14% for the displacements and of 5% for the strains. Moreover, it is also observed that this increase in the dynamic response is accompanied by uncertainties which originate in great part from considering road unevenness. The response's means and standard deviations are used for computing the total uncertainty according to Equation (5.2).

The value of $V(\epsilon^{ref})$ is unknown, however, it is assumed to take on different values, and their influence on the total uncertainty of a model prediction is examined. The model $M_i$ with the lowest $V_{M_i}(Y)$ is assumed to be the most fit model since there is a balance between the better prediction and its uncertainty. The influence of the tested values of $V(\epsilon^{ref})$ affects as expected the qualitative evaluations of the $V_{M_i}(Y)$, but it does not affect the ranking of the single models. For example, Figures 5.6(g), 5.6(h), and 5.6(i) depict the standard deviation of the models' predictions for different dynamic responses when the eight-degree-of-freedom vehicle model travels at a speed of 84 km/h considering Class B roadway. For every response measure, a model dominates with the lowest or the highest uncertainty. The model most fit can be assigned by the lowest total uncertainty. It can be said that with regard to serviceability measures (displacements) and vibrational serviceability measures (accelerations) the models considering the bridge-vehicle interaction can be considered the most fit. On the other hand, with regard to the strains, the uncertainties of input parameters and processes outweigh the better response of the coupled subsystems when road unevenness is considered. The investigation is performed in a similar manner for all vehicle models and speeds. The complete total uncertainty results for the studied critical speeds considering Class A and B roadways are depicted in Figures 5.5 and 5.6.

TABLE 5.15: Mean values and standard deviations for the dynamic responses considering the (2DOF) vehicle model

(a) Mean values and standard deviations for the dynamic responses for the vehicle model traveling at a speed of 84 km/h considering Class A roadways

| Model | $DIF_u$ | | $DIF_\epsilon$ | | Norm. Acceleration | |
|---|---|---|---|---|---|---|
| | Mean | Std | Mean | Std | Mean | Std |
| Model 1 | 1.071 | 0.000 | 1.041 | 0.000 | 0.0197 | 0.000 |
| Model 2 | 1.041 | 0.002 | 1.011 | 0.001 | 0.0196 | 0.001 |
| Model 3 | 1.178 | 0.097 | 1.099 | 0.089 | 0.0499 | 0.015 |
| Model 4 | 1.189 | 0.098 | 1.096 | 0.091 | 0.0531 | 0.016 |

(b) Mean values and standard deviations for the dynamic responses for the vehicle model traveling at a speed of 130 km/h considering Class A roadways

| Model | $DIF_u$ | | $DIF_\epsilon$ | | Norm. Acceleration | |
|---|---|---|---|---|---|---|
| | Mean | Std | Mean | Std | Mean | Std |
| Model 1 | 1.132 | 0.000 | 1.093 | 0.000 | 0.031 | 0.000 |
| Model 2 | 1.104 | 0.002 | 1.073 | 0.002 | 0.030 | 0.001 |
| Model 3 | 1.212 | 0.113 | 1.124 | 0.110 | 0.057 | 0.017 |
| Model 4 | 1.231 | 0.114 | 1.143 | 0.117 | 0.059 | 0.018 |

(c) Mean values and standard deviations for the dynamic responses for vehicle model traveling at a speed of 84 km/h considering Class B roadways

| Model | $DIF_u$ | | $DIF_\epsilon$ | | Norm. Acceleration | |
|---|---|---|---|---|---|---|
| | Mean | Std | Mean | Std | Mean | Std |
| Model 1 | 1.071 | 0.000 | 1.041 | 0.000 | 0.0197 | 0.000 |
| Model 2 | 1.041 | 0.002 | 1.011 | 0.001 | 0.0196 | 0.001 |
| Model 3 | 1.341 | 0.182 | 1.237 | 0.152 | 0.0968 | 0.028 |
| Model 4 | 1.372 | 0.181 | 1.237 | 0.157 | 0.0992 | 0.029 |

(d) Mean values and standard deviations for the dynamic responses for the vehicle model traveling at a speed of 130 km/h considering Class B roadways

| Model | $DIF_u$ | | $DIF_\epsilon$ | | Norm. Acceleration | |
|---|---|---|---|---|---|---|
| | Mean | Std | Mean | Std | Mean | Std |
| Model 1 | 1.132 | 0.000 | 1.093 | 0.000 | 0.031 | 0.000 |
| Model 2 | 1.104 | 0.002 | 1.073 | 0.002 | 0.030 | 0.001 |
| Model 3 | 1.383 | 0.182 | 1.246 | 0.153 | 0.105 | 0.028 |
| Model 4 | 1.408 | 0.208 | 1.249 | 0.185 | 0.110 | 0.037 |

TABLE 5.16: Mean values and standard deviations for the dynamic responses considering the (8DOF) vehicle model

(a) Mean values and standard deviations for the dynamic responses for the vehicle model traveling at a speed of 84 km/h considering Class A roadways

| Model | $\text{DIF}_u$ | | $\text{DIF}_\epsilon$ | | Norm. Acceleration | |
|---|---|---|---|---|---|---|
| | Mean | Std | Mean | Std | Mean | Std |
| Model 1 | 1.065 | 0.000 | 1.017 | 0.000 | 0.011 | 0.000 |
| Model 2 | 1.064 | 0.001 | 1.016 | 0.001 | 0.011 | 0.000 |
| Model 3 | 1.071 | 0.028 | 1.021 | 0.027 | 0.017 | 0.003 |
| Model 4 | 1.085 | 0.029 | 1.027 | 0.028 | 0.019 | 0.003 |

(b) Mean values and standard deviations for the dynamic responses for the vehicle model traveling at a speed of 130 km/h considering Class A roadways

| Model | $\text{DIF}_u$ | | $\text{DIF}_\epsilon$ | | Norm. Acceleration | |
|---|---|---|---|---|---|---|
| | Mean | Std | Mean | Std | Mean | Std |
| Model 1 | 1.119 | 0.000 | 1.065 | 0.000 | 0.020 | 0.000 |
| Model 2 | 1.133 | 0.002 | 1.076 | 0.002 | 0.019 | 0.001 |
| Model 3 | 1.140 | 0.062 | 1.080 | 0.056 | 0.024 | 0.004 |
| Model 4 | 1.160 | 0.065 | 1.086 | 0.058 | 0.026 | 0.004 |

(c) Mean values and standard deviations for the dynamic responses for the vehicle model traveling at a speed of 84 km/h considering Class B roadways

| Model | $\text{DIF}_u$ | | $\text{DIF}_\epsilon$ | | Norm. Acceleration | |
|---|---|---|---|---|---|---|
| | Mean | Std | Mean | Std | Mean | Std |
| Model 1 | 1.065 | 0.000 | 1.017 | 0.000 | 0.011 | 0.000 |
| Model 2 | 1.064 | 0.001 | 1.016 | 0.001 | 0.011 | 0.000 |
| Model 3 | 1.121 | 0.064 | 1.046 | 0.066 | 0.034 | 0.009 |
| Model 4 | 1.135 | 0.059 | 1.043 | 0.063 | 0.036 | 0.009 |

(d) Mean values and standard deviations for the dynamic responses for the vehicle model traveling at a speed of 130 km/h considering Class B roadways

| Model | $\text{DIF}_u$ | | $\text{DIF}_\epsilon$ | | Norm. Acceleration | |
|---|---|---|---|---|---|---|
| | Mean | Std | Mean | Std | Mean | Std |
| Model 1 | 1.119 | 0.000 | 1.065 | 0.000 | 0.020 | 0.000 |
| Model 2 | 1.133 | 0.002 | 1.076 | 0.002 | 0.019 | 0.001 |
| Model 3 | 1.202 | 0.149 | 1.116 | 0.149 | 0.038 | 0.010 |
| Model 4 | 1.220 | 0.151 | 1.118 | 0.155 | 0.039 | 0.010 |

(a) Speed = 84 km/h

(b) Speed = 84 km/h

(c) Speed = 84 km/h

(d) Speed = 130 km/h

(e) Speed = 130 km/h

(f) Speed = 130 km/h

Considering Class A roadways

(g) Speed = 84 km/h

(h) Speed = 84 km/h

(i) Speed = 84 km/h

(j) Speed = 130 km/h

(k) Speed = 130 km/h

(l) Speed = 130 km/h
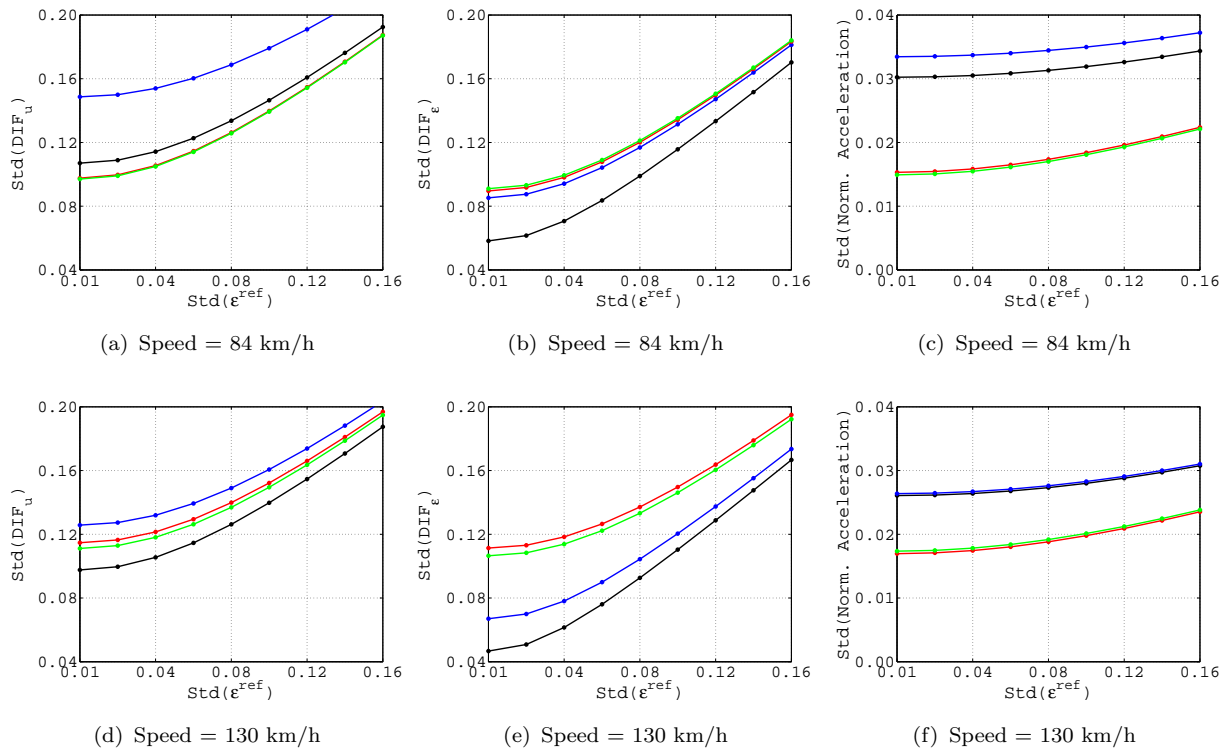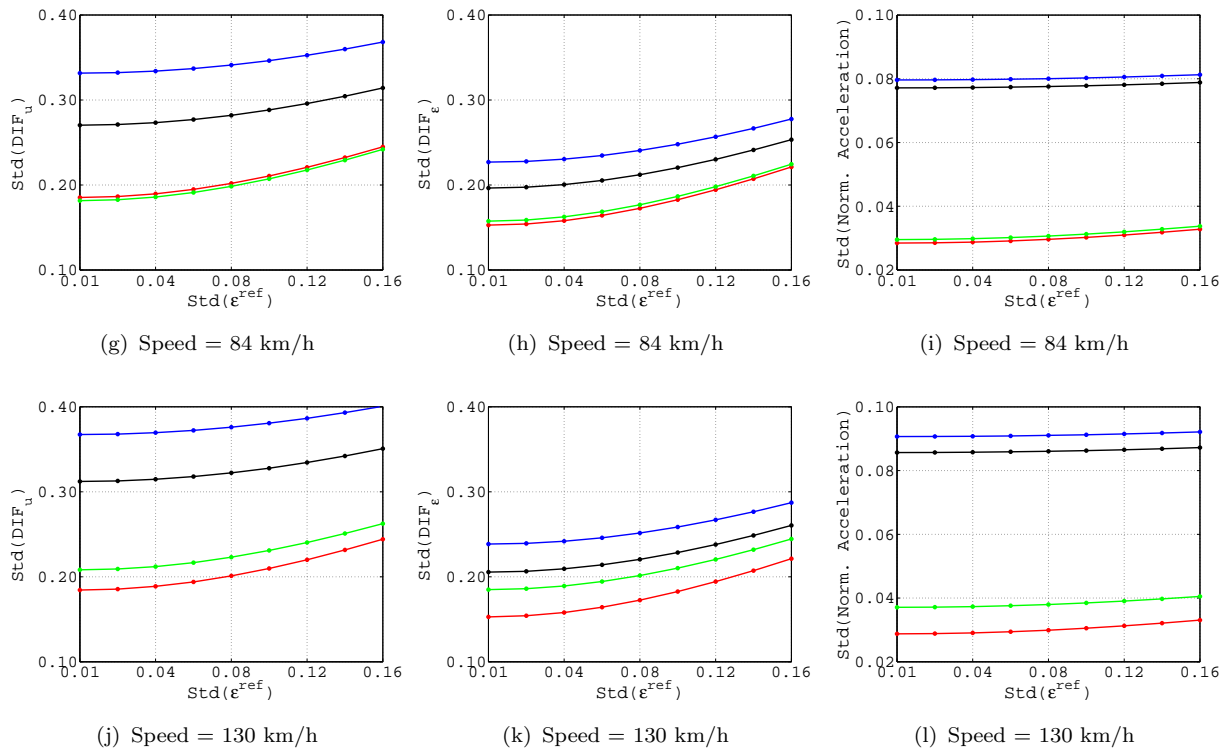
Considering Class B roadways

FIGURE 5.5: Total model uncertainty of responses due to 2DOF vehicle traveling over the bridge considering different classes of roadways: (—) Dynamic response due to a moving weight, (—) Dynamic response considering BVI without road unevenness, (—) Dynamic response considering BVI with road unevenness, (—) Dynamic response considering BVI with road unevenness and elastomeric bearings

(a) Speed = 84 km/h

(b) Speed = 84 km/h

(c) Speed = 84 km/h

(d) Speed = 130 km/h

(e) Speed = 130 km/h

(f) Speed = 130 km/h

Considering Class A roadways

(g) Speed = 84 km/h

(h) Speed = 84 km/h

(i) Speed = 84 km/h

(j) Speed = 130 km/h

(k) Speed = 130 km/h

(l) Speed = 130 km/h

Considering Class B roadways

FIGURE 5.6: Total model uncertainty of responses due to 8DOF vehicle traveling over the bridge considering different classes of roadways: (—) Dynamic response due to a moving weight, (—) Dynamic response considering BVI without road unevenness, (—) Dynamic response considering BVI with road unevenness, (—) Dynamic response considering BVI with road unevenness and elastomeric bearings

The following are the concluded observations from Figures 5.5 and 5.6:

- Considering Class A roadways: With regard to the two-degree-of-freedom vehicle model, it can be said that the couplings of the bridge subsystems (Model 4) are of significance at the first critical speed 84 km/h for the serviceability measure (displacements) and vibrational serviceability measure (accelerations). With regard to the more realistic vehicle model, i.e., the eight-degree-of-freedom model, the effects of couplings are clear for the accelerations, whereas the decoupled model of moving weights (Model 1) can be described as the adequate model with the lowest total uncertainty for the displacements and strains. When the eight-degree-of-freedom vehicle travels at a speed of 130 km/h, the moving weight solution (Model 1) is no longer conservative compared with the coupled models (Models 2, 3, and 4). Therefore, the bridge-vehicle interaction is of greater significance for the displacements and strains.
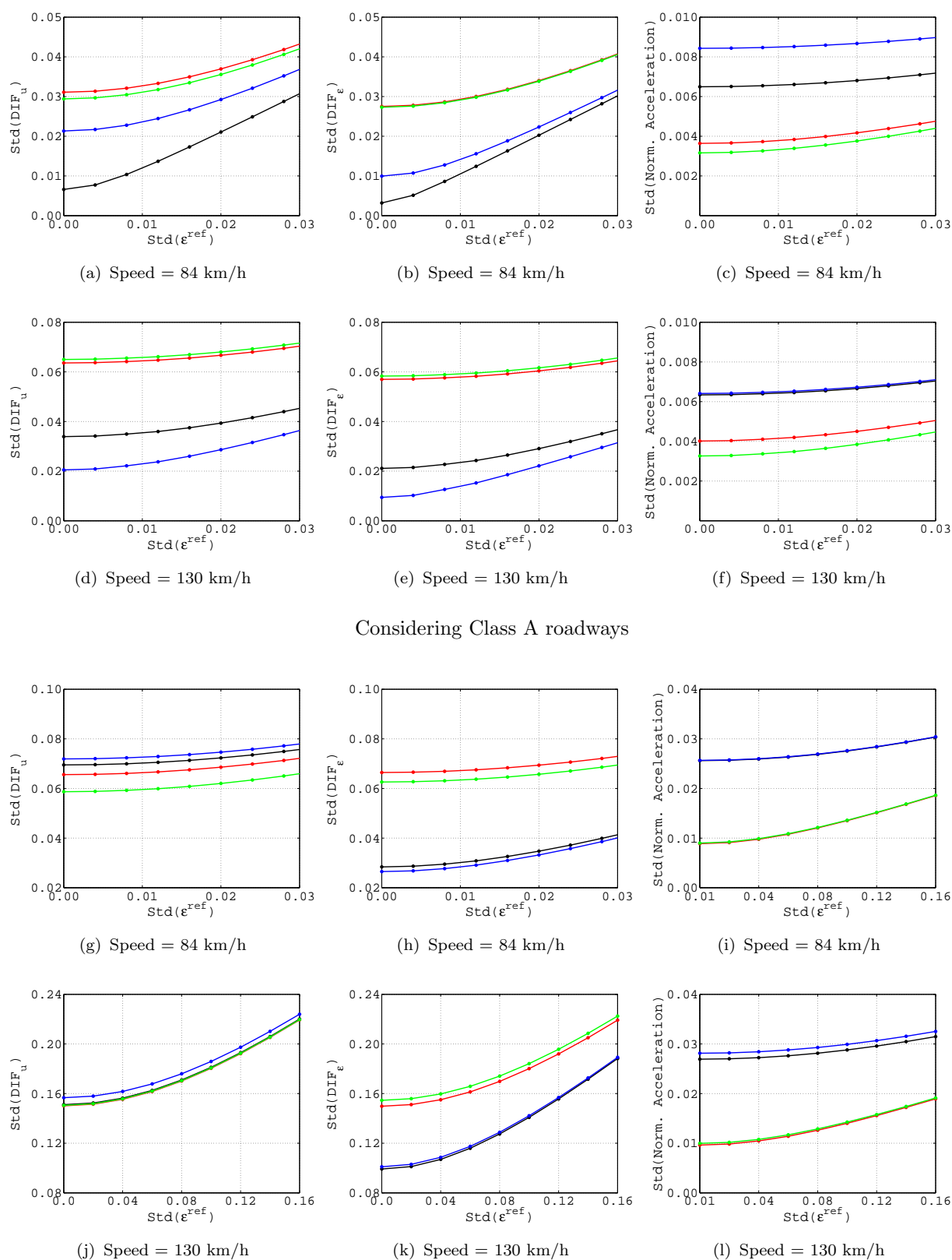
- Considering Class B roadways: With regard to the two-degree-of-freedom vehicle model, the couplings of the bridge subsystems (Model 3 and Model 4) are important at both critical speeds for all response measures studied. In contrast, with regard to the more realistic vehicle model, i.e., the eight-degree-of-freedom model, the effect of the couplings on the obtained uncertainties is clear for the displacements and the accelerations. With regard to the strains, the simpler models (Model 1 and Model 2) can be described as adequate enough.

The ranking of the models depends on the vehicle's speed and the investigated response, however, the conclusions drawn above can apply to the critical frequency ratios derived earlier. These ratios represent the make up of the maximum dynamic response for classes of bridges and speeds discussed in Section 4.3.5. In addition, the class of the roadways has a major influence on determining the significance of the coupled subsystems in bridge engineering. The rougher the road surfaces, the more important the bridge-vehicle interaction becomes. Nevertheless, such a study is an attempt to support the application of detailed models over simpler ones. The first critical speed 84 km/h is a practical speed for heavy vehicles (eight-degree-of-freedom), and it has been observed that the use of moving weight model solutions (Model 1) to get the global displacements and strains of the bridge's superstructure can be sufficient assuming that the road profiles are very good. However, when

rougher road profiles (Class B) are used, displacements have an increase of 13.5% if the bridge subsystems are coupled (Model 4) and this better response is not overpowered by the accompaying uncertainty, therefore, this model is considered to be appropriate for the case being studied. The strains show lower sensitivity for the coupling effects since the simpler models (Model 1 and Model 2) are still considered to be fit for Class B of the road profiles.

## 5.6    Conclusions

As to be expected, the main players of the dynamic response when a heavy vehicle is passing is the speed. However, the vehicle dynamics also contributes here, and its collective attribution depends on the response estimate investigated and the vehicle model used. The variance of the displacements and accelerations are more dependent on modeling the bridge-vehicle interaction. This is even more the case with rougher roadways. Whereas strains are more resilient to the effects of the couplings when compared with the displacements and accelerations.

Total model uncertainty can be used to balance the better response of the model to its uncertainty in order to select the model that is most fit for a certain response. The plausible models tested are the following: coupled model of the bridge and vehicle considering random vibrations with elastic supports (Model 4), coupled model of the bridge and vehicle considering random vibrations (Model 3), coupled model of the bridge and vehicle without considering random vibrations (Model 2), decoupled model of a moving weight (Model 1). The model which gives the lowest total uncertainty is recommended for the response examined. For the first chosen critical speed 84 km/h which is a practical speed for heavy vehicles (eight-degree-of-freedom), the moving weight model (Model 1) is sufficient for obtaining the global displacements and strains of the bridge system assuming that the road profiles are very good. However, for rougher road profiles (Class B), the modeling of bridge-vehicle interaction is considered appropriate as the increase of 13.5% in the displacements is not overpowered by the accompaying uncertainty. The strains are still governed by the simpler models (Model 1 and Model 2) for Class B road profiles. Whereas, the accelerations are

mainly governed by the models that consider bridge-vehicle interaction for both classes of road profiles.

The observations drawn can apply to the derived critical frequency ratios. Furthermore, the rougher the road surfaces, the greater the importance of the interaction between the bridge and vehicle.

# Chapter 6

# Assessment of Coupled Partial Models

## 6.1 Introduction

Structural engineering uses different partial models of materials, structural elements, loading, to name a few, to represent real structures. These classes of models are often referred to as partial models, which are looked at separately to allow a thorough study and avoid excessive complexity in handling the engineering problem. However, different classes of partial models may interact with each other and influence the global response.

Every class of a partial model may be presented by different plausible descriptions, which emulate a behavior, a phenomenon or an action, however, these descriptions may also show inconsistencies or incompatibilities. The engineer has to make sure that the partial models affecting the engineering problem are considered. Moreover, the engineer has to decide on the appropriate plausible description to obtain a reliable prognosis. Therefore, a systematic procedure that assesses coupled partial models in quantitative measures is needed. This investigation tries to address the questions related to the importance of considering a class of a partial model in the analysis, the interactions between the partial models, and the quality of a combination between plausible descriptions of partial models.

Since heavier vehicles now travel on road networks, existing highway bridges are checked for their adequacy in handling this increase in the dynamic loadings. The conditions of the bridge, like the long-term deflections, may be of importance since they excite the vehicle traversing the bridge. Therefore, the model of the bridge-vehicle interaction (loading) and the model for the long-term deflections (material) are coupled to study their effects on the dynamic response of the bridge.

The first part of this chapter describes the partial models studied for the engineering problem. The second part discusses the assessment method of the response of the coupled partial models. An application example of the assessment procedure is presented for the response scenarios selected for the dynamic problem.

## 6.2  Partial Models

Deflections may develop in concrete beam bridges due to long-term deformations. These deformations often cause harmonic excitation in a vehicle traveling over the bridge at a constant speed. Thus, the dynamic effects due to the bridge-vehicle interaction are influenced by these static deformations. In other words, there is an interaction between the loading model of a traveling vehicle and the creep model of the bridge's material. Within the current research area, very few studies have been involved in such a topic. The effects of road surface roughness and the long-term deflection of prestressed concrete bridges on the dynamic effects due to moving vehicles were examined in [104]. The concrete bridges studied were multi-span girder bridges and cable-stayed bridges. The authors concluded that the effects of random road unevenness on the dynamic impact induced by moving vehicles is significant for girder bridges, while that of long-term deflections of the concrete deck is small to moderate. However, the authors conducted the study by a direct comparison between the responses. The issues of the response quality or the significance of considering long-term deflections were not addressed. In this examination, the partial models of loading and material are coupled and the quality of the response of the global model is examined.

## 6.2.1 Creep Models

The creep models describe the time-dependent increase of the creep compliance $C_{c,cr}$ over time. $C_{c,cr}$ is defined for constant stresses, and it depends on the specifics of the creep model. Thus, the creep strain $\varepsilon_{c,cr}$ is computed as:

$$\varepsilon_{c,cr} = \sigma_c C_{c,cr}\left(t, t_0\right), \tag{6.1}$$

where $\sigma_c$ is the stress in concrete, $t$ is the actual concrete age and $t_0$ is the age of concrete at the beginning of loading. The stresses vary when analyzing prestressed and reinforced concrete structures. Therefore, in order to use the creep compliance models, the stress history $\sigma_c\left(t\right)$ is integrated over time using numerical algorithms, i.e. the Boltzmann principle of superposition.

The creep models vary in their level of complexity, theoretical background, and input parameters. The following four creep models examined are those according to:

- The American Concrete Institute ACI209 [105]

- The Model Code 90-99 MC99 [106] - incorporated in the recent publication of Model Code 10 [107]

- B3 by Bažant and Bajewa [108]

- GL2000 by Gardner and Lockman [109].

Model ACI209 and MC99 are built according to the product-ansatz, by combining the ultimate creep value $\varphi_{c,\infty}$ with a time function. The ultimate creep value $\varphi_{c,\infty}$ indicates that the creep deformations hit a plateau after approximately 70 years of loading, whereas, model B3, which follows the summation ansatz to include the viscoelastic, viscoplastic and drying creep contributions, shows a steady increase over time without an ultimate creep value. Model GL2000 is purely an empirical model which is created by fitting experimental data.

The creep strains are considered as additional terms to the strains in the concrete, which leads to an increase of the total strains $\varepsilon_{c,tot}$ of the concrete over time, and is expressed as:

$$\varepsilon_{c,tot}\left(t\right) = \varepsilon_{c,el}\left(t\right) + \varepsilon_{c,cr}\left(t\right), \tag{6.2}$$

with $\varepsilon_{c,el}\left(t\right)$ as the time-dependent elastic strains.

The modeling and the assessment of the examined creep models are found in the study of [110]. The author's assessment is based on the uncertainty of the model's prognosis, combining parameter and model uncertainties. Their results have been used in this investigation.

## 6.2.2 Loading Model of a Heavy Vehicle

The loading model of a heavy vehicle traveling over a bridge has been treated in several studies, which were reviewed in Section 3.1. The loading describing a single heavy truck traveling over a bridge is considered to be a partial model with the following plausible descriptions:

- A model of a moving weight at a constant speed

- A model for the bridge-vehicle interaction without considering road unevenness

- A model for the bridge-vehicle interaction considering road unevenness

The problem of the bridge-vehicle interaction is solved in the time domain performing a direct time integration algorithm, Newmark-$\beta$ algorithm, in a non-iterative procedure conditioning over a very small time step [21]. The solution algorithm and its verification were presented in Section 3.1.3. Road unevenness is characterized as a Gaussian random process. A description of the process and its realization can be found in Section 3.1.4.

The quality of the individual loading model is determined using the total uncertainty presented in Section 5.5. The model with the lowest uncertainty is given a quality of 1 and the rest of the models are graded proportionally for the response investigated.

## 6.3 Numerical Analysis

The quality of the response of the coupled partial models is examined. Therefore, there is a need to consider the effects of the partial models combined on the global response. For the partial models studied, the main steps in performing the dynamic analysis considering bridge-vehicle interaction and long-term deflections are depicted in Figure 6.1.
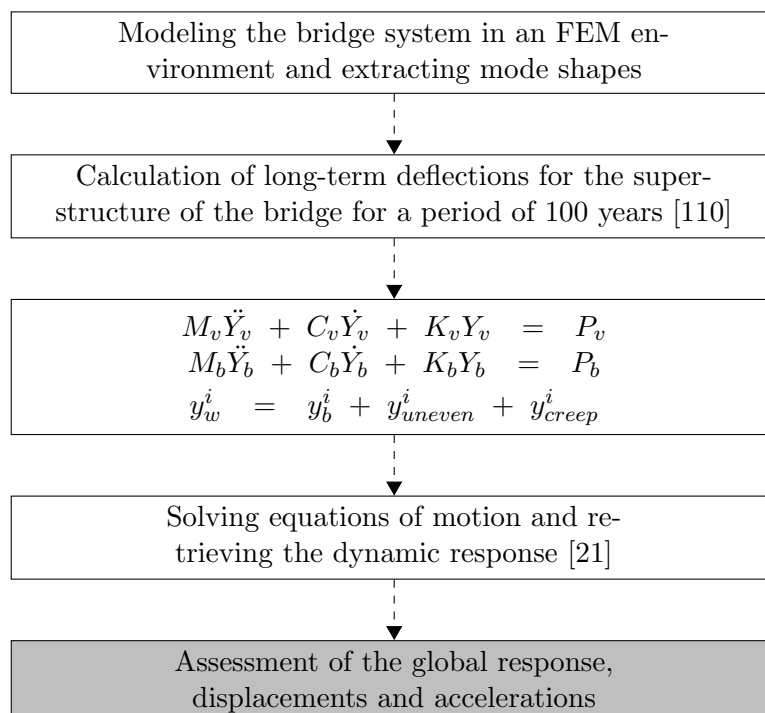


FIGURE 6.1: Flowchart of the numerical analysis

# 6.4 Assessment Method

The assessment approach used extends the concepts of sensitivity analysis presented in Section 2.4.1. As previously mentioned, the sensitivity analysis can be performed for a general family of inputs. These inputs could be simply input parameters or models. The possibility of investigating the influence of model selection on the variance of the output, in addition to model input parameters was addressed by [47]. This kind of investigation was carried out by [76], in which the influences of the model choice and input parameters on the uncertainty of the model prognosis were investigated. The author introduced a random variable with discrete values to describe the input parameter related to the choice of a model. The contributions of the input parameters and the model choice serve as guidelines for the direction of further research. An extension of the idea using graph theory and sensitivity analysis is proposed in a joint publication [111]. The proposed algorithm first identifies the partial models that are of relevance to a specific response and then estimates a measure for determining the reliability of the prognosis based on the influence of a partial model description.

In the following subsection, the main description of the assessment method is illustrated. A detailed account of the proposed procedure and its extended application can be found in [111].

## 6.4.1 Graphical Representation

A graph is used to map the combinations of partial models for an engineering problem. Thus, the vertices of a graph correspond to the partial models and the edges correspond to the coupling of the partial models as shown in Figure 6.2. The path through the graph presents a possible global coupled model of the engineering problem studied [112], e.g., the path is indicated by the shaded vertices and their solid line edges in Figure 6.2.

In addition, the vertices may have additional attributions, such as weighting factors. These factors, e.g., $(b_5), (b_6)$, etc., are denoted as the quality of the partial models. The plausible descriptions of a partial model, e.g., C-1, C-2, and C-3 in Figure 6.2, are grouped in one

class of a partial model C. For example, model class C may contain the different descriptions of the loading model on a bridge due to a moving heavy vehicle on it. Connections between C-1 and C-2 are not allowed. In other words, two or multiple descriptions of a partial model cannot be simultaneously assigned to another class of a partial model.
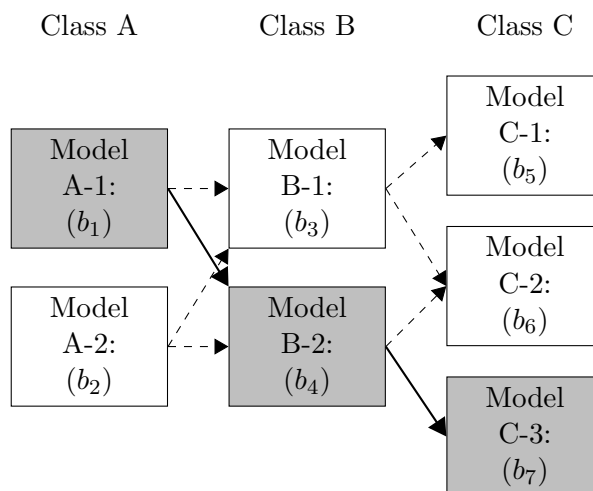


FIGURE 6.2: Example of a graph grouping seven partial models (boxes) into three different classes (A, B, and C) connecting them through the couplings (dashed and solid lines)

## 6.4.2 Sensitivity to a Partial Model Class

For engineering applications, several classes of partial models $M_i$ are often coupled to represent a global model. The influence of a class of a partial model $M_i$ on the global response can be identified using sensitivity indices.

A classical description of a variance-based sensitivity analysis is given in Section 2.4.1. It basically examines how the output uncertainty of a model is apportioned to the model's input uncertainties. In this case, the same concept is employed to apportion the output uncertainty to the classes of partial models. The estimated first order $S_i^M$ and total effect $S_{Ti}^M$ indices indicate the influence of a class of a partial model on the uncertainty of the global behavior. A high value of $S_{Ti}^M$ indicates that $M_i$ influences the response of the global model significantly, whereas a very low value of $S_{Ti}^M$ indicates that the influence of this model class on the global behavior is negligible. Moreover, the sensitivity analysis detects and quantifies the interrelation between the partial model classes, $S_{Ti}^M - S_i^M$, which may have a physical interpretation. Such an examination would categorize the model classes into

influential or non-influential classes. Partial model classes that are labeled as non-influential may be excluded from further examinations.

Each $M_i$s are described using an uncorrelated, uniformly distributed, discrete random parameter as follows:

$$X_i^M \in \{0, 1\}, \text{ with } i = 1, \ldots, n_M, \tag{6.3}$$

where $n_M$ is the number of classes of the partial models examined. The values of $X_i$ are either 0 or 1, where 0 indicates a deactivated model class and 1 indicates an activated model class. An activated model class simply means that its corresponding partial model is involved in building the global one; and a deactivated model class means that its corresponding partial model is not considered in building the global one. For example, the loading model class of a heavy vehicle traveling over a bridge can be deactivated by ignoring the additional dynamic effects of a moving vehicle or activated by considering the dynamics of the vehicle, its speed, and interaction with the bridge.

For these $n_M$ random variables, the sensitivity indices are estimated following the relationships explained in Section 2.4.1. The input parameters $X_i$ have discrete values that enable an efficient calculation of the sensitivity indices using Equations (2.7) and (2.9). The combinations between the possible values of the discrete input parameters are limited. The model output of each of these combinations is retrieved and the terms $V(E(Y|X_i))$, $V(E(Y|X_{\sim i}))$, and $V(Y)$ can be calculated directly without the need for the full sensitivity scheme by *Saltelli et al.* [47].

## 6.4.3 Sensitivity to the Description within a Partial Model Class

Each partial model can have multiple descriptions, thus, it is important to identify the influence of the model choice within a class of a partial model. Such an examination quantifies the influence that the selection of the appropriate plausible description from a partial model class $M_i$ has on the variance of the global response. As previously mentioned, [76] proposed introducing an additional input parameter for describing the model choice. The sensitivity indices for the model's input parameters and the model choice parameter are computed and used to estimate the contribution of the input parameters and the model choice to the

output uncertainty. Thus, the values of the sensitivity indices indicate whether it is the description of the model or its input parameters that most contribute to the uncertainty of the output and guide the examination accordingly. The proposed method extends this idea for investigating the significance of the model choice considering multiple classes of partial models, which are coupled to build a global model.

As in the previous section, an uncorrelated, uniformly distributed, discrete random variable is introduced, which is expressed as:

$$X_i^{MC} \in \{1, 2, \ldots, n_{PM_i}\} \ , \text{ with } i = 1, \ldots, \ n_M, \tag{6.4}$$

where $n_{PM_i}$ is the number of the plausible descriptions of a partial model within a model class $M_i$, and the variable $X_i^{MC}$ resembles the choice of the $j^{th}$ description of a partial model $PM_{i,j}$ from class $M_i$. For the global model in Figure 6.2, $X_i^{MC}$ can have the values of 1, 2 or 3, which correspond to the models C-1, C-2, and C-3 of model class $C$. The combinations between the possible values of the discrete input parameters of the different partial models $X_i^{MC}$ are also finite. The output of each of these combinations is obtained and the terms $V(E(Y|X_i))$, $V(E(Y|X_{-i}))$, and $V(Y)$ are computed.

The total effect sensitivity indices $S_{Ti}^{MC}$ are computed to the input parameters of the model choice. A high $S_{Ti}^{MC}$ indicates that the choice of description of a partial model within a model class $M_i$ leads to a high variation in the global model response. In other words, the choice of description from group $M_i$ is significant for the quality of the output response. A low $S_{Ti}^{MC}$ means, that the choice of the models within $M_i$ has a minor effect on the response and consequently the response quality. These cases occur when the different descriptions of the partial model within $M_i$ cause similar effects on the response studied.

In short, the sensitivity regarding the model choice is a measure of how much the model choice within a model class $M_i$ contributes to the variation of the output. Therefore, it follows that the more the variation of the response can be attributed to the choice of model within a class $M_i$, the more important it is to choose the most appropriate model from $M_i$, in order to obtain a better global response quality. Therefore, $S_{Ti}^{MC}$ index can be used as a weighting factor of a partial model class, considering its plausible descriptions, when coupled with other partial model classes. This weighting factor is combined with the

individual quality of the partial models within a class $M_i$, and the global model quality $(MQ_{GM})$ can be computed.

### 6.4.4 Quality of Coupled Partial Models

The weighting factor of the vertex $(b_{ij})$ is denoted as the quality of the partial model $PM_{i,j}$ within the global coupled model. This factor is computed as follows:

$$b_{ij} = \frac{S_{Ti}^{MC} \cdot MQ_{PM_{i,j}}}{\sum_{i=1}^{n_M} S_{Ti}^{MC}}, \text{ with } \quad PM_{i,j} \in M_i, \tag{6.5}$$

where $MQ_{PM_{i,j}}$ is the quality of a studied response using the $j^{th}$ description of the partial model $PM_{i,j}$ from class $M_i$ which is examined individually, and $S_{Ti}^{MC}$ is the estimate for the significance of a chosen description from the model class $M_i$ on the quality of the global response (see Section 6.4.3). The sum of the total effect indices $\sum_{i=1}^{n_M} S_{Ti}^{MC}$ may be larger than one for a non-additive global model, and since this may affect the computation of the quality of the global model, a normalizing constant of $\sum_{i=1}^{n_M} S_{Ti}^{MC}$ is used in the calculation of $b_{ij}$.

Accordingly, the global model quality $MQ_{GM}$ can be determined as follows:

$$MQ_{GM} = \sum_{i=1}^{n_M} \frac{S_{Ti}^{MC} \cdot MQ_{PM_{i,j}}}{\sum_{i=1}^{n_M} S_{Ti}^{MC}}, \text{ with } \quad PM_{i,j} \in M_i, \tag{6.6}$$

$MQ_{GM}$ is a quantitative measure for the quality of the global model, which has a value of between 0 and 1, with 1 representing the best quality.

## 6.5 Numerical Example

### 6.5.1 General Description

The system of the multi-span continuous bridge and the two-degree-of-freedom vehicle model described in Section 4.2.1 and Section 4.2.2.1, respectively, are used in the analysis. The

characteristics of the vehicle are given in Table 4.3. The modal information of the bridge and the vehicle are shown in Table 4.2 and Table 4.4, respectively. In addition, the superstructure is a prestressed concrete box girder. The considered load cases are the dead load of the superstructure and pavement $g$=166 kN/m, and a uniformly distributed traffic load of $p$=46 kN/m following *DIN EN 1991-2* [113].



(a) Structural system



(b) Geometry of the prestressing



(c) Cross section deck

|  | **Deck** |
| --- | --- |
| **Concrete** | C 50/60 |
| CEM | II,52.5N |
| $E_{co}$ [MN/m$^2$] | 38500 |
| $E_{cm}$ [MN/m$^2$] | 32800 |
| $f_{cm}$ [MN/m$^2$] | 58 |
| $c$ [kg/m$^3$] | 400 |
| $w$-$c$ [$-$] | 0.4 |
| $f$-$a$ [$-$] | 0.5 |
| $sl$ [m] | 0.15 |
| $a$ [$-$] | 0.015 |
| $f_{ctm}$ [MN/m$^2$] | 4.1 |
| $\varepsilon_{c1}$ | -0.0026 |
| $\beta_{ct}$ | 0.4 |
| **Steel** | prestessed Y1770C |
| $E_p$ [MN/m$^2$] | 190000 |
| $f_{p0.1}$ [MN/m$^2$] | 1500 |

(d) Material parameters
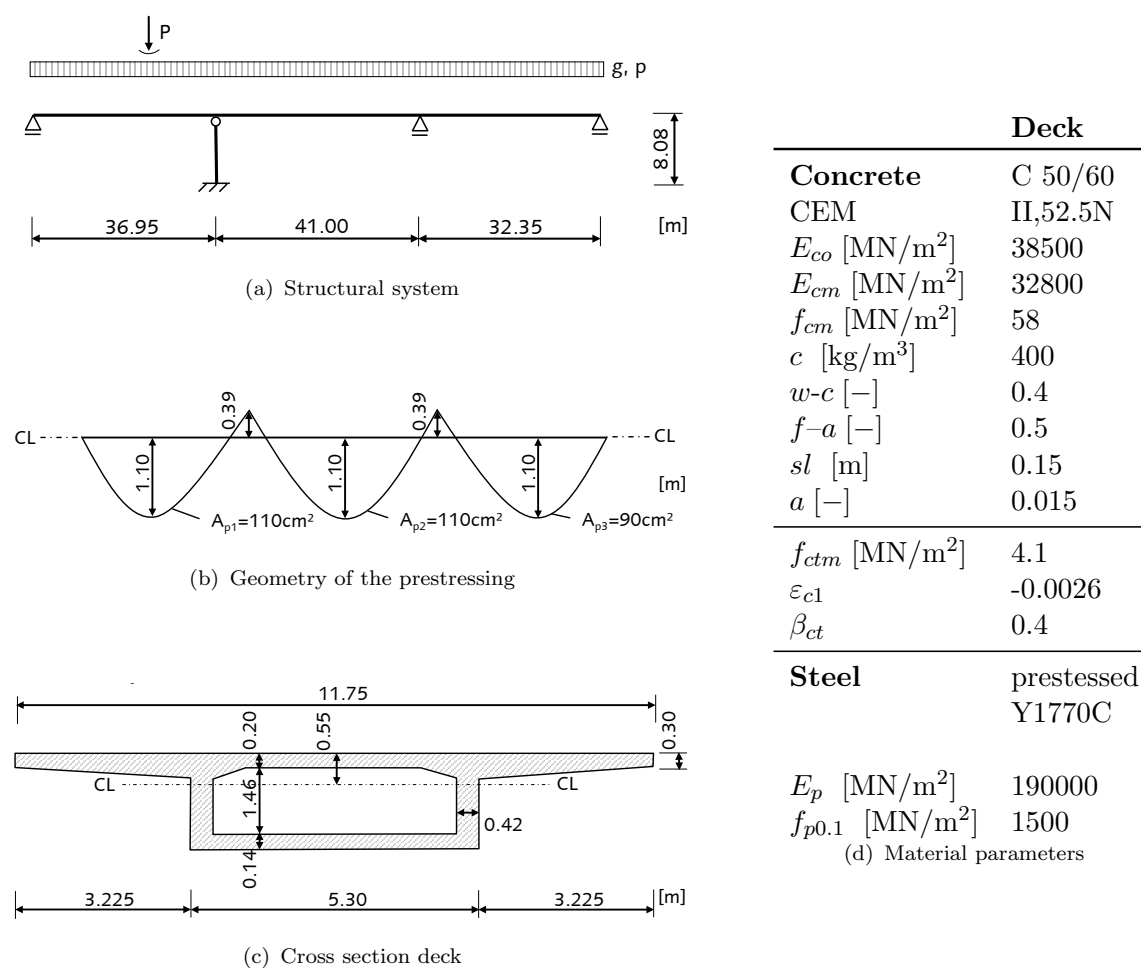
FIGURE 6.3: Bridge geometry and materials

The creep deformations are calculated for quasi-permanent loading for a load duration of 100 years. A heavy vehicle is assumed to traverse the bridge at $t - t_0$=100 y, therefore, the state of the bridge at $t - t_0$=100 y considering the long-term deflections of the superstructure is computed and employed in the dynamic analysis. Moreover, random road unevenness is generated by means of the Monte Carlo simulation and considered in the dynamic analysis. In total, 500 samples of random profiles simulated with the following properties: $S_{FF}(\kappa_0)$ = 0.5 × 10$^{-6}$ m$^3$/cycle [27], $\omega_l$ = 7 rad/s, $\omega_u$ = 35 rad/s, and $N$ = 320. The road surfaces

generated are passed through a moving average filter to take the tire envelopment of road unevenness into account [89].

The dynamic response due to the bridge-vehicle interaction considering the initial conditions of the superstructure is obtained. The numerical estimates used for the assessment are the Dynamic Incremental Factor for the displacements $\text{DIF}_u$ and the maximum normalized accelerations at the middle of the first span.

## 6.5.2 Dynamic Response

The following is an analysis sample of the dynamic displacement of the bridge when the bridge-vehicle interaction is considered with long-term deflections and road unevenness. Both road conditions are a source of excitation for the vehicle, which introduces additional dynamic effects on the bridge. The combination of these excitations constitutes the dynamic response. For a better understanding of the effects of the initial conditions of the bridge superstructure on the dynamic response, four schemes are analyzed;

- Scheme 1: a perfect straight smooth road

- Scheme 2: long-term deflections only

- Scheme 3: road unevenness only

- Scheme 4: long-term deflections and road unevenness

For the analysis sample examined in this section, GL2000 creep model is used to compute the long-term deflections of the superstructure at $t - t_0 = 100$ y. The first mid-span displacement of the bridge considering the different schemes for a vehicle traveling at a speed of 90 km/h (25 m/s) is depicted in Figure 6.4. It follows then that the dynamic effects are not only affected by road unevenness, but they are also affected by the long-term deflections of the superstructure.

The frequency content of the dynamic response is examined in Figures 6.5 and 6.6. This investigation examines the responsive behavior of the dynamic response of the bridge to the
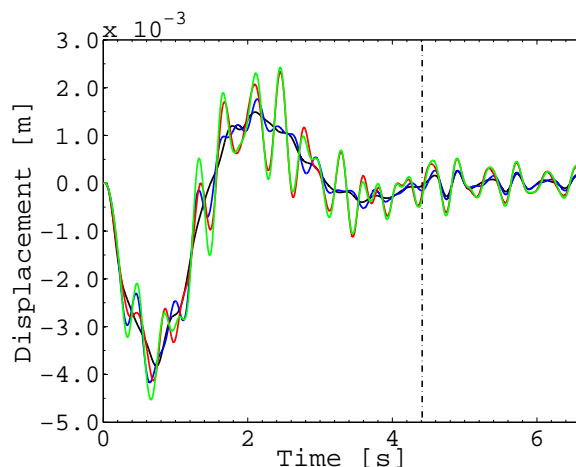
FIGURE 6.4: First mid-span displacement considering different schemes: (—) Scheme 1, (—) Scheme 2, (—) Scheme 3, (—) Scheme 4

sources of excitation considered. The highest amplitudes are at low frequencies, which correspond to the excitation caused by the moving weight of the vehicle as shown in Figure 6.5. However, other peaks appear around the first and second natural bending frequencies of the bridge (2.5 Hz and 3.6 Hz). Also, when Scheme 2 or Scheme 3 are considered, the main additional contributions to the response amplitudes are at 2.5 Hz and 3.6 Hz.
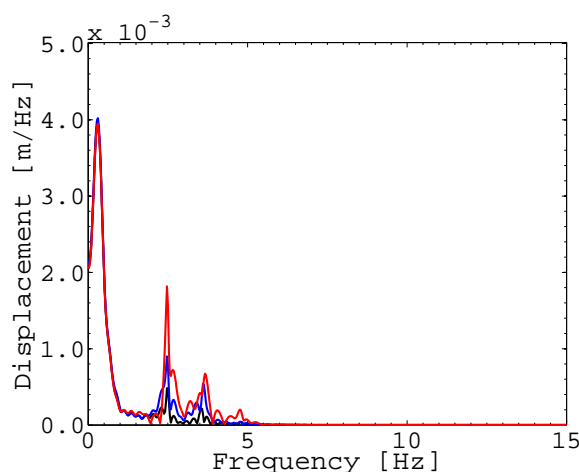


FIGURE 6.5: Fourier amplitude spectrum of the bridge's first mid-span displacement: (—) Scheme 1, (—) Scheme 2, (—) Scheme 3

The response measure studied reacts differently to the type of excitation (Scheme 2 or Scheme 3) as the response amplitudes increase in variant portions around the natural frequencies of the bridge as shown in Table 6.1. The conclusion that could be drawn after investigating the amplitude spectra of the dynamic response is that the initial state of the bridge when the vehicle traverses a bridge is of importance, not only because of road unevenness, but
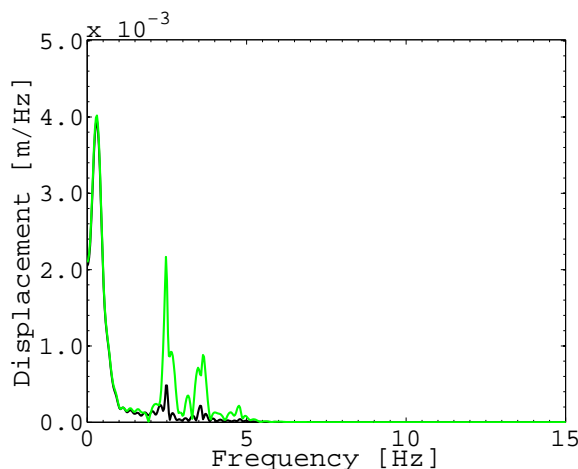
FIGURE 6.6: Fourier amplitude spectrum of the bridge's first mid-span displacement: (—) Scheme 1, (—) Scheme 4

also because of the long-term deflections. Therefore, it would be of interest to estimate the influence of creep models and dynamic loading models on the dynamic response using quantified measures. Such measures help in assessing the reliability of the prognosis.

TABLE 6.1: Factors for the increase in the response amplitudes of the displacements

|  | at 2.5 Hz | at 3.6 Hz |
| --- | --- | --- |
| Scheme 2 | 1.86 | 2.54 |
| Scheme 3 | 3.76 | 3.06 |
| Scheme 4 | 4.51 | 4.15 |

### 6.5.3   Assessment Results

The classes of the partial models examined are the creep model of concrete and the loading model of a heavy vehicle traveling over the bridge. In the following section, the assessment results obtained for two response scenarios are presented, which are the $\text{DIF}_u$ and the maximum normalized accelerations.

#### 6.5.3.1   Scenario I: $\text{DIF}_u$

In this scenario, the influence that the examined partial models have on the $\text{DIF}_u$ for the first mid-span displacement is studied. According to the procedure described in Section 6.4, the influence of a class of partial models is investigated first. The classes of the partial models

are denoted as creep (C) $M_1$ and loading (L) $M_2$. The parameters $X_i^M$, with $i = 1, 2$ are sampled for the sensitivity analysis and the first order $S_i^M$ and total effect $S_{Ti}^M$ sensitivity indices are calculated as shown in Table 6.2. The loading model is the dominant partial model, with a $S_i^M = 0.94$. This is to be expected since the loading class is the main model for estimating $\text{DIF}_u$. It can be observed that the creep model class has a small influence on $\text{DIF}_u$. Studying the difference $S_{Ti}^M - S_i^M$, it is clear that there is an interaction between the creep and loading model classes as indicated by the higher values of $S_{Ti}^M$. The loading model is affected by the material model since long-term deflections can be treated as an excitation for the vehicle model (loading) and this relation may be reflected in the difference $S_{Ti}^M - S_i^M$.

TABLE 6.2: Sensitivity indices for the $\text{DIF}_u$

|  | C | L |
|---|---|---|
| $S_i^M$ | 0.03 | 0.94 |
| $S_{Ti}^M$ | **0.06** | **0.97** |
| $S_{Ti}^M - S_i^M$ | 0.03 | 0.03 |
| $S_i^{MC}$ | 0.09 | 0.86 |
| $S_{Ti}^{MC}$ | **0.14** | **0.91** |
| $S_{Ti}^{MC} - S_i^{MC}$ | 0.05 | 0.05 |

The first examination identifies the key classes of partial models affecting the $\text{DIF}_u$. The importance of the choice of a plausible description within a class of a partial model is then investigated. The two parameters $X_1^{MC}$ and $X_2^{MC}$ are considered, where $X_1^{MC}$ represents the choice for the creep model and $X_2^{MC}$ the choice for the loading model. The possible discrete values of $X_i^{MC}$ are shown in Table 6.3, and the estimated $S_i^{MC}$ and $S_{Ti}^{MC}$ are presented in Table 6.2. The choice of the loading model is of great importance. This means that selecting the moving weight, or BVI with or without road unevenness when running the dynamic analysis has a major influence on the $\text{DIF}_u$. However, the choice of the creep model still has a significant influence with a contribution of $S_{Ti}^{MC} = 0.14$. Thus, the quality of the global model depends on the quality of the chosen loading and creep models.

The quality of the individually examined partial models has to be retrieved in a preliminary step. This has been obtained for the creep models from the study of [110]. The total model uncertainty is used for the loading models, which has been explained in Section 6.2.2. The qualities of the partial models are given in Table 6.3. For a combination of a creep and a loading model described by a path in the graph, a quality $MQ_{GM}$ can be computed using

TABLE 6.3: PM descriptions and qualities for the $DIF_u$

| $X_1^{MC}$ | Creep | $MQ_{PM}$ | $X_2^{MC}$ | Loading | $MQ_{PM}$ |
|---|---|---|---|---|---|
| 1 | ACI209 | 0.68 | 1 | Moving weight | 0.91 |
| 2 | MC10 | 0.76 | 2 | BVI without uneven-ness | 1.00 |
| 3 | B3 | 1.00 | 3 | BVI with unevenness | 0.84 |
| 4 | GL2000 | 0.92 | | | |

Equation (6.6). This is shown in Figure 6.7 for a combination of the creep model ACI209 and loading model considering the bridge-vehicle interaction without road unevenness, where the $MQ_{GM} = 0.96$.
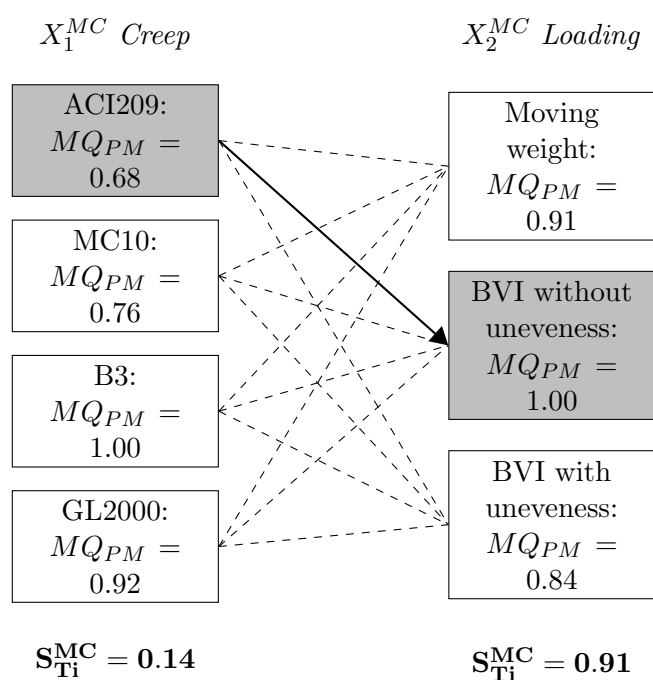


FIGURE 6.7: Graph of significant model classes for the $DIF_u$

### 6.5.3.2 Scenario II: Normalized Accelerations

The same steps are applied for the second response scenario, the maximum normalized accelerations. First, the influence of partial model classes is estimated for the accelerations. It can be seen from Table 6.4 that the loading model class with $S_{Ti}^{MC} = 0.98$ is the leading model class. The effect of the creep model class on the accelerations is of a lower order when compared with the displacements. In addition, the influence of the choice from the plausible descriptions of the model class is examined. $X_1^{MC}$ contributes the choice of the

creep model and $X_2^{MC}$ contributes the choice of the loading model. The estimated $S_i^{MC}$ and $S_{Ti}^{MC}$ are presented in Table 6.4. The choice of loading model has a major influence on the accelerations. The choice of creep model also has an influence with a contribution of $S_{Ti}^{MC} = 0.07$, however, it is not as strong as its influence on the $\text{DIF}_u$. The quality of the accelerations retrieved from the global model still depends on the quality of the selected loading and creep models.

TABLE 6.4: Sensitivity indices for the normalized accelerations

|  | C | L |
|---|---|---|
| $S_i^M$ | 0.02 | 0.97 |
| $S_{Ti}^M$ | **0.03** | **0.98** |
| $S_{Ti}^M - S_i^M$ | 0.01 | 0.01 |
| $S_i^{MC}$ | 0.04 | 0.93 |
| $S_{Ti}^{MC}$ | **0.07** | **0.96** |
| $S_{Ti}^{MC} - S_i^{MC}$ | 0.03 | 0.03 |

The quality of the individually examined partial models are given in Table 6.5. Figure 6.8 shows a combination of creep model ACI209 and loading model considering bridge-vehicle interaction without road unevenness, where the $MQ_{GM} = 0.68$.

TABLE 6.5: PM descriptions and qualities for the normalized accelerations

| $X_1^{MC}$ | Creep | $MQ_{PM}$ | $X_2^{MC}$ | Loading | $MQ_{PM}$ |
|---|---|---|---|---|---|
| 1 | ACI209 | 0.68 | 1 | Moving weight | 0.72 |
| 2 | MC10 | 0.76 | 2 | BVI without unevenness | 0.73 |
| 3 | B3 | 1.00 | 3 | BVI with unevenness | 1.00 |
| 4 | GL2000 | 0.92 | | | |

The quality of the response is 0.96 for the $\text{DIF}_u$ and 0.68 for the normalized accelerations when considering the same model combinations. This difference shows that the quality of the response heavily relies on the response itself, therefore, generalized conclusions need thorough examination of the responses of interest. In addition, these findings also rely on the plausible descriptions of the partial model classes considered. It is necessary to point out that the results of the assessment for this example depend on the level of road unevenness considered in the dynamic analysis. The road profiles generated here represent very good roadways, which is the status of most highway bridges. However, when much rougher road profiles are chosen, it is to be expected that the excitations of the vehicle due to
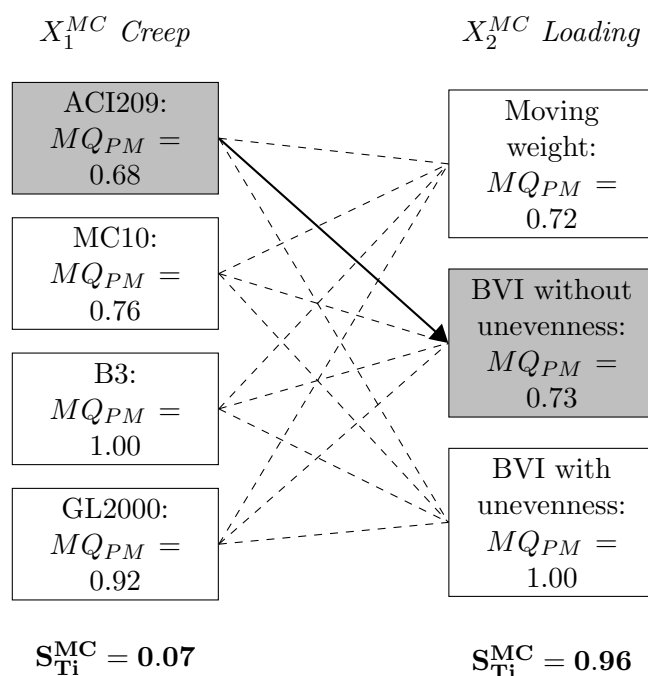
FIGURE 6.8: Graph of significant model classes for the normalized accelerations

unevenness would surpass the excitation caused by long-term deflections. Nevertheless, such an examination is of significance and practical relevance as it helps in choosing appropriate descriptions of the partial models and calculating better estimates for the dynamic response.

## 6.6   Conclusions

The dynamic effects due to the bridge-vehicle interaction are influenced by the creep deformations. The two partial models with their plausible descriptions of the dynamic loading and material are interrelated. The assessment procedure extends the use of sensitivity analysis to quantify the influence of model choice on the global response. It first identifies the influence of the partial models on a specific response and detects interactions that may exist between the partial models classes. And second it estimates a quantified measure for the dependency of the response quality on the descriptions of the partial model.

The response measures used in the assessment are the Dynamic Incremental Factor for the displacements $\text{DIF}_u$ and the maximum normalized accelerations. The main conclusion to be drawn from these measures is that different qualities for the response can be computed for

the same combinations of partial models. This finding points the fact that the quality of the response heavily relies on the response itself, therefore, generalized statements need careful examination of responses of interest. These findings also rely on the plausible descriptions of the partial model classes considered. Nevertheless, the procedure can be applied to different engineering problems.

# Chapter 7

# Conclusions and Recommendations for Further Research

## 7.1 General Conclusions

The objective of this study has been to suggest tools that can help to assess the dynamic responses of coupled models in bridges. This branch of structural dynamics lacks the quantified measures and mathematical expressions that could serve as guidelines in assessing the fitness of a model. Motivated by the interest of considering road unevenness in the dynamic analysis, a probabilistic study was performed. This study has been used to examine the concepts of sensitivity and uncertainty analyses to assess the dynamic output.

Sensitivity analysis is used to apportion the output uncertainty to its inputs, which could be useful in detecting the relatively important inputs for determining the output. The mathematical measures for this relative importance are the sensitivity indices, which are the first order indices $S_i$ and total order indices $S_{Ti}$. A high value of the sensitivity index indicates that the input parameter influences the output significantly, whereas a very low value indicates that the input parameter has a negligible influence. This might help the modeler or engineer to investigate the influential inputs and their underlying subsystems or partial models in greater detail since ignoring the effects of these influential inputs would affect the reliability of the output of the coupled model. Such an analysis utilizes the model

itself with no need for measurements or reference solutions. A setting for the sensitivity analysis is proposed, which enables performing the sensitivity analysis considering random stochastic processes. The classical and proposed sensitivity settings are used to identify the relevant inputs and subsystems that have the most influence on the variance of the dynamic response.

Concepts of total uncertainty based on the additive adjustment factor are used to rank the models built for the dynamic problem. The balance between the better response of the model and its uncertainty can be used to choose the model that is most fit for the response to be examined. The plausible models tested are as follows:

- The decoupled model of a moving weight (Model 1)

- The coupled model of the bridge and the vehicle without considering random vibrations (Model 2)

- The coupled model of the bridge and the vehicle considering random vibrations (Model 3)

- The coupled model of the bridge and the vehicle considering random vibrations with elastic supports (Model 4)

The model with the lowest total uncertainty is recommended for the response being examined.

In addition, the influence of partial models on the dynamic responses has been examined. A discrete input parameter was introduced to represent a partial model with its plausible descriptions. The estimated sensitivity indices for this input parameter is considered as a measure of how much the partial model affects the quality of the output of coupled partial models.

Before stating the main conclusions regarding the assessment of the dynamic output, the main observations from a general dynamic analysis considering bridge-vehicle interaction are determined and are as follows:

- Compared to the continuous system, the single-span bridge system representing short to medium bridges offers the highest dynamic amplifications in the responses resulting from a heavy vehicle traveling on it. The responses obtained from the simplified two-degree-of-freedom vehicle model are rather conservative compared with the responses obtained from the more realistic eight-degree-of-freedom vehicle model.

- Modeling elastomeric bearings also has an effect on the displacements and accelerations, however, these effects are not significant compared with those of the bridge-vehicle interaction considering road unevenness.

- The response obtained due to the moving weight is of a low frequency content. However, when considering the bridge-vehicle interaction, other peaks appear, and their magnitudes and positions depend on the frequencies of the bridge system and vehicle. The displacements and strains amplitude spectra show the same trend when compared with those of the accelerations. Furthermore, the response estimates studied react differently to the excitation caused by road unevenness since the response amplitudes increase in variant portions around the bridge's natural frequency.

- The conclusion that can be drawn after investigating the amplitude spectra of the responses is that the estimate of the displacements and accelerations are highly dependent on the bridge-vehicle interaction considering road unevenness, followed by the strains. In addition, these results depend on the vehicle model used in the dynamic analysis; the response obtained with the two-degree-of-freedom vehicle model shows higher sensitivity to road unevenness when compared with the one obtained with the eight-degree-of-freedom vehicle model.

- The critical ratios that envelop the maximum dynamic response are obtained. These ratios indicate a strong relationship between the speed of the vehicle and the first natural frequency of the bridge. The values of the Dynamic Incremental Factor (DIF) is highly dependent on the speed. By the identification of these critical ratios, critical speeds and their corresponding reasonable measure of DIF can be calculated and used for designing or upgrading bridges.

The observations above may help in explaining some of the results obtained by the sensitivity and uncertainty analyses. The following conclusions can be drawn for the vehicle models examined:

- As to be expected, the main input affecting the dynamic response when a heavy vehicle is passing is the speed.

- The vehicle dynamics also contributes here. Its collective attribution depends on the response estimate investigated and the vehicle model. For the eight-degree-of-freedom vehicle model, the stiffness of the tractor suspension has an impact on the variances of the displacements and strains. The stiffness of the tractor suspension is significant for the accelerations, but it is the damping of the tractor suspension that has a higher contribution to the variance of the acceleration.

- The contribution of the stiffness of the elastomeric bearings is examined. It was found that the bearings can have the most impact on the variance of displacements.

- It can be said that the displacements and accelerations are more dependent on the modeling of the bridge-vehicle interaction considering elastomeric bearings. This is even more the case with rougher roadways. Furthermore, strains show lower sensitivity to the previously mentioned couplings.

- The ranking of the coupled models examined by using total uncertainty depends on the speed of the vehicle and the response studied. The conclusions drawn from this apply to the critical ratios derived. Also, the class of the roadway has a major influence on determining the significance of the coupled subsystems in bridge engineering. The rougher the road surfaces, the greater the importance of the interaction between the bridge and vehicle is.

- The first critical speed considered for the bridge (84 km/h) is a practical speed for heavy vehicles (eight-degree-of-freedom). The use of the moving weight model (Model 1) to obtain the global displacements and strains of the bridge system can be sufficient assuming that the road profiles are very good. However, for rougher road profiles (Class B), the displacements increase by 13.5% if the bridge subsystems are coupled

(Model 4) and this better response is not overpowered by the accompanying uncertainty, therefore, (Model 4) is considered to be the appropriate model for the case studied. The strains are still governed by the simpler models (Model 1 and Model 2) for Class B road profiles.

- Another investigation is run that considers the long-term deflections of concrete in the dynamic analysis. It has been shown that the partial models of creep have an influence on the dynamic output for the case studied, however, this finding is highly dependent on the level of road unevenness considered.

These conclusions are drawn for the global responses of the beam bridges studied. The conclusions could be different for other responses. However, the general assessment procedure providing mathematical expressions regarding model assessment can be applied in a similar manner regardless of the type of model. It is worth mentioning that the main setback of such a study is the computational cost of the entire analysis, however, once the output is obtained, it can be used for other purposes as well.

## 7.2 Recommendations for Further Research

Model quality and assessment have not been areas of interest in bridge dynamics. Other disciplines, such as material, geo-technical, or mechanical engineering, are more advanced in using model quality and assessment in their applications. Therefore, this has been an attempt to include concepts of model assessment in the dynamic problem of bridge engineering. Based on the observations made during the course of this research, a number of directions for further research are recommended for the assessment of models and the engineering problem studied:

- The adaptation of the sensitivity analysis to include random processes in its application and the use of the total uncertainty in ranking plausible numerical models is generic in application. These assessment procedures can be used for other engineering applications, in which probabilistic studies are used to solve the randomness of the system

and the computational cost is not too high. A further extension of model assessment can be the adaptation and the use of Bayesian model selection without measurement data in model selection from plausible sets of models in engineering applications.

- The engineering problem in hand can be elaborated further as the following:

  - The analysis that has been presented was run for one type of heavy vehicle. Considering other models for trucks traveling on the road networks would make the study more comprehensive. Each of these vehicles have a different set of input parameters. In addition to the inputs of the vehicles, an input parameter can be introduced to represent the choice of a vehicle model, which is selected from the complete set of plausible vehicles. This combined with the traffic data, which is often expressed using probabilistic descriptions, general assessment of loading models of bridges can be developed

  - A 3D model of the vehicle subsystem can be used, in which rolling effects are included. Consequently, a 3D model for the bridge and elastomeric bearings can be used. The assessment of local behaviors may be of more interest and significance, e.g., the life span of expansion joints when introducing local irregularities in the road profiles

  - Other boundary conditions for the bridge may be included by integrating the soil in the numerical model to check whether the vibrations due to traffic can affect the settlements in the soil and whether differential settlements of the soil can excite the vehicle enough to influence the dynamic response

# Bibliography

[1] Y.B. Yang, J.D. Yau, and Y.S. Wu. *Vehicle-Bridge Interaction Dynamics*. World Scientific Publishing Co. Pte. Ltd., 2004.

[2] L. Frýba. *Dynamics of Railway Bridges*. Thomas Telford Ltd, 2007.

[3] S. Kim and A.S. Nowak. Load Distribution and Impact Factors for I-girder Bridges. *Journal of Bridge Engineering, ASCE*, 2(3):97–104, 1984.

[4] Y.L. Xu and W.H. Guo. Effects of Bridge Motion and Cross Wind on Ride Comfort of Road Vehicles. *Journal of Wind Engineering and Industrial Aerodynamics*, 92: 641–662, 2004.

[5] M.F. Green, D. Cebon, and D.J. Cole. Effects of Vehicle Suspension Design on Dyanmics of Highway Bridges. *Journal of Structural Engineering*, ASCE, 121(2):272–282, 1995.

[6] C.W. Kim, M. Kawatani, and W.S. Hwang. Reduction of Traffic-Induced Vibration of Two-Girder Steel Bridge seated on Elastomeric Bearings. *Engineering Structures*, 26:2185–2195, 2004.

[7] W. Weaver, S.P. Timoshenko, and D.H. Young. *Vibration Problems in Engineering*. John Wiley & Sons, 1990.

[8] R.T. Wang. Vibration of Multi-Span Timoshenko Beams to a Moving Force. *Journal of Sound and Vibration*, 207(5):731–742, 1997.

[9] D.Y. Zheng, Y.K. Cheung, F.T.K. Au, and Y.S. Cheng. Vibration of Multi-span Non-Uniform Bridges under Moving Loads by using Modified Beam Vibration Functions. *Journal of Sound and Vibration*, 212:455–467, 1998.

[10] G.V. Rao. Linear Dynamics of an Elastic Beam under Moving Loads. *Journal of Vibration and Acoustics*, 122(7):281–289, 2000.

[11] A.V. Pesterev, B. Yang, L.A. Bergman, and C.A. Tan. Revisiting the Moving Force Problem. *Journal of Sound and Vibration*, 261:75–91, 2003.

[12] M.M. Stanišič. On a New Theory of the Dynamic Behavior of the Structures carrying Moving Masses. *Ingenieur-Archiv*, 55:176–185, 1985.

[13] J.E. Akin and M. Mofid. Numerical Solution for Response of Beams with Moving Mass. *Journal of Structural Engineering*, ASCE, 115(1):120–131, 1989.

[14] J.L. Humar and A.M. Kashif. Dynamic Response of Bridges under Travelling Loads. *Canadian Journal of Civil Engineering*, 20:287–298, 1993.

[15] M.F. Green and D. Cebon. Dynamic Response of Highway Bridges to Heavy Vehicle Loads: Theory and Experimental Validation. *Journal of Sound and Vibration*, 170(1)(170):51–78, 1994.

[16] M. Fafard, M. Laflamme, and M. Savard. Dynamic Analysis of Existing Continuous Bridge. *Journal of Bridge Engineering*, 3(1):28–37, 1998.

[17] P.K. Chatterjee, T.K. Datta, and C.S. Surana. Vibration of Suspension Brigdes under Vehicular Movement. *Journal of Structural Engineering*, ASCE, 120(3):681–703, 1994.

[18] G.H. Tan, G.H. Brameld, and D.P. Thambiratnam. Development of an Analytical Model for Treating Brigde-Vehicle Interaction. *Engineering Structures*, 20(1):54–61, 1998.

[19] F. Yang and G.A. Fonder. An Interative Solution Method for Dynamic Resposne of Bridge-Vehicle Systems. *Earthquake Engineering and Structural Dynamics*, 25:195–215, 1996.

[20] Y.K. Cheung, F.T.K. Au, D.Y. Zheng, and Y.S. Cheng. Vibration of Multi-Span Non-Uniform Bridges under Moving Vehicles and Trains by using Modified Beam Vibration Functions. *Journal of Sound and Vibration*, 228:611–628, 1999.

[21] K. Liu, G. De Roeck, and G. Lombaert. The Effect of Dynamic Train-Bridge Interaction on the Bridge Resposne during a Train Passage. *Journal of Sound and Vibration*, 325:240–251, 2009.

[22] V.K. Garg and R.V. Dukkipati. *Dynamics of Railway Vehicle Systems*. Academic Press, New York, 1984.

[23] Y.B. Yang and B.H. Lin. Vehicle-Bridge Interaction Analysis by Dynamic Condensation Method. *Journal of Structural Engineering*, ASCE, 121(11):1636–1643, 1995.

[24] Y.B. Yang and Y.S. Wu. A Versatile Element for Analysing Vehicle-Bridge Interaction Response. *Engineering Structures*, 23:452–469, 2001.

[25] L. Ding, H. Hao, and X. Zhu. Evaluation of Dynamic Vehicle Axle Loads on Bridges with Different Surface Conditions. *Journal of Sound and Vibration*, 323:826–848, 2009.

[26] C.J. Dodds and J.D. Robson. The Description of Road Surface Roughness. *Journal of Sound and Vibration*, 31(2):175–183, 1973.

[27] ISO8608. *Mechanical Vibration, Road Surface Profiles*. Reporting of measured data, 1991.

[28] M.J. Inbanathan and M. Wieland. Bridge Vibration due to Vehicle Moving over a Rough Surface. *Journal of Structural Engineering*, ASCE, 133(9):1994–2008, 1987.

[29] O. Coussy, M. Said, and J.P. van Hoove. The Influence of Random Surface Irregularities on the Dynamic Response of Bridges under Suspended Moving Loads. *Journal of Sound and Vibration*, 130(2):313–320, 1989.

[30] E.S. Hwang and A.S. Nowak. Simulation of Dynamic Load for Bridges. *Journal of Structural Engineering*, ASCE , 117(5)(5):1413–1434, 1991.

[31] K. Henchi, M. Fafard, M. Talbot, and G. Dhatt. An Efficient Algorithm for Dynamic Analysis of Bridges under Moving Vehicles using a Coupled Modal and Physical Components Approch. *Journal of Sound and Vibration*, 212(4):663–683, 1998.

[32] C.H. Chang. Modeling of Laminated Rubber Bearings using an Analytical Stiffness Matrix. *International Journal of Solids and Structures*, 39:6055–6078, 2002.

[33] G.P. Warn, A.S. Whittaker, and M.C. Constantinou. Vertical Stiffness of Elastomeric and LeadRubber Seismic Isolation Bearings. *Journal of Structural Engineering, ASCE*, 133:1227–1236, 2007.

[34] J.D. Yau, Y.S. Wu, and Y.B. Yang. Impact Response of Bridges with Elastic Bearings to Moving Loads. *Journal of Sound and Vibration*, 248(1):9–30, 2001.

[35] R. Vogt. *Analyse des Tragverhaltens bewehrter Elastomerlager unter Verwendung der Methode der Finiten Elemente*. PhD thesis, Professur Verkehrsbau, Bauhaus Unversität, Weimar, 2009.

[36] W. Gao, N. Zhang, J.C. Ji, and H.P. Du. Dynamic Analysis of Vehicles with Uncertainty. *Automobile Engineering*, 222:657–664, 2008.

[37] D. Cebon. *Handbook of Vehicle-Road Interaction*. Taylor & Francis, 1999.

[38] P.H. Kirkegaard and S.R.K. Nielsen. Influence of Uncertainty of Vehicle Dynamics on the Dynamic Response of Minor Highway Bridges. In *Proceedings of the 4th International Conference on Stochastic Dynamics*, pages 507–512, University of Notre Dame, USA, August 1998.

[39] S.R.K. Nielsen and P.H. Kirkegaard. Influence of Surface Irregularities on the Dynamic Response of Minor Highway Bridges. In *Proceedings of the 4th International Conference on Stochastic Dynamics*, pages 507–512, University of Notre Dame, USA, August 6-8 1998.

[40] A. González, E. Obrien, D. Cantero, Y.Li, J. Dowlings, and A. Žnidarič. Critical Speed for the Dynamics of Truck Events on Bridges with a Smooth Road Surface. *Journal of Sound and Vibration*, 329(11):2127–2146, 2010.

[41] F. Lu, J.H. Lin, D. Kennedy, and F.W. Williams. An Algorithm to Study Non-stationary Random Vibrations of Vehicle-Bridge Systems. *Computers and Structures*, 87:177–185, 2009.

[42] G. Lombaert and J. Conte. Vehicle-Bridge Interaction in the Presence of Random Track Unevenness. Technical report, Structural Mechanics Division, Katholieke Universiteit Leuven, Belgium, 2010.

[43] S.S. Law and S.Q. Wu. Dynamic Analysis of Bridge with Non-Gaussian Uncertainties under a Moving Vehicles. *Probabilistic Engineering Mechanics*, 26:281–293, 2011.

[44] N. Liu, W.Gao, C.M. Song, and N. Zhang. Probabilistic Dynamic Analysis of Vehicle-Bridge Interaction with Uncertain Parameters. *Computer Modeling in Engineering & Sciences*, 72(2):72–102, 2011.

[45] M. Shinozuka and G. Deodatis. Simulation of Stochastic Processes by Spectral Representation. *Applied Mechanics Reviews*, 44(4):191–204, 1991.

[46] P. Paultre, O. Chaallai, and J. Proulx. Bridge Dynamics and Dynamic Amplification Factors - A Review of Analytical and Experimental Findings. *Canadian Journal of Civil Engineering*, 19:260–278, 1992.

[47] A. Saltelli, M. Ratto, T. Andres, F. Campolongo, J. Cariboni, D. Gatelli, M. Saisana, and S. Tarantola. *Global Sensitivity Analysis*. John Wiley & Sons Ltd, 2008.

[48] I. Babuska and J.T. Oden. Verification and Validation in Computational Engineering and Science: Basic Concepts. *Computer Methods in Applied Mechanics and Engineering*, 193:4057–4066, 2004.

[49] J.T. Oden and S. Prudhomme. Estimation of Modeling Error in Computational Mechanics. *Journal of Computational Physics*, 182:496–515, 2002.

[50] E. Zio and G.E. Apostolakis. Two Methods for the Structural Assessment of Model Uncertainty by Experts in Performance Assessments of Radioactive Waste Repositories. *Reliability Engineering and System Safety*, 54:225–241, 1996.

[51] J.C. Helton, J.D. Johnson, C.J. Sallaberry, and C.B. Storlie. Survey of Sampling-Based Methods for Uncertainty and Sensitivity Analysis. *Reliability Engineering and System Safety*, 91:1175–1209, 2006.

[52] H. Akaike. A New Look at the Statistical Model Identification. *IEEE Transactions on Automatic Control*, AC-19:716–723, 1974.

[53] G. Schwarz. Estimating the Dimension of a Model. *The Annals of Statistics*, 6(2): 461–464, 1978.

[54] S.F. Gull. Bayesian Inductive Inference and Maximum Entropy. In G.J. Erickson and C.R. Smith, editors, *Maximum entropy and Bayesian methods in science and engineering, vol.1: Foundations.* Kluwer, 1988.

[55] D.J.C. Mackay. Bayesian Interpolation. *Neural Computation*, 4(3):415–447, 1992.

[56] D.S. Sivia. *Data Analysis: A Bayestian Tutorial.* Oxford Science Publications, Oxford, United Kingdom, 1996.

[57] J.L. Beck and K.V. Yuen. Model Selection Using Response Measurements: A Bayesian Probabilistic Approach. *Journal of Engineering Mechanics*, 130:192–203, 2004.

[58] T. Nilsen and T. Aven. Models and Model Uncertainty in the Context of Risk Analysis. *Reliability Engineering and System Safety*, 79:309–317, 2003.

[59] S.D. Snowling and J.R. Kramer. Evaluating Modelling Uncertainty for Model Selection. *Ecological Modelling*, 138:17–30, 2001.

[60] J.C. Helton and F.J. Davis. Illustrations of Sampling-Based Methods for Uncertainty and Sensitivity Analysis. *Risk Analysis*, 22:591–622, 2002.

[61] A. Saltelli, S. Tarantola, F. Campolongo, and M. Ratto. *Sensitivity Analysis in Practice: A Guide to Assessing Scientific Models.* John Wiley & Sons Ltd, 2004.

[62] J.E. Hurtado and A.H. Barbat. Monte Carlo Techniques in Computational Stochastic Mechanics. *Archives of Computational Methods in Engineering*, 5:3–30, 1998.

[63] J.C. Helton and F.J. Davis. Latin Hybercube Sampling and the Propagation of Uncertainty in Analyses of Complex Systems. *Reliability Engineering and System Safety*, 81:23–69, 2003.

[64] A. Matala. Sample Size Requierement for Monte Carlo - Simulations using Latin Hypercube Sampling. Technical report, Department of Engineering Physics and Mathematics, Helsinki University of Technology, 2008.

[65] D.C. Montgomery and G.C. Runger. *Applied Statistics and Probability for Engineers, Third Edition.* Wiley, 2003.

[66] E. Parzen. *Stochastic Processes.* holden-Day, San Francisco, 1962.

[67] I.M. Sobol. On Freezing Unessential Variables. *Vestnik Moskovskogo Universiteta,* Serija Matematika 6:9294, 1996.

[68] S. Hora and R. Iman. A Comparison of Maximum/Bounding and bayesian/monte carlo for Fault Tree Uncertainty Analysis. Technical report, Report SAND85-2839, Sandia Laboratories, 1986.

[69] P. Lancaster and K. Salkauskas. Surfaces Generated by Moving Least Squares Methods. *Mathematics of Computation*, 37:141–158, 1981.

[70] P. Lancaster and K. Salkauskas. *Curve and Surface Fitting: An Introduction.* Academic Press Ltd, 1990.

[71] A.A. Giunta and L.T. Watson. A Comparison of Approximating Modeling Technigues: Polynomial versus Interpolating Models. Technical Report 98-4758, American Institute of Aeronautics and Astronautics, 1998.

[72] U. Alibrandi. A Response Surface Method for Nonlinear Stochastic Dynamic Analysis. In *Applications of Statistics and Probability in Civil Engineering.* Tylor & Francis Group, London, 2011.

[73] T. Most. Efficient Sensitivity Analysis of Complex Engineering Problems. In *Proceedings of the 11th International Conference on Applications of Statistics and Probability in Civil Engineering*, Zurich, August 1-4, 2011.

[74] A. Forrester, A. Sobester, and A. Keane. *Engineering Design via Surrogate Modeling: A Practical Guide.* John Wiley & Sons Ltd, 2008.

[75] I. Park, H.K. Amarchinta, and R. Grandhi. A Bayesian Approach for Auantification of Model Uncertainty. *Reliability Engineering and System Safety*, 95:777–785, 2010.

[76] T. Most. Some aspects on model assessment in a probabilistic context. *Computers and Structures*, Preprint submitted, 2011.

[77] C.W. Kim, M. Kawatani, and K.B. Kim. Three Dimentional Dynamic Analysis for Bridge-Vehicle Interaction with Roadway Roughness. *Computers & Structures*, 83: 1627–1645, 2005.

[78] L. Deng and C.S. Cai. Development of Dynamic Impact Factor for Performance Evaluation of Exicting Multi-Girder Concrete Bridges. *Engineering Structures*, 32: 21–31, 2010.

[79] M.M. ElMadany. Design and Optimization of Truck Suspensions using Covariance Analysis. *Computers and Structures*, 28:241–246, 1988.

[80] N.K. Harris, E.J. OBrien, and A.González. Reduction of Bridge Dynamic Amplification through Adjustment of Vehicle Suspension Damping. *Journal of Sound and Vibration*, 302:471–485, 2007.

[81] D. Cantero, A. González, and E.J. OBrien. Maximum Dynamic Stress on Bridges Traversed by Moving Loads. *Proceedings of the ICE - Bridge Engineering*, 162:75–85, 2009.

[82] W.R. Clough and J. Penzien. *Dynamics of Structures*. McGraw-Hill, 1993.

[83] Mathworks. *The Language of Technical Computing*. Version 7, 2008.

[84] ANSYS. *Mechanical APDL Product*. Release 12.0, 2009.

[85] W. Schiehlen. Colored Noise Excitation of Engineering Structures. In *Computational Methods in Structural Dynamics and Earthquake Engineering*, 2009.

[86] S.O. Rice. *Selected Papers on Noise and Stochastic Processes*. Dover Publications, 1954.

[87] D.E. Newland. *An Introduction to Random Vibrations, Spectral and Wavelet Analysis*. Dover Publications, Inc., 1993.

[88] D.E. Newland. The Effect of a Footprint on Perceived Surface Roughness. *Proceedings of the Royal Society of London, Series A : Mathematical, Physical sciences & Engineering Sciences*, 405:303–327, 1986.

[89] M.W. Sayers and S.M. Karamihas. Interpretation of Road Roughness Profile Data. Technical report, University of Michigan Transportation Research Institute (UMTRI) Report (96-19), 1996.

[90] K.M. Captain, A.B. Boghani, and D.N. Wormley. Analytical Tire Models for Dynamic Vehicle Simulation. *Vehicle System Dynamics*, 8:1–32, 1979.

[91] H. Eggert and W. Kauschke. *Structural Bearings*. Ernst & Sohn, 2002.

[92] M. Kawatani, Y. Kobayashi, and H. Kawaki. Influence of Elastomeric Bearings on Traffic-Induced Vibration of Highway Bridges. *Transportation Research Record*, 1696: 76–82, 2000.

[93] I.P. Swan. *The Effect of Elastomeric Bearing Degradation on Bridge Dynamic Response*. PhD thesis, School of the Built Environment, Napier University, Edinburgh, United Kingdom, 2006.

[94] EN 1337-3:2005 (E). *Structural Bearings - Part 3: Elastomeric Bearings*. European Committee for Standardization, Brussels, March 2005.

[95] S.P. Brady, E.J. O'Brien, and A. Žnidarič. The Effect of Vehicle Velocity on the Dynamic Amplification of a Vehicle Crossing a Simply Supported Bridge. *American Society of Civil Engineering*, 11:241–249, 2006.

[96] R. Cantieni. Dynamic Behavior of Highway Bridges under the Passage of Heavy Vehicles. Technical report, EMPA, Switzerland, 1992.

[97] B. Bakht and S.G. Pinjarkar. Review of Dynamic Testing of Highway Bridges. Technical report, Structural Research Report SRR-89-01, Ministry of Transportation of Ontario, 1989.

[98] M. Kawatani, S. Nishiyama, and Y. Yamada. Dynamic Response Analysis of Highway Girder Bridges under Moving Vehicles. Technical Report 2137, Osaka University, April 1993.

[99] S. Grave. *Modelling of Site-Specific Traffic Loading on Short to Medium Span Bridges*. PhD thesis, Trinity Colleg Dublin, Ireland, 2001.

[100] AS 5100.4-2004. *Bridge Design - Bearings and Deck Joints*. Standards Australia, April 2004.

[101] M. Gao, J. Xiong, and J. Zhan. Sensitive Wavelength of Track Irregularity and its Influence on Dynamic Responses of Train-Bridge System in High-Speed Railway. In *8th International Conference on Structural Dynamics, EURODYN2011*, 4-7 July 2011.

[102] V. Bayer and C. Bucher. Importance Sampling for First Passage Problems of Nonlinear Structures. *Probabilistic Engineering mechanics*, 14(1-2):27–32, 1999.

[103] X. Yin, Z. Fang, C.S. Cai, and L. Deng. Non-Stationary Random Vibration of Bridges under Vehicles with Variable Speed. *Engineering Structures*, 32:2166–2174, 2010.

[104] F.T.K. Au, Y.S. Cheng, and Y.K. Cheung. Effects of Random Road Surface Roughness and Long-Term Deflection of Prestressed Concrete Girder and Cable-Stayed Bridges on Impact due to Moving Vehicles. *Computers and Structures*, 79:853–872, 2001.

[105] ACI209. Prediction of Creep, Shrinkage, and Temperature Effects in Concrete Structures. Norm, American Concrete Institute, 1992.

[106] CEB - Comité Euro-International du Beton. Structural Concrete: Textbook on Behaviour, Design and Performance - Updated Knowledge of the CEB/FIP Model Code 90 : Volume 1-3. Technical report, Comité Euro-International du Beton, 1999.

[107] CEB - Comite Euro-International du Beton. CEB-FIP Model Code 2010 - First Complete Draft - Volume 1. Technical report, Comite Euro-International du Beton, 2010.

[108] Z.P. Bažant and S. Bajewa. Justificaton and Refinements of Model B3 for Concrete Creep and Shrinkage 2. Updating and Theoretical Basis. *Materials and Structures*, 28: 488–495, 1995.

[109] N.J. Gardner and M.J. Lockman. Design Provisions for Drying Shrinkage and Creep of Normal-Strength Concrete. *ACI Materials Journal*, 98:159–167, 2001.

[110] H. Keitel and A. Dimmig-Osburg. Uncertainty and Sensitivity Analysis of Creep Models for Uncorrelated and Correlated Input Parameters. *Engineering Structures*, 32 (11):3758–3767, 2010.

[111] H. Keitel, G. Karaki, T. Lahmer, S. Nikulla, and V. Zabel. Evaluation of Coupled Partial Models in Structural Engineering using Graph Theory and Sensitivity Analyses. *Engineering and Structures (accepted)*, 2011.

[112] A. Kaveh. Graphs and Structures. *Computers and Structures*, 40(4):893–901, 1991.

[113] DIN Deutsches Institut für Normung e. V. DIN EN 1991-2: Einwirkungen auf Tragwerke - Teil 2: Verkehrslasten auf Brücken. Norm, Beuth Verlag, Berlin, 2010.

# Modeling

## .1    Mass, damping and stiffness matrices: 8DOF

When deriving the equations of motion from the equilibrium of forces and moments acting on each mass of the eight-degree-of-freedom model, the following matrices are formulated for the vehicle model.

$$
\mathbf{M}_v =
\begin{pmatrix}
(m_T + m_S) & b_5 m_S & b_4 m_S \\
b_5 m_S & \left(I_T + b_5^2 m_S + \frac{m_4 m_5}{m_4 + m_5} a_1^2\right) & \left(b_4 b_5 m_S - \frac{m_4 m_5}{m_4 + m_5} a_1 a_2\right) \\
b_5 m_S & \left(I_T + b_5^2 m_S + \frac{m_4 m_5}{m_4 + m_5} a_1^2\right) & \left(b_4 b_5 m_S - \frac{m_4 m_5}{m_4 + m_5} a_1 a_2\right) \\
0 & 0 & 0 \\
0 & 0 & 0 \\
0 & 0 & 0 \\
0 & 0 & 0 \\
0 & 0 & 0
\end{pmatrix}
$$

$$
\begin{pmatrix}
0 & 0 & 0 & 0 & 0 \\
0 & 0 & 0 & 0 & 0 \\
0 & 0 & 0 & 0 & 0 \\
m_1 & 0 & 0 & 0 & 0 \\
0 & m_2 & 0 & 0 & 0 \\
0 & 0 & m_{31} & 0 & 0 \\
0 & 0 & 0 & m_{32} & 0 \\
0 & 0 & 0 & 0 & m_{33}
\end{pmatrix}
\tag{1}
$$

$$
\mathbf{C}_v =
\begin{pmatrix}
(c_1 + c_2 + c_{31} + c_{32} + c_{33}) & [-b_1 c_1 + b_2 c_2 + b_5(c_{31} + c_{32} + c_{33})] \\
-b_1 c_1 + b_2 c_2 + b_5(c_{31} + c_{32} + c_{33}) & [b_1^2 c_1 + b_2^2 c_2 + b_5^2(c_{31} + c_{32} + c_{33})] \\
(b_{31} + b_4)c_{31} + (b_{32} + b_4)c_{32} + (b_{33} + b_4)c_{33} & b_5[(b_{31} + b_4)c_{31} + (b_{32} + b_4)c_{32} + (b_{33} + b_4)c_{33}] \\
-c_1 & b_1 c_1 \\
-c_2 & -b_2 c_2 \\
-c_{31} & -b_5 c_{31} \\
-c_{32} & -b_5 c_{32} \\
-c_{33} & -b_5 c_{33}
\end{pmatrix}
$$

$$
\begin{array}{cccccc}
[(b_{31} + b_4)c_{31} + (b_{32} + b_4)c_{32} + (b_{33} + b_4)c_{33}] & 0 & 0 & 0 & 0 & 0 \\
b_5[(b_{31} + b_4)c_{31} + (b_{32} + b_4)c_{32} + (b_{33} + b_4)c_{33}] & 0 & 0 & 0 & 0 & 0 \\
(b_{31} + b_4)c_{31} + (b_{32} + b_4)c_{32} + (b_{33} + b_4)c_{33} & 0 & 0 & 0 & 0 & 0 \\
0 & c_1 & 0 & 0 & 0 & 0 \\
0 & 0 & c_2 & 0 & 0 & 0 \\
-(b_{31} + b_4)c_{31} & 0 & 0 & c_{31} & 0 & 0 \\
-(b_{32} + b_4)c_{32} & 0 & 0 & 0 & c_{32} & 0 \\
-(b_{33} + b_4)c_{33} & 0 & 0 & 0 & 0 & c_{33}
\end{array}
$$

$$(2)$$

$$
\mathbf{K}_v =
\begin{pmatrix}
(k_1 + k_2 + k_{31} + k_{32} + k_{33}) & [-b_1 k_1 + b_2 k_2 + b_5(k_{31} + k_{32} + k_{33})] \\
-b_1 k_1 + b_2 k_2 + b_5(k_{31} + k_{32} + k_{33}) & [b_1^2 k_1 + b_2^2 k_2 + b_5^2(k_{31} + k_{32} + k_{33})] \\
(b_{31} + b_4)k_{31} + (b_{32} + b_4)k_{32} + (b_{33} + b_4)k_{33} & b_5[(b_{31} + b_4)k_{31} + (b_{32} + b_4)k_{32} + (b_{33} + b_4)k_{33}] \\
-k_1 & b_1 k_1 \\
-k_2 & -b_2 k_2 \\
-k_{31} & -b_5 k_{31} \\
-k_{32} & -b_5 k_{32} \\
-k_{33} & -b_5 k_{33}
\end{pmatrix}
$$

$$
\begin{array}{cccccc}
[(b_{31} + b_4)k_{31} + (b_{32} + b_4)k_{32} + (b_{33} + b_4)k_{33}] & 0 & 0 & 0 & 0 & 0 \\
b_5[(b_{31} + b_4)k_{31} + (b_{32} + b_4)k_{32} + (b_{33} + b_4)k_{33}] & 0 & 0 & 0 & 0 & 0 \\
(b_{31} + b_4)k_{31} + (b_{32} + b_4)k_{32} + (b_{33} + b_4)k_{33} & 0 & 0 & 0 & 0 & 0 \\
0 & (k_1 + k_{t1}) & 0 & 0 & 0 & 0 \\
0 & 0 & (k_2 + k_{t2}) & 0 & 0 & 0 \\
-(b_{31} + b_4)k_{31} & 0 & 0 & (k_{31} + k_{t31}) & 0 & 0 \\
-(b_{32} + b_4)k_{32} & 0 & 0 & 0 & (k_{32} + k_{t32}) & 0 \\
-(b_{33} + b_4)k_{33} & 0 & 0 & 0 & 0 & (k_{33} + k_{t33})
\end{array}
$$

$$(3)$$

where $m_T$ is the tractor sprung mass, $m_S$ is the semi-trailer sprung mass, $m_1$ is the tractor front axle mass, $m_2$ is the tractor rear axle mass, $(m_{31}, m_{32}, m_{33})$ are semi-trailer tridem masses, $I_T$ is the tractor pitch moment of inertia, $I_S$ is the semi-trailer pitch moment of inertia, $c_1$ is the damping of the tractor front axle suspension system, $c_2$ is the damping of the tractor rear axle suspension system, $(c_{31}, c_{32}, c_{33})$ are the damping of the semi-trailer tridem axle suspension systems, $k_1$ is the stiffness of the tractor front axle suspension system, $k_2$ is the stiffness of the tractor rear axle suspension system, $(k_{31}, k_{32}, k_{33})$ are the stiffness of the semi-trailer tridem axle suspension systems, $k_{t1}$ is the stiffness of the tractor front axle tire, $k_{t2}$ is the stiffness of the tractor rear axle tire, and $(k_{t31}, k_{t32}, k_{t33})$ are the stiffness of the semi-trailer tridem axle tires.

# Additional: Probabilistic Study

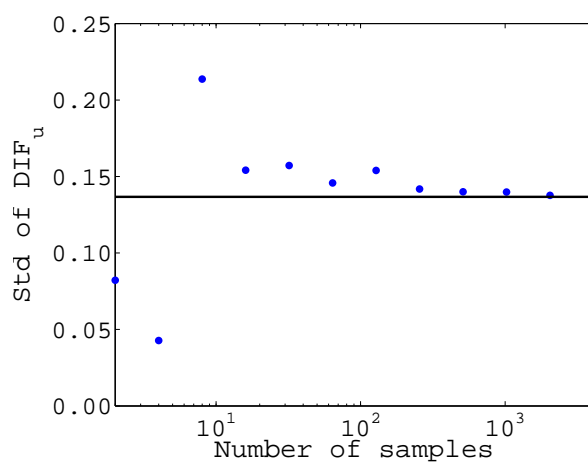## .2 Minimum number of road profiles considered in the dynamic analysis



FIGURE 1: Effect of number of samples on the deviation of the dynamic response estimate ($DIF_u$) due to the excitation of 2DOF vehicle: ( • ) Monte Carlo Simulation, (—) Convergence limit
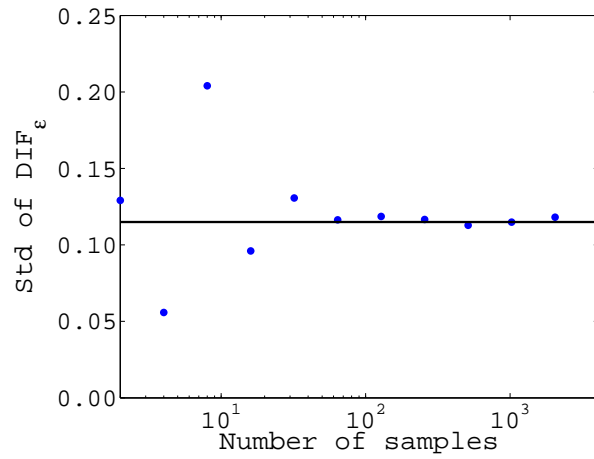
FIGURE 2: Effect of number of samples on the deviation of the dynamic response estimate (DIF$_\epsilon$) due to the excitation of 2DOF vehicle: ( • ) Monte Carlo Simulation, (—) Convergence limit
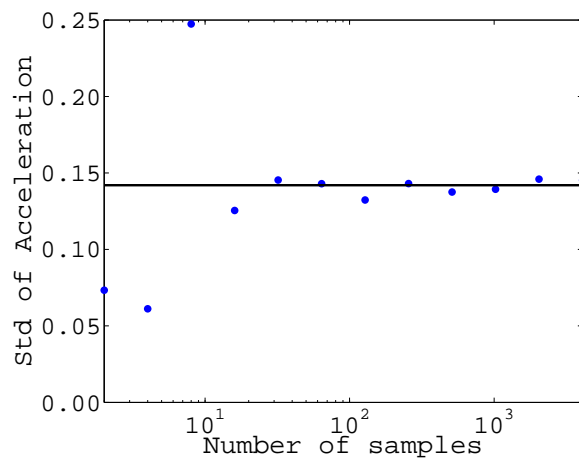


FIGURE 3: Effect of number of samples on the deviation of the bridge acceleration due to the excitation of 2DOF vehicle: ( • ) Monte Carlo Simulation, (—) Convergence limit
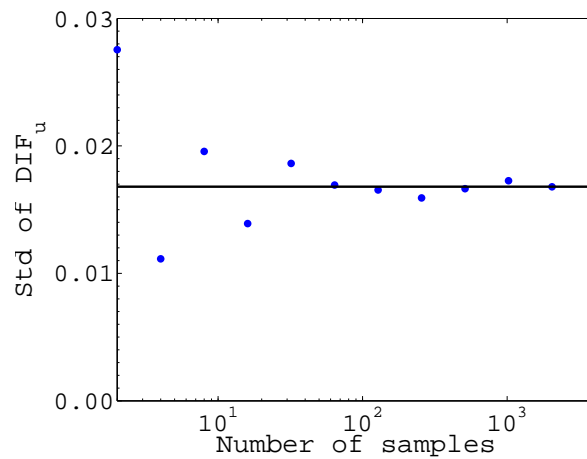
FIGURE 4: Effect of number of samples on the deviation of the dynamic response estimate ($\mathrm{DIF}_u$) due to the excitation of 8DOF vehicle: ( • ) Monte Carlo Simulation, (—) Convergence limit
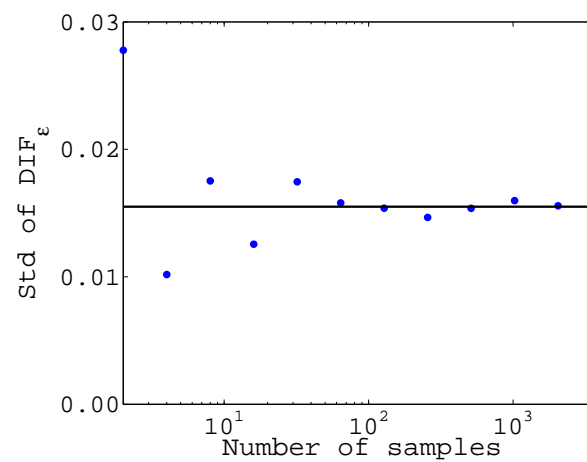


FIGURE 5: Effect of number of samples on the deviation of the dynamic response estimate ($\mathrm{DIF}_\epsilon$) due to the excitation of 8DOF vehicle: ( • ) Monte Carlo Simulation, (—) Convergence limit
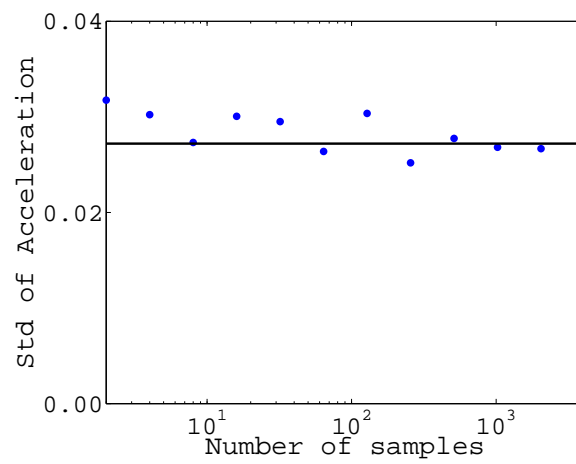
FIGURE 6: Effect of number of samples on the deviation of the bridge acceleration due to the excitation of 8DOF vehicle: ( • ) Monte Carlo Simulation, (—) Convergence limit

## .3 Log-likelihood estimates for the fitted distributions

TABLE 1: Log-likelihood estimates for the fitted distributions to the analyzed responses due to moving 2DOF

|  | Normal | Log-normal | Extreme value |
|---|---|---|---|
| $DIF_u$ | 482.70 | 493.05 | 503.46 |
| $DIF_\epsilon$ | 493.32 | 501.18 | 507.31 |
| Norm. acceleration | 265.07 | 284.34 | 285.46 |

TABLE 2: Log-likelihood estimates for the fitted distributions to the analyzed responses due to moving 8DOF

|  | Normal | Log-normal | Extreme value |
|---|---|---|---|
| $DIF_u$ | 2466.01 | 2468.63 | 2477.48 |
| $DIF_\epsilon$ | 2501.05 | 2502.62 | 2506.06 |
| Norm. acceleration | 2534.77 | 2554.72 | 2557.59 |

TABLE 3: Log-likelihood estimates for the fitted distributions to the analyzed responses due to moving 2DOF considering elastic spring supports

|  | Normal | Log-normal | Extreme value |
|---|---|---|---|
| $DIF_u$ | 480.66 | 489.42 | 499.13 |
| $DIF_\epsilon$ | 547.68 | 555.92 | 564.06 |
| Norm. acceleration | 218.46 | 248.31 | 249.58 |

TABLE 4: Log-likelihood estimates for the fitted distributions to the analyzed responses due to moving 8DOF considering elastic spring supports

|  | Normal | Log-normal | Extreme value |
|---|---|---|---|
| $DIF_u$ | 2440.47 | 2443.76 | 2451.05 |
| $DIF_\epsilon$ | 2472.89 | 2473.72 | 2476.36 |
| Norm. acceleration | 2532.84 | 2551.42 | 2553.74 |